POLITECNICO
MILANO 1863

SCUOLA DI INGEGNERIA INDUSTRIALE
E DELL'INFORMAZIONE

Characterization of a test bench for the certification of protection smart terminations used in secondary substations

TESI DI LAUREA MAGISTRALE IN
ELECTRICAL ENGINEERING
INGEGNERIA ELETRICA

Author: **Luigi Riccio**

Student ID: 966786
Advisor: Gabriele D'Antona
Academic Year: 2021-22

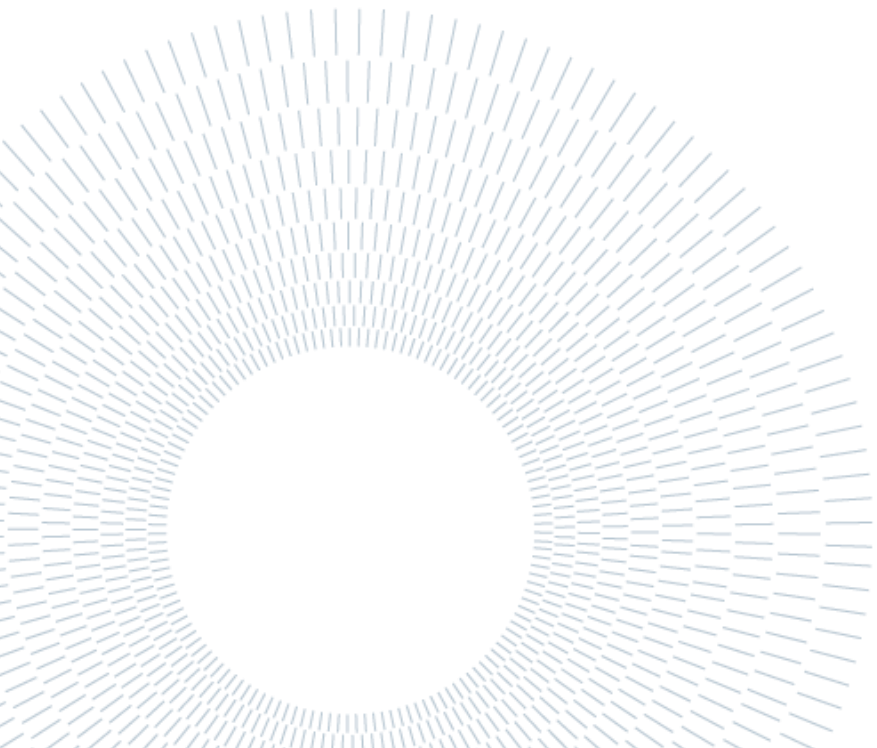

Abstract

The accuracy of a test bench is crucial for obtaining reliable information about the devices being tested and how they interact. This thesis addresses the calibration of a test bench used by Gridspertise, an ENEL group company, to test the sensors of a secondary substation. Specifically, the thesis investigates the accuracy of the test bench related to the studying of an unexpected delay and to the error introduced by transformers, which don't work at nominal conditions.

The method of solving is divided into two parts. The first part involves laboratory tests to collect data, while the second part involves data analysis using the Non-linear Least-Square method implemented in Matlab to obtain recursive estimates. The results show the accuracy of the devices and identify conditions in which they should not be used to avoid significant uncertainty. The delay was found to be caused by a lack of synchronization between the two devices.

The thesis concludes by providing new accuracy tables for future work and suggesting further tests to explore certain aspects in greater depth. Overall, this research contributes to a better understanding of the accuracy of test benches and how to improve their calibration.

Key-words: Calibration, secondary substation, smart termination.

Sommario

L'accuratezza del banco da lavoro è fondamentale per ottenere maggiori informazioni sui dispositivi testati e su come essi interagiscono tra di loro. L'obiettivo di questa tesi è la stima della calibrazione del banco da lavoro adottato da Gridspertise, una compagnia del gruppo ENEL, usato per testare i sensori delle cabine secondarie. In particolare questa tesi si focalizza sullo studio di un inaspettato ritardo e sugli errori introdotti dai trasformatori, i quali non lavorano a condizione nominale.

Il metodo di risoluzione è diviso in 2 parti. La prima si basa su dei test in laboratorio al fine di raccogliere i dati necessari mentre la seconda si basa sull'analisi di quest'ultimi usando il metodo dei minimi quadrati implementato su Matlab. I risultati mostrano le accuratezza dei dispositivi per ogni condizione identificando i casi da evitare per non incorrere in incertezze significative. Per quanto riguarda il ritardo si è scoperto che è causato da una mancanza di sincronizzazione tra gli strumenti adoperati.

La tesi si conclude presentando nuove tabelle di accuratezza da adoperare per futuri lavori e proponendo nuovi test da eseguire per poter approfondire il lavoro svolto. Complessivamente, questo studio fornisce una buona visione per quanto riguarda l'accuratezza del banco da lavoro e ne approfondisce la calibrazione.

Parole chiave: Calibrazione, cabina secondaria, smart termination.

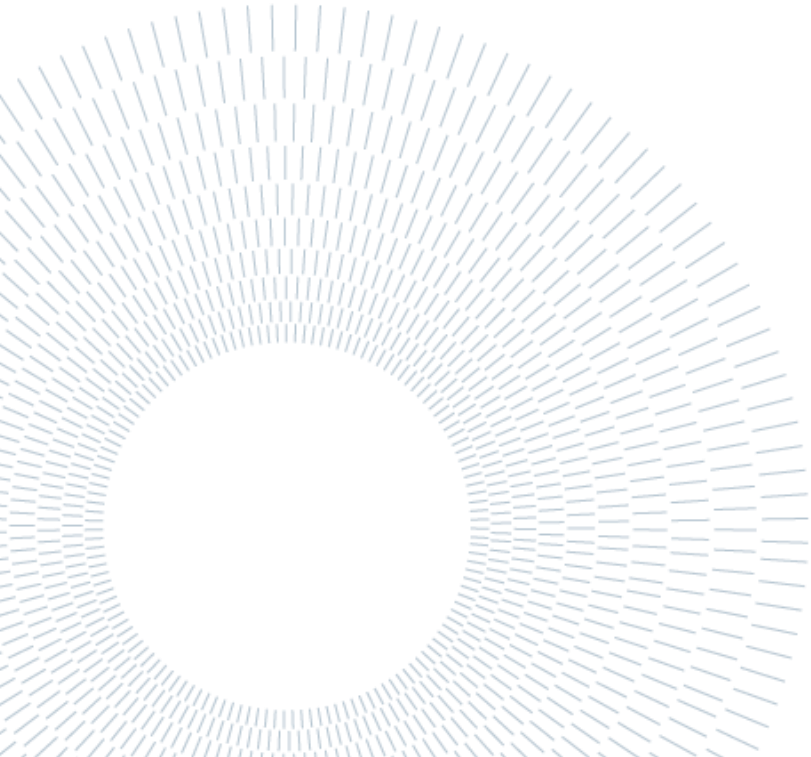

Contents

Introduction

The secondary station is one of the most important elements of the electric power system. It belongs to the distribution grid and it connects the medium voltage network to the low voltage one delivering electricity to the small costumers, like our houses.

For this reason protection system for MV/LV stations is fundamental. ENEL, Ente Nazionale per l'energia Elettrica, introduced a new device for this sector, RGDM (Rilevatore di Guasto e Di Misura). Which is an evolution of the previous device RGDAT (Rilevatore Guasto e Di Assenza Tensione) adopted to detect faults and voltage presence.

Instead, RGDM is able to detect faults, detect voltage presence/absence, adopt a logic selection of the fault, communicate with the main switch and exchange of data/signal by IEC 61850, the dominant international sub-station communication standard.

RGDM receives as input the signals acquired by sensors called smart terminations. To guarantee optimal working conditions all the devices must be calibrated. This thesis was proposed by Gridspertise, a company of the ENEL group, which wanted to understand the accuracy of their test bench, composed of secondary substation equipped with a test smart terminations and RGDM.

Their request was related to the accuracy of the acquisition chain, characterised by current and voltage transformers which don't work at nominal condition, and to the studying of an unexpected delay between the acquired current signal and the acquired voltage signal.

As a consequence, this paper is divided into two sections focusing on these two different topics.

For each case it was done a first laboratory test, in order to collect data. All the test were done in the Gridspertise's structure and all of them were agreed upon with the staff of Gridspertise.

Afterward, the data were analysed adopting the software Matlab, in order to obtain the error introduced by the transformers, the delay and their accuracy range.

A brief summary of the project is hereafter presented:

- Chapter 1: Substation and the protection system, where the electric power system is summarized focusing on MV grid and its protection system

- Chapter 2: Test set up, where the test bench of Gridspertise's laboratory is introduced.
- Chapter 3: Calibration chain, where topics are explained in deep focusing on the results and how all the data are acquired.
- Chapter 4: Conclusions, overall work of thesis results are summarized and conclusions are taken

The bibliography of this paper is constituted of slide courses of my personal university career, standards, documents sent by the staff of Grispertise and the manuals of the adopted instruments.

At the end of the thesis is presented an appendix where the Matlab codes are present.

1 | Substation and the protection system

In this chapter the configuration of the MV network is recalled, focusing on MV protection system.

This part is written based on the sources: [1] [2] [4].

1.1 The power system

In this section the power system will be briefly introduced, analysing its infrastructures

1.1.1 EHV-HV Network

The first part of the power system is the generation side, where the energy is produced by huge size power plants (Nuclear, Coal, Hydro-electric) and it pass from medium voltage side to extreme high (380-275 kV) voltage side by the station.

At this point, we talk about the transmission network, which consists of extreme high and high voltage network.

The transmission network is mashed, it means that each bus may be supplied by, at least, 2 ways. It guarantees a very good continuity of service, because in case of fault, at least, one way is available. It assures very good short circuit power, high short circuit currents, very good voltage profile and very good power flow. It is adopted for long distance electric power transmission.

89% of the HV line is composed of overhead lines, Figure 1.1. They are, typically, made of a core of steel surrounded by aluminium. It guarantees to respect the constraints considering all the characteristics of the HV network, like its huge extension (hundreds of kilometres) that is linked to higher losses .

Figure 1.1: HV overhead lines

On the HV network energy could be injected by medium sized power plants, also in this case it is produced in medium voltage and it is increased, and it can be delivered to HV costumers like industries and factories, Figure 1.2, 1.3.

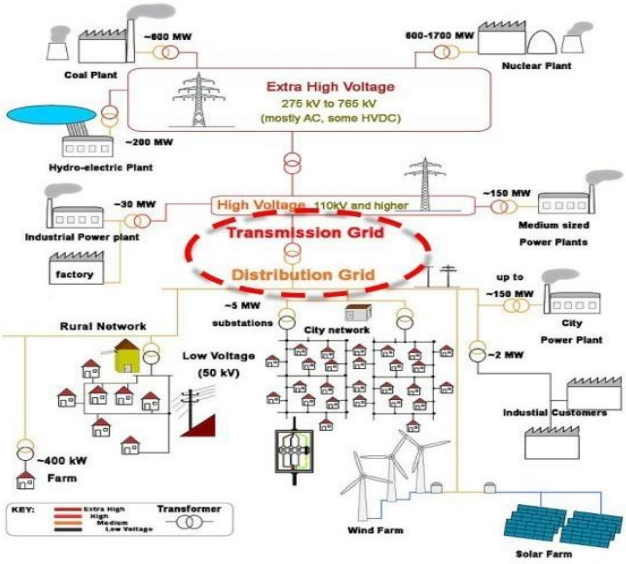

Figure 1.2: Example of electric power system [2]

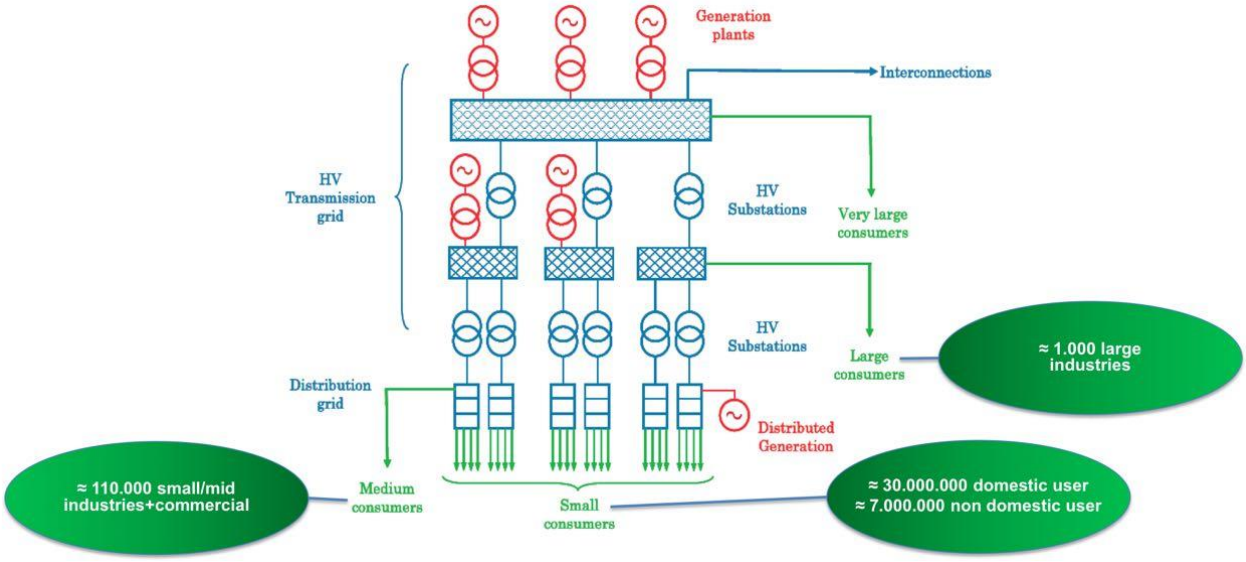

Figure 1.3: Example of electric power system [1]

Than the energy is delivered to the distribution grid, MV and LV side, the point of common coupling between the grids is called "primary substation".

1.1.2 EHV-HV protection

In Europe the neutral of HV network is effectively connected to the ground, it means that the voltage to ground of the healthy phases, excluding the transient period, does not exceed 80% of the nominal phase to phase voltage at steady state. It implies high current also in case of earth fault, almost equal to short circuit current, and a low voltage on healthy phases, figure 1.4.

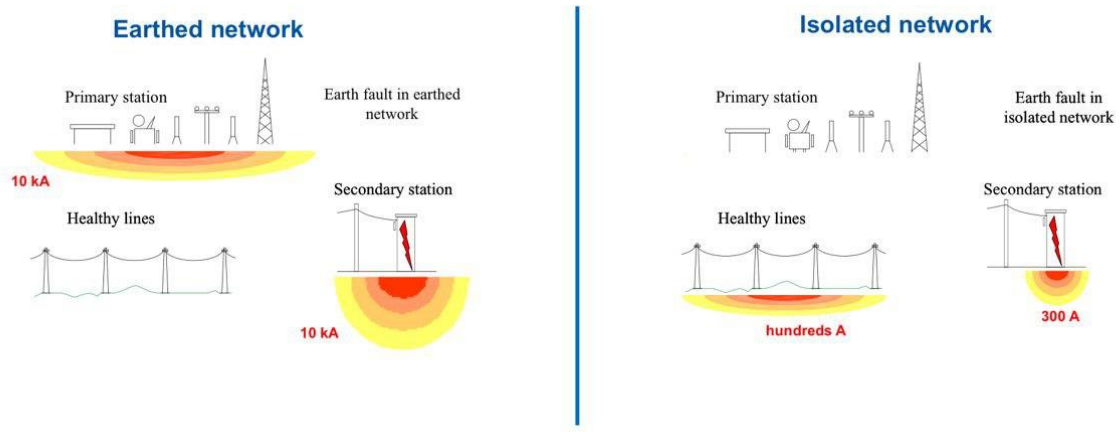

Figure 1.4: Differences between earthed network and isolated network [1]

Due to the mashed structure of the transmission network, simple relays cannot be used because all of them would trip.

It is necessary to use distance relay, specific relay which recognizes the position of the fault measuring its distance.

Its operation principle is based on the estimation of the impedance seen (Z_y) at the point of installation.

The imaginary part of the calculated impedance X_y is proportional to the fault distance, instead, the real part includes also the fault resistance and for this reason Is not proportional too.

$$V = (\mathrm{Zy} + \mathrm{Rf}) * I \rightarrow \frac{V}{I} = (\mathrm{Ry} + \mathrm{Rf} + \mathrm{j} * \mathrm{Xy})(R * y + Rf + j * y) \tag{1.1}$$

Where:

- y stands for the distance
- R_f stands for the fault resistance
- R_y stands for the real part of Z_y
- X_y stands for the imaginary part of Z_y

If the imaginary part is positive the fault is downstream respect to the distance relay and the current is 0°-90° lagging from voltage. On the contrary if it is negative the fault is upstream respect to the distance relay and the current is 180°-270° leading from voltage.

The performance of distance relay is defined in terms of reach accuracy, that is related to the impedance calculation, and the operating time, which can vary with fault current, measuring techniques and errors produced by CTs and VTs.

Distance relays are not expensive, fast, with a good reliability and a good selection of fault. They are based on 2 telecommunication skills: permissive over-reach scheme or blocking over-reaching schemes. They are used to coordinate 2 relays at both the ends of the line.

In case of EHV network, large generators are connected and for this reason a very short time is needed to eliminate faults for stability reasons. Teleprotection schemes are used in the protection system.

1.1.3 Primary substation

The primary substation is the connection point between the transmission network (EHV-HV grid) and the distribution network (MV-LV grid) , Figure 1.5.

In Italy, there are around 2500 primary substations categorized for their nominal power. The most common size is 25 MVA, that shares the 60%, the other sizes are: 16 MVA (25%), 40 MVA (15%) and 63 MVA (1-2%).

The classical structure of the primary substation is the following one:

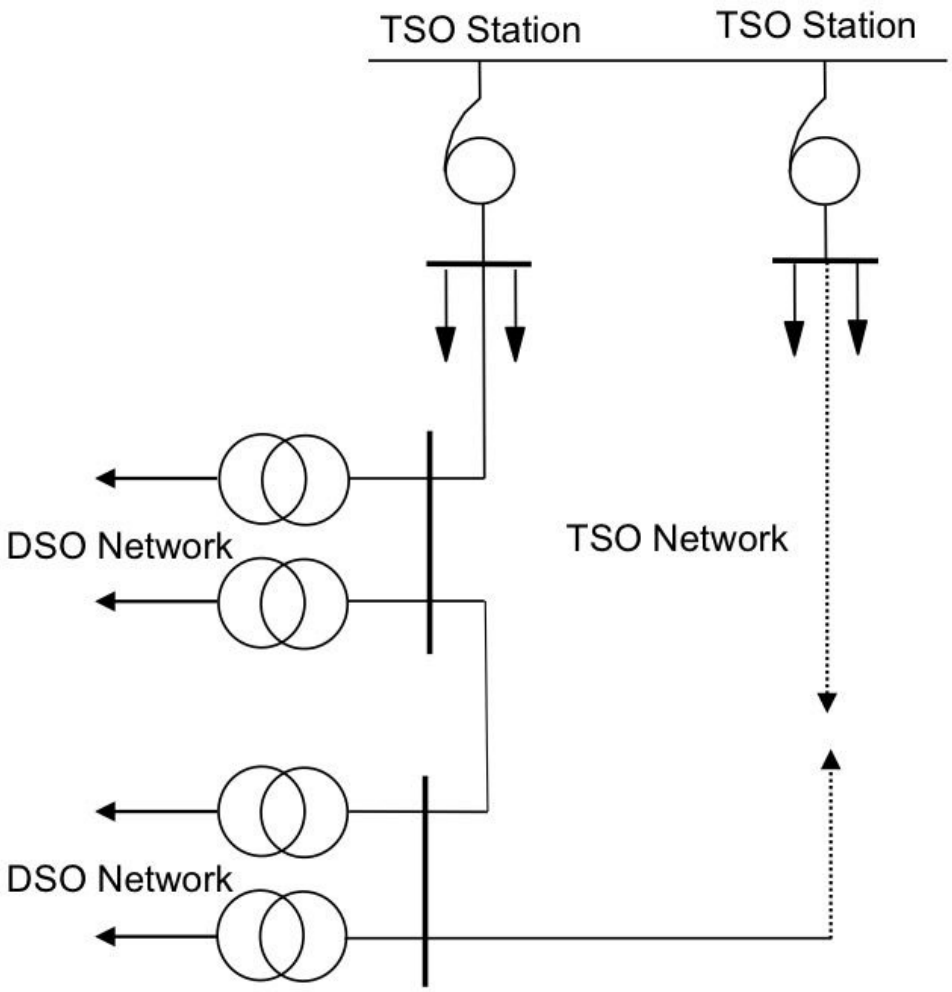

Figure 1.5: Example of primary substation [1]

As we can notice, due to the mashed structure of the HV network, for each Primary substation we have at least 2 transformers. For each transformer there is a current transformer in order to monitor and protect. Electric protections are coupled with circuit breakers to protect transformers and each single feeder.

Another component of the primary substation is the HV-MV tap changer. It is used by the Distributive System Operator(DSO) to control the voltage profile over the MV feeders in order to not succeed the constraint, Figure 1.6. Acting on the tap changer the ratio of the transformer will be changed. The ratio will decrease when, for whatever reason, the load tends to decrease and on the contrary, it will increase if the load increases.

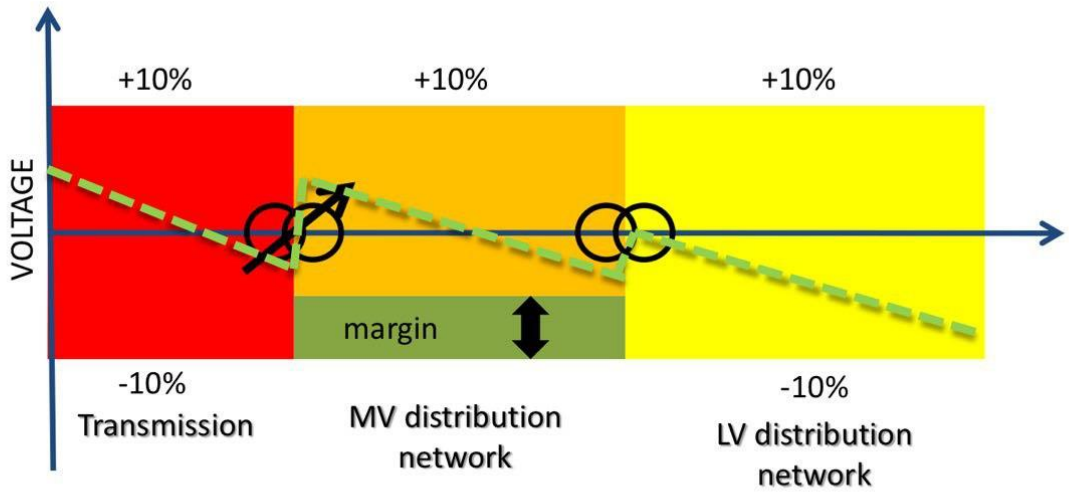

Figure 1.6: Example of voltage behavior in electric power system [2]

The tap ratio can varies between 0,95 and 1,05 of the nominal value.

While the HV side is effectively connected to the earth, the MV side can be isolated, directly connected to earth by a very low resistance or compensated network, Figure 1.7. We talk about compensated network if it is connected to earth through inductance (Petersen coil) or an impedance.

The neutral point connection to earth has no influence in case of normal operation and in case of phase-to-phase fault, it acts only in case of earth fault on currents and voltages.

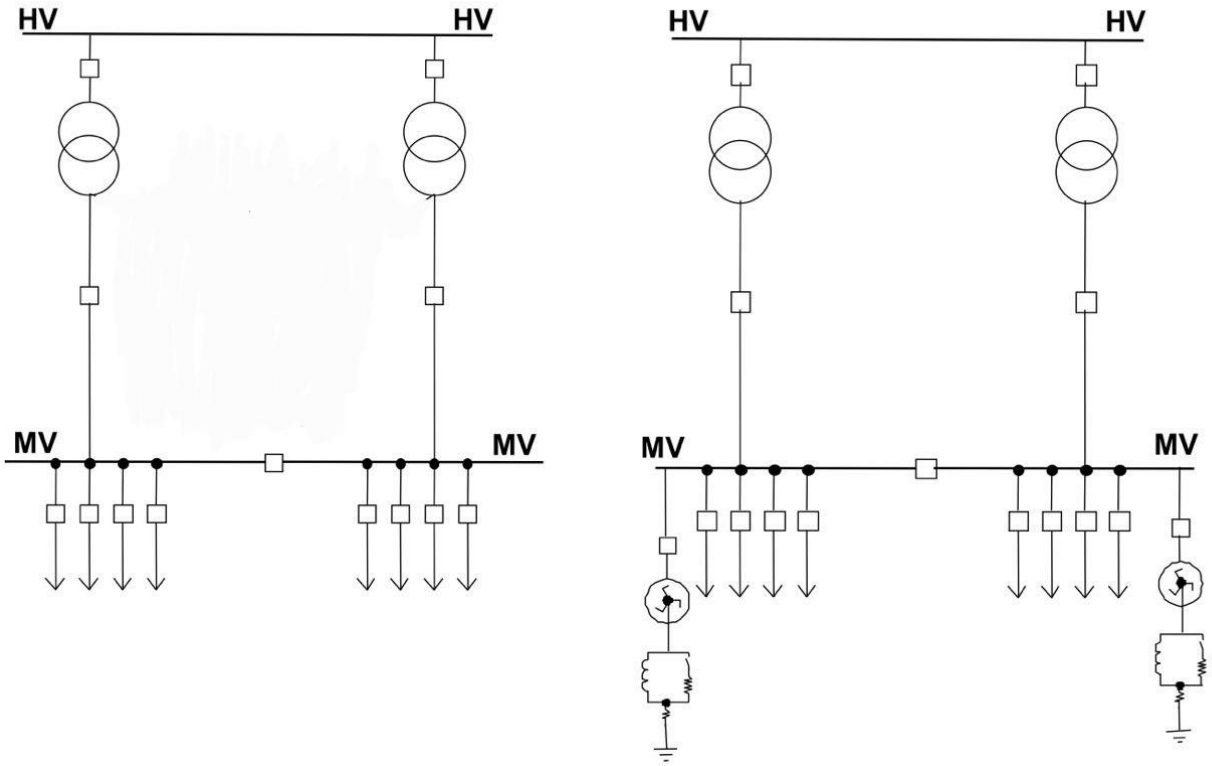

Figure 1.7: Examples of isolated and compensated MV network [1]

The compensated network works limiting the earth fault current and automatically detecting the fault at the same time.

The imaginary part of the impedance, the Petersen coil, has the function to reduce the reduce the module of the fault current. Instead, the parallel resistance has the function to change the angle of the faulty current, at least 13° counterclockwise from the healthy one, to allow the protection system to trip. Parallel resistance has been chosen in order to have 25-35 A of additional resistive component, Figure 1.8, 1.9, 1.10.

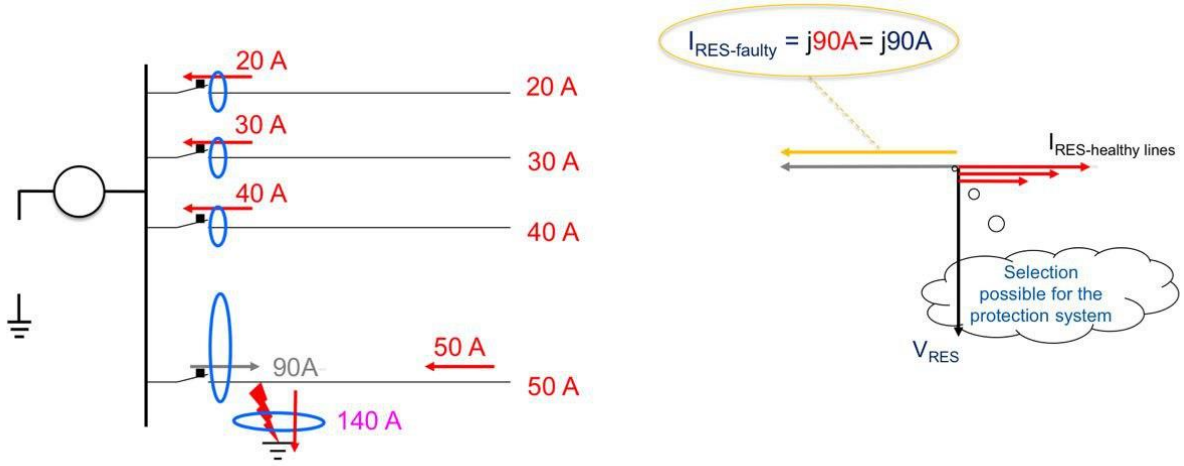

Figure 1.8: Case of isolated MV network [1]

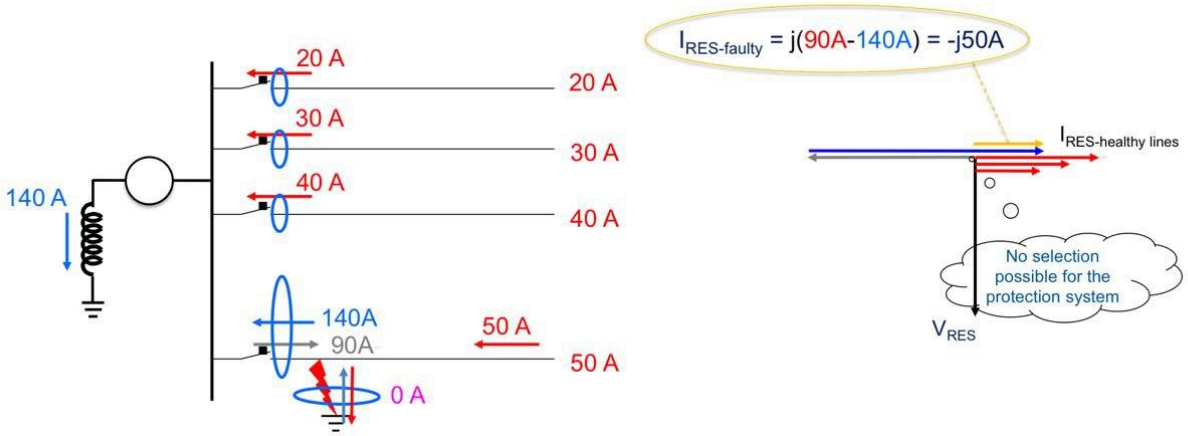

Figure 1.9: Case of compensated MV network with a pure Petersen coil[1]

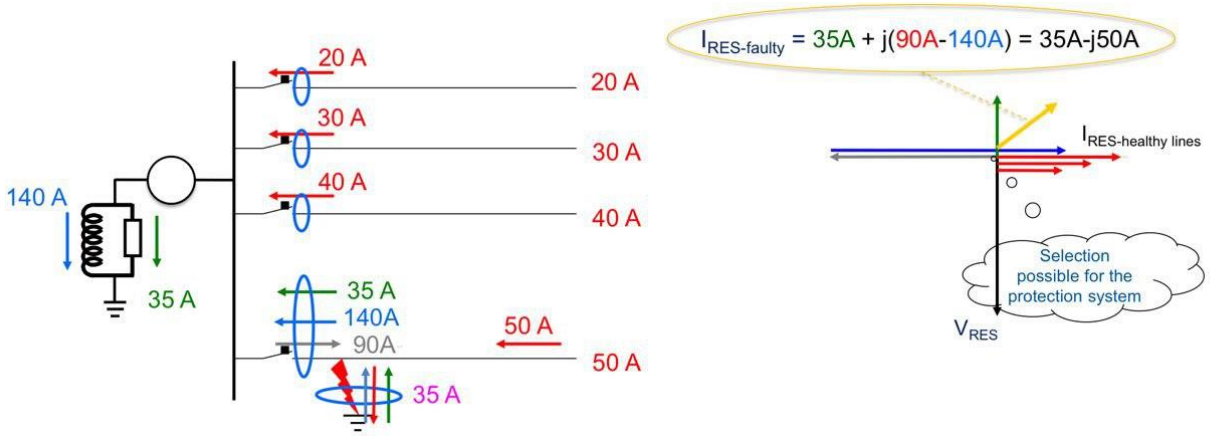

Figure 1.10: Case of compensated MV network with an impedance [1]

Another resistance, in series with the impedance, is necessary in order to limit the saturation of the current transformer. Its value is in the order of few ohms, depending on the coil position, in order to limit the time constant of earth fault current to 150 ms. This means that after 500 ms (3 times time constant) CT is no more saturated and the protection system can surely work.

To set the desired value of the Petersen coil the network analyser is used. It measures the residual voltage, which depends form the not transposed MV feeders, in different tuning position, to do this the network analyser has to calculate the capacitance. Where the max value stands for the 100% of tuning. An under compensation, around the 90%, is preferable in order to guarantee an higher angel between the faulty current and the healthy one.

The network analyser measures typically every 3 minutes, in no fault conditions, and it stops the tuning process in fault condition.

To use this solution ENEL adopts a three winding transformer (DT1096), Figure 1.11 where the first and the second winding are respectively used for Petersen coil and parallel resistance and the third one is used for current injection for tuning.

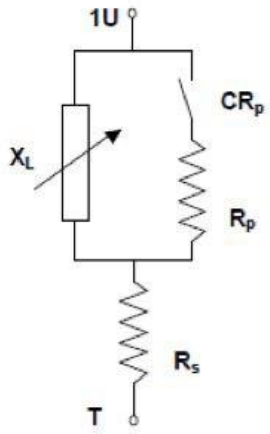

Figure 1.11: DT 1096, three winding transformer used by Enel [1]

1.2 MV Network

The MV network, Figure 1.12, is the first part of the distribution grid. It is generally radial, with the possibility to be re-supplied by other paths thanks to the installation of many reconfiguration points. In this way there is the possibility to change the grid topology in order to allow more reliable management of the grid, feeding as many customers as possible.

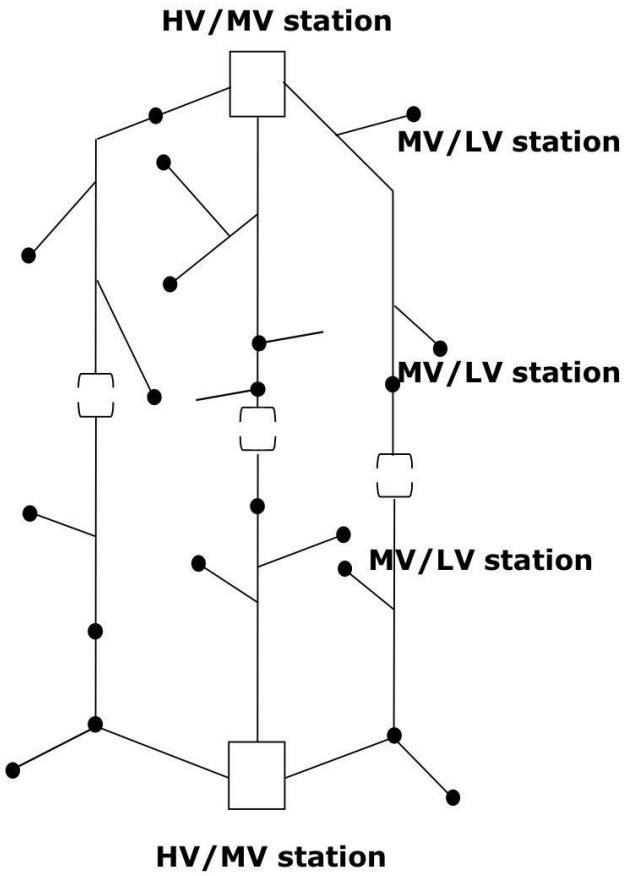

Figure 1.12: Example of MV network [1]

It is fed by primary substations and also by distributed generations, like wind and solar plant, which inject directly to the load without passing through the transmission grid.

It delivers the energy, directly, to the MV customers, like city power plant or small industrial, or to the LV customers passing through the MV/LV transformers, the Secondary Substation.

The 41% of the MV cables are underground lines, like in the city, and the other 59% is overhead lines, like in rural area. In the first case they are underground insulated cables and in the second case they could be naked or elicord,

In case of Emergency country, MV distribution grids have very long feeders, very heterogenous users and fluctuating load. For this reason they are designed at 33kV or, sometimesoltc, even 66 kV and the primary substation could be designed with a power higher than 100 MVA.

1.2.1 MV Voltage regulation

The customers, of all sizes, operate at the best, in terms of performance and continuity, when they are supplied at the nominal voltage, any deviation deteriorates the performance.

The variation of voltage, in terms of amplitude, at which consumers are supplied is one of the elements characterizing the Quality of Service. They are correlated with disturbance, like load variation, and control actions of reactive power sources, like synchronous machines and condensers.

The voltage regulation is the set of actions carried out in order to keep the voltage in all busses within values, in the range of the nominal one, that ensure the good operation of the load.

The voltage variation, excluding the periods with interruptions, should not exceed the range of 90-110% of the nominal voltage. This range could vary in particular cases like special remote network users or networks not interconnected with transmission systems.

As was explained in the paragraphs below, the transformers, both HV/MV and MV/LV, cover an important role in the voltage regulation in a MV Grid working on the tap ratio of the substations. For economic reason, secondary substations are not provided with on-load tap changer (OLTC), like primary one, but merely with no-load-tap-changer. There is a number of taps, usually 5, connected to a charger which is adjustable when the transformer is installed. For this reason it is not an automatic regulation like HV/MV side.

One of the most important regulations is the voltage compound, Figure 1.13. It is based on sanding to the tap positioner of the transformer the difference between the substation voltage set point and the measured voltage.

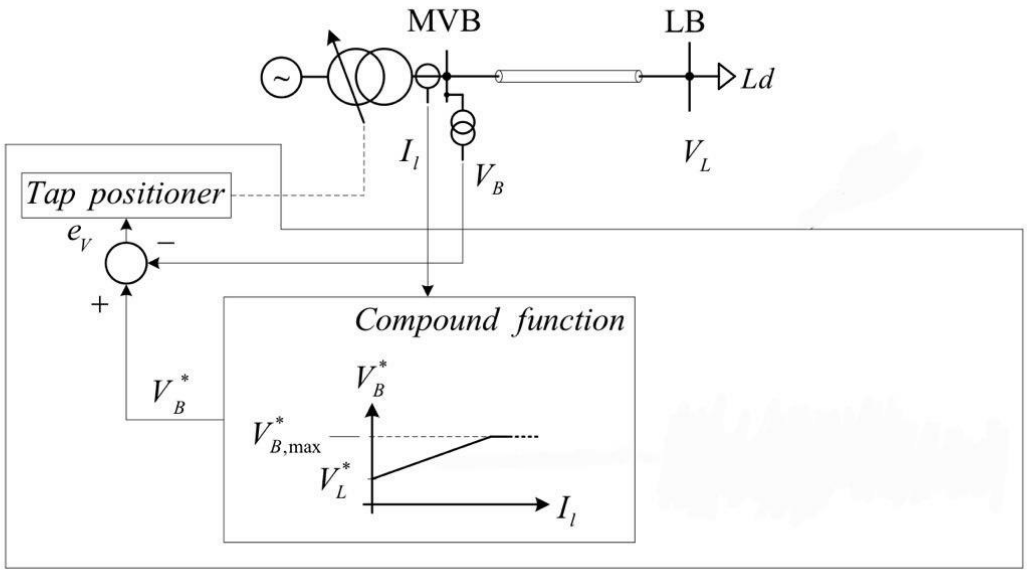

Figure 1.13: Example of compound [4]

$$e_v = V^*{}_B - V_B \tag{1. 2}$$

$$V^*{}_B = V_L + \sqrt{3} I_l (R_l cos\varphi_l + X_l sin\varphi_l) \tag{1. 3}$$

Where:

- e_v stands for the voltage error
- $V^*{}_B$ stands for the substation voltage set point
- V_B stands for the measured voltage
- V_L stands for the desired voltage on load busbar
- R_l is the line resistance
- X_l is the line inductance
- φ_l is the load angle

There is another kind of compound function, the partial compound where a coefficient is added. It value is between 0, when there is no compensation, and 1, where the compound is total.

$$V^*{}_B = V_L + \sqrt{3} I_l (aR_l cos\varphi_l + aX_l sin\varphi_l) \tag{1. 4}$$

Another significant problem in the MV voltage regulation, is the presence of distributed generation units. They impact on the feeders voltage profile, increasing the

voltage at the Point of Common Coupling. In this case it is no longer possible to solve the problem simply adjusting the tap ratio.

$$\Delta\dot{V} = \frac{\sqrt{3}(RIcos\varphi + XIsen\varphi)}{V_2}\frac{V_2}{V_2} = \frac{RP_2 + XQ_2}{{V_2}^2} \tag{1. 5}$$

In case of DG, the real power P_2, is injected and for this reason the voltage drop will be reduced, Figure 1.14.

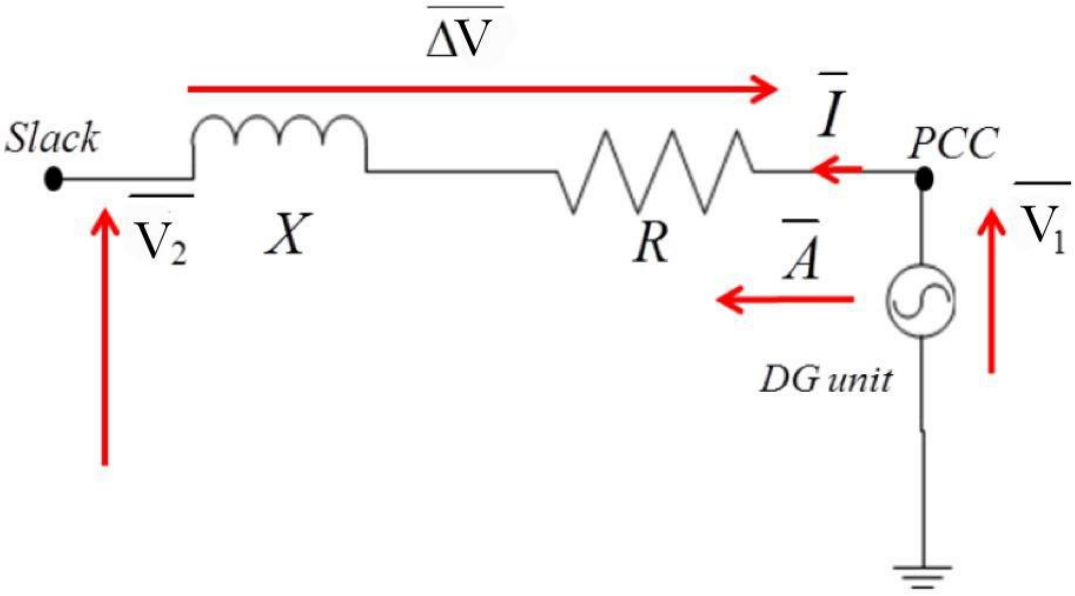

Figure 1.14: DG unit injecting complex power $\overline{A}$ in the PCC [2]

Consequently, it is necessary to identify a method involved to estimate what is the maximum penetration of DG units, compliant with the grid constraints. It is commonly named hosting capacity.

This method is based on the selection of performance indices for the grid and their limits. The hosting capacity, Figure 1.15, is the amount of new production or consumption where the first performance index reaches its limit.

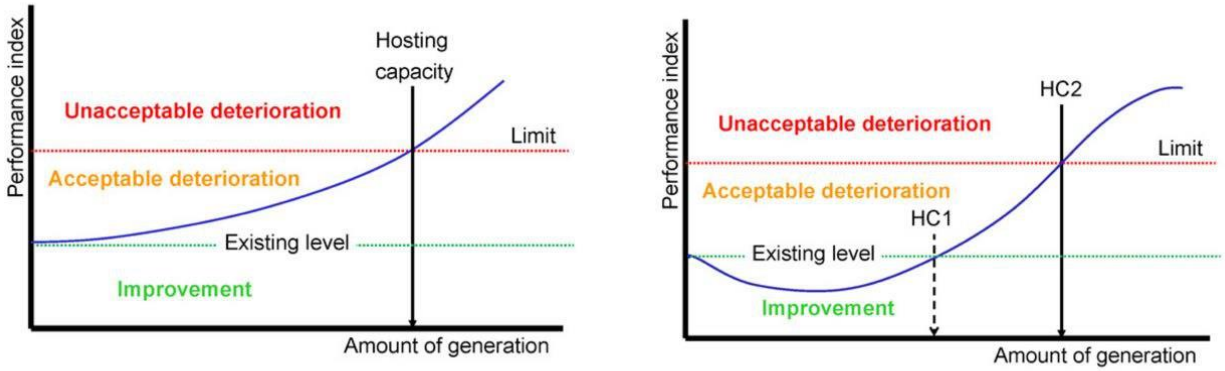

Figure 1.15: Example of impact of hosting capacity on performance index [2]

The value of the hosting capacity could be changed if the DSOs find a new feasible solutions. Obviously, limits have to be defined in order to properly regulate network developments.

The main constraints related to the hosting capacity are the followings:

- Thermal loading of all network equipment, which imposes a maximum value of current per each branches.
- Voltage limits, in this case the steady state voltages are checked against the predefined minimum and maximum voltage limits, ±10% of the nominal value.
- Rapid voltage changes, caused by the sudden fluctuations of the connected DG units, it impose a limit of 4-6% of variation in a short time.

In order to not succeed these ranges and regulate the voltage profile in a MV feeder with the penetration of DG, it could be possible operate on the injections of real and reactive power. The possibilities are to decrease real power injections, increase reactive power injections and change both P and Q injections.

$$\frac{\partial U_1}{\partial P}\Delta P + \frac{\partial U_1}{\partial Q}\Delta Q = \Delta U_1 \tag{1. 6}$$

The regulation of reactive power liked to a voltage value closes to the limit is linked to the local voltage regulation. In this case the reactive power regulation is a function of the local measured voltage at DG delivery point.

Instead we talk about centralized voltage regulation when voltage exceeds its limits and for this reason the local voltage regulation fails its goal and the generator become an Out-threshold Generator (OTG). The OTG sends a signal to the Centralized Voltage Regulation, VCS; which chooses the Best Generator, BG, which have the greatest voltage influence on the OTG. It is chosen by a sensitivity approach.

The sensitivity approach is based on deriving each single node voltage E_i per each single node reactive power Q_j. In this way the matrix of reactive power sensitivity, S_Q , is defined:

$$\begin{bmatrix} \Delta E_1 \\ \vdots \\ \Delta E_i \\ \vdots \\ \Delta E_n \end{bmatrix} = \begin{bmatrix} \frac{\delta E_1}{\delta Q_1} & \frac{\delta E_1}{\delta Q_2} & \frac{\delta E_1}{\delta Q_3} & \frac{\delta E_1}{\delta Q_4} & \frac{\delta E_1}{\delta Q_5} \\ \vdots & \vdots & \vdots & \vdots & \vdots \\ \frac{\delta E_i}{\delta Q_1} & \frac{\delta E_i}{\delta Q_2} & \frac{\delta E_i}{\delta Q_3} & \frac{\delta E_i}{\delta Q_4} & \frac{\delta E_i}{\delta Q_5} \\ \vdots & \vdots & \vdots & \vdots & \vdots \\ \frac{\delta E_n}{\delta Q_1} & \frac{\delta E_n}{\delta Q_2} & \frac{\delta E_n}{\delta Q_3} & \frac{\delta E_n}{\delta Q_4} & \frac{\delta E_n}{\delta Q_5} \end{bmatrix} \begin{bmatrix} \Delta Q_1 \\ \vdots \\ \Delta Q_i \\ \vdots \\ \Delta Q_n \end{bmatrix} \tag{1. 7}$$

At this point the VCS can determine the BG in base at the highest value on the row of the OTG node.

This approach could be adopted both for MV feeders and for LV feeders but the sensitivity will result higher for MV nodes than LV ones, it is due to the higher R/X ratio for the last one.

1.3 MV protection system

The main goal of the protection system is to maintain a very high level of continuity of service and in case it is not possible to minimize the outage time. Even if the distributed network is full of protocols and systems to prevent the failures they are impossible to totally avoid. Natural events, physical accidents, equipment failure and human error are impossible to prevent. For this reason the most important thing is to minimize the following damages.

The most common fault is the single phase to ground one, it covers the 70-80%, the others are the phase to phase to ground (10-17%), the phase to phase (8-10%), the three phase(2-3%) and the cross-country fault.

Another important aspect to detect the fault is understand if it is balanced, unbalanced or series. In order to obtain this information the Fortescue transformation is used.

1.3.1 phase to phase short circuit

In case of phase to phase short circuit there are high currents involved which are limited only by series elements, the neutral connection has no effect. For this reason a very fast fault clearing is needed. In fact, the energy in cable during short circuit, the Joule effect, depends on the value of the current flowing in the cable and the time to clear the fault. For this reason high current implies short elimination time and low current implies long elimination time.

The most important thing in this case is that the energy produced during the short circuit doesn't succeed the energy stored in the cable until the fault clearing.

$$I^2t \leq K^2S^2 \tag{1. 8}$$

Where

$$K = \sqrt{\frac{c}{\alpha\rho_0} ln\left(\frac{1+\alpha\theta}{1+\alpha\theta_0}\right)} \tag{1. 9}$$

- ρ_0 stands for the resistivity
- c stands for the specific heat
- α stands for the temperature coefficient for resistivity
- θ stands for the final temperature
- θ_0 stands for the initial temperature
- I stands for the flowing current

- *t* stands for the elimination time
- S stands for the section of the cable

During the phase to phase short circuit there is the minimum short circuit current, instead the maximum value happens during the three phase short circuit, it is related to an increment of the voltage, which reaches 110% of its value.

1.3.2 Cross-country fault

The cross country fault is a fault which involves both two phases and the earth. It typically happens because of the increasing of the voltage due to an earth fault. It happens in the healthy phases caused by the losing of isolation by some point. The residual currents in the two lines are composed into two component: the first one similar to the earth fault current and the second one similar to a phase-to-phase short circuit. The second one is higher than the first one and for this reason the two residual current in the two line are quite opposite, as shown in the Figure 1.16.

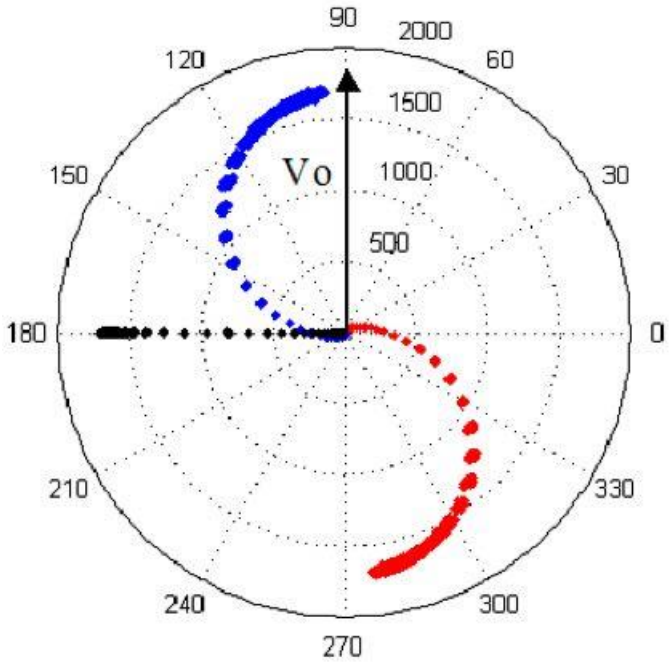

Figure 1.16: Example of Cross-country fault [1]

1.3.3 Involved relays

The relays involved in the MV protection system have to guarantee the function of metering and monitoring and the function of event record.

The first one is related to measure the rms value and the phase displacement of voltages and current, the active and reactive power and the frequency. The second function has to record tripping operations, alarms, fault record, including data and time of operation, failures detected by automatic supervision, change of relay setting and change of state of binary inputs/outputs.

This kind of relays detect at the same time both voltage and current, for this reason the Inter-Range Instrumentation Group (IRIG-B) is used. It is a time protocol which ensures accurate time synchronization. Internal auxiliary transformers are used to isolate and to adopt input from voltage and current transformers.

Instead for what concerns the record process the Memory Protection Unit (MPU) allows to define memory access permission. The output signals are converted into digital data for processing: signal processing, protection algorithm, logic schemes, output signals and control and handing of human interface.

All this process is summed-up in the Figure 1.17

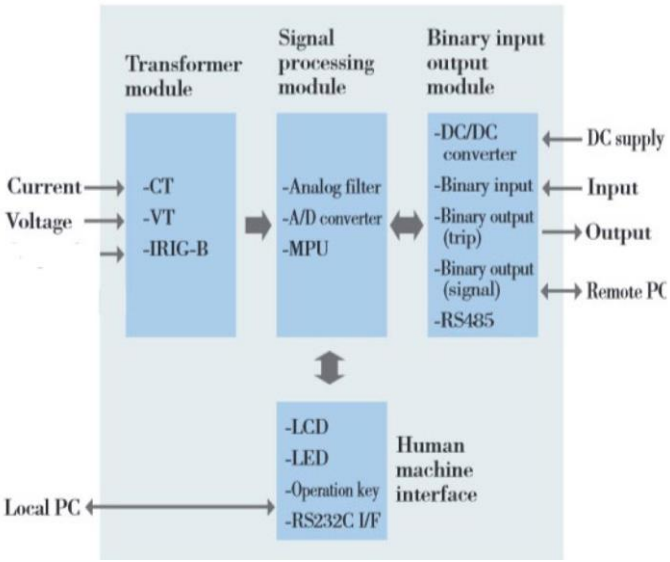

Figure 1.17: Hardware block diagram [1]

The main hardware and software function are permanently verified in background, the most basic function is the parity check data in which microprocessor continues to verify that is able to make the simple operation. More sophisticated and expensive

function are the reference voltages, in which the microprocessor can check the presence of the input voltage, and the input/output channels.

Due to its radial structure, during a short circuit caused by a phase-to-phase fault a simple overcurrent relay is needed, unless the presence of DG. Otherwise directional overcurrent relays are used. Instead in case of earth fault, because of the neutral point not directly connected to earth to earth, overcurrent relays can't be used, in fact directional residual overcurrent relay are adopted with a trip time which depend on earth plant design for earth faults. Also in case of cross-country earth fault directional residual overcurrent relays are necessary.

Let's start to talk about the difference between directional and non-directional relays. The second one operate detecting just one quantity, in case of overcurrent relay it detect only if the current succeed the range but it can't distinguish the position, if the fault is downstream or upstream.

Instead the directional relay operates detecting more information, in case of directional overcurrent relay it detects the current and the reference voltage to distinguish the fault position.

Another distinction for relays is if they are time dependent or time independent. In the second case the trip time doesn't depends on the current value, if it succeeds the set value the relays will trip with the set tripping time. Instead in case of time dependent relays, Figure 1.18, high current corresponds to a fast tripping time and low current to long tripping time.

$$t = \frac{K}{(I/I_1)^m - 1} \tag{1. 10}$$

Where k and m are two factors which vary if the tripping curve is set in case of inverse, very inverse or extremely inverse.

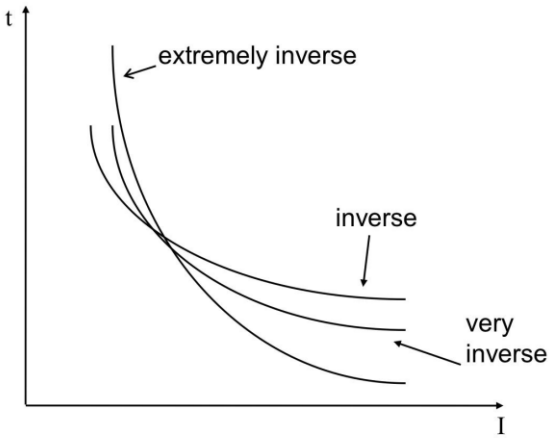

Figure 1.18: Tripping curve [1]

The involved relay in MV protection system are:

- overcurrent relays (ANSI code 50/51), Figure 1.19, the difference between 50 and 51 is that the last one operate with an integrated delay. They could be both time dependent and independent

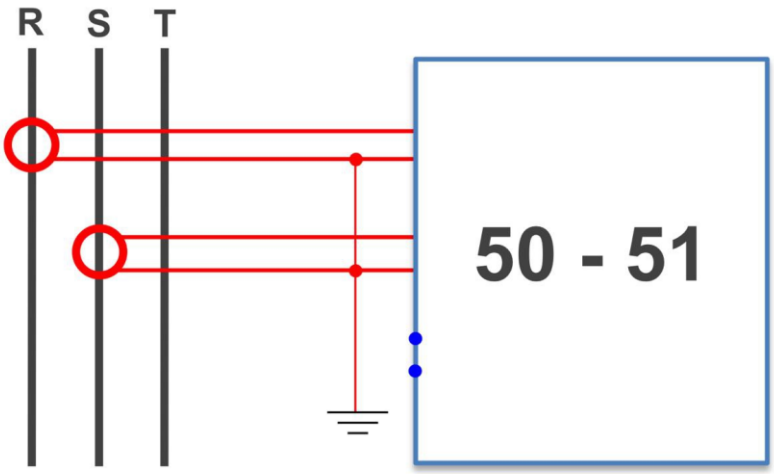

Figure 1.19: Connection scheme of overcurrent relay (ANSI code 50/51) [1]

- directional overcurrent relay (ANSI code 67), Figure 1.20, it detects the direction of the fault in base if the current is lagging or leading referred to the voltage. It is time independent

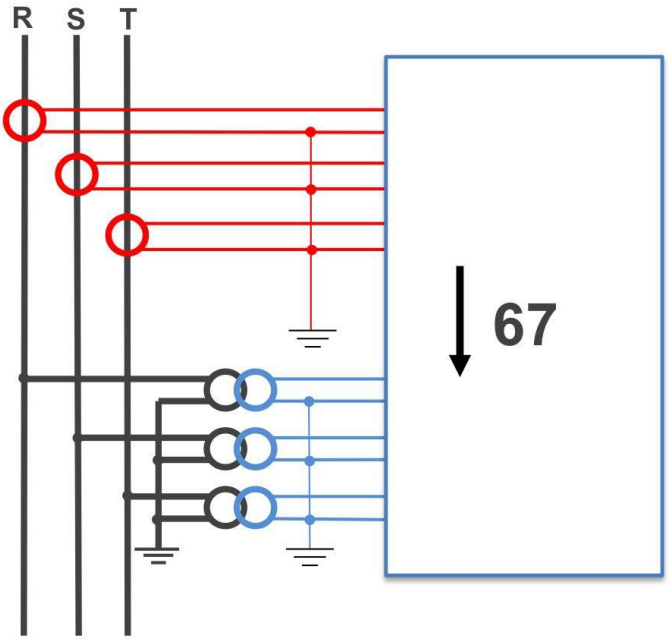

Figure 1.20: Connection scheme ofdirectional overcurrent relay (ANSI code 67) [1]

- residual directional overcurrent relay (ANSI code 67N) , Figure 1.21.

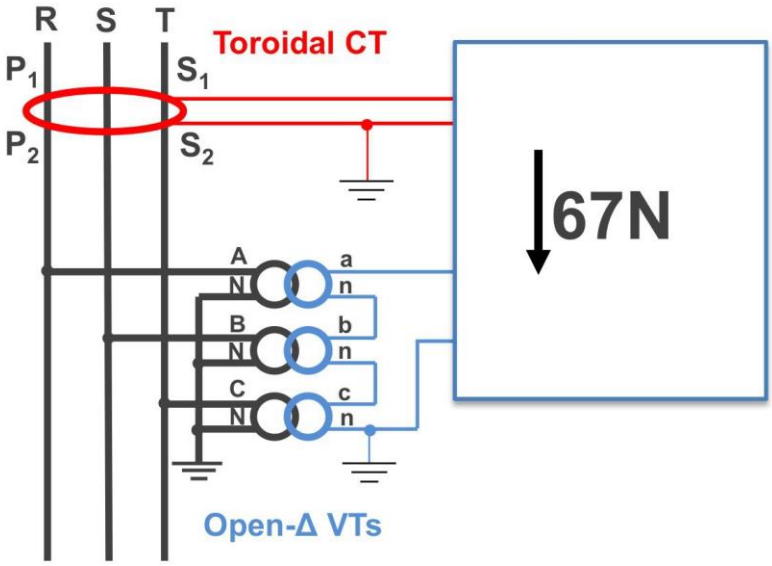

Figure 1.21: Connection scheme of residual directional overcurrent relay (ANSI code 67N) [1]

In a MV network, at least, three kind of residual directional overcurrent relays are used:

- 67.S1, it is used in compensated networks and it is set with a tripping current equal to 2 A, a tripping voltage of 6% of the secondary voltage and a tripping phase of 60-257° clockwise from the residual voltage.
- 67.S2, it is used in isolated networks and it is set with a tripping current equal to 2 A, a tripping voltage of 2% of the secondary voltage and a tripping phase of 60-120° clockwise from the residual voltage.
- 67.S3, it is used both in isolated and compensated networks to eliminate fault along the lines and it is set with a tripping current equal to 150 A, a tripping voltage of 2% of the secondary voltage and a tripping phase of 190-10° clockwise from the residual voltage.

They operate at the same time and for this reason a synchronization is needed in other to avoid that more than one relays trip at the same time for the same fault.

Three different tripping times are set for each relays, Figure 1.22, 67.S3 is the quickest tripping after 100 ms, the second one is 67.S2 after 400 ms and the last one is 67.S1 after 20s.

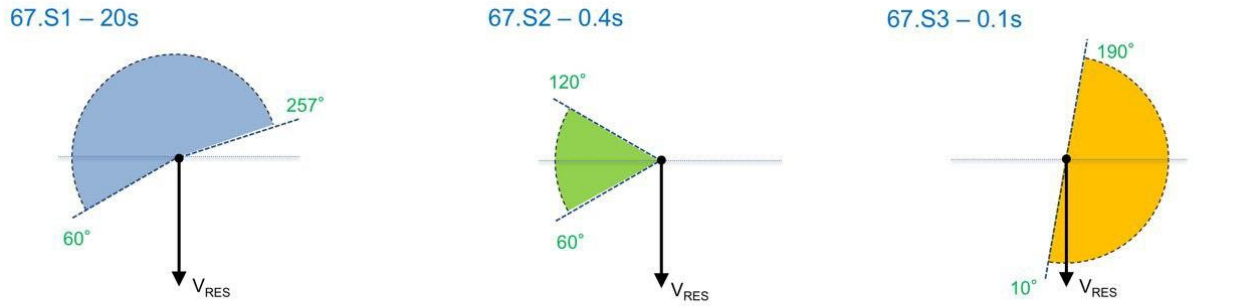

	TRIP CURRENT	TRIP VOLTAGE	PHASE	TIME
67 S1	2A	6%	60°- 257°	20s
67 S2	2A	2%	60°- 120°	400ms
67 S3	150A	2%	190°- 10°	100ms

Figure 1.22: Tripping zone of residual directional overcurrent [1]

1.3.4 MV Network automation

The equipment in MV network is structured in the following way, Figure 1.23: from the primary station to the secondary one there is the protection system in primary station, DV901, the line circuit breaker on each MV line and the protection system in secondary station, Figure 1.24, that could be RGDAT (Rilevatore Guasto e Di Assenza Tensione) or RGDM (Rilevatore di Guasto e Di Misura). Between the secondary station there are also feeder sectionalizers, IMS, or circuit breakers, DY800.

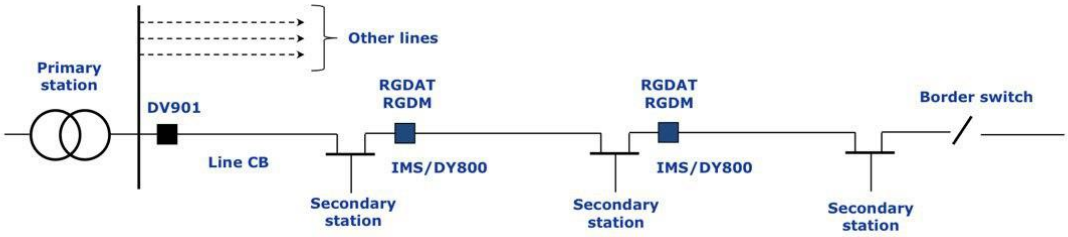

Figure 1.23: Equipment in MV networks [1]

Let's focus on the differences between RGDAT and RGDM. RGDAT is an equipment able to detect faults, like earth faults or short circuits, and to detect the presence or the absence of the voltage. RGDM is an evolution which can do a logic section of the fault, it communicates with GD and exchange data and signal by IEC 61850 protocol. RGDM can also measure power, frequency and the second harmonic and can work on intermittent arc.

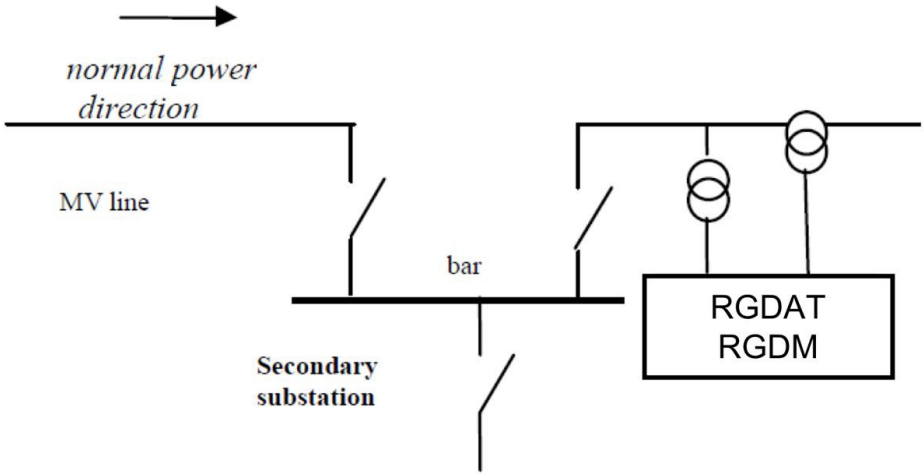

Figure 1.24: Protection system in Secondary Station [1]

In case of fault ENEL operates 3 kind of automation: FNC, FRG and FSL

The FNC (Funzione Neutro Compensato) automation is adopted only in case of earth fault on cable, aerial and mixed networks with compensated neutral.

After the detection of the fault a signal is sent to each IMS/DY800. These instruments aren't interconnected to each other, so for this reason a delay is imposed. It is higher if IMS/DY800 is farther from the fault. The delay, represented by clock in the picture below, is a multiple of 5 seconds for IMS or less for DY800, Figure 1.25.

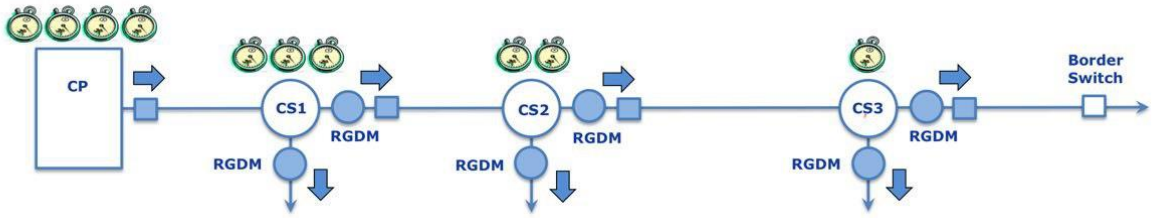

Figure 1.25 FNC automation scheme [1]

The first IMS/DY800 upstream to the fault opens and its RGDAT/RGDM sends a message to the control room indicating block in open. Then the operator in the control room opens the closest IMS/DY800 to the fault, closes the IMS in the border secondary substation within 180 seconds and configures the RGDAT/RGDM, downstream to the fault, in the reverse direction.

The FRG (Funzione di Ricerca Guasto) automation is adopted on cable, aerial and mixed networks in case of earth fault, only when the neutral is isolated, short circuit and cross-country fault.

After the detection of the fault the first step of the FRG automation is the opening of the circuit breaker in the protection (CP) in 0.1 seconds and the following re-closure in 0.6 seconds.

If the fault is still present the fault can't be categorized as a transient interruption, when it lasts less than 1 second, and it became a short supply interruption, when it last more than 1 second and less than 3 minutes.

Than circuit breaker opens in CP in 0.1 seconds and waits 30 seconds before re-closing. After that all IMS/DY800 open upstream the fault detected by RGDAT/RGDM.

Starting from the farter IMS/DY800, everyone recloses after 5 seconds, in this way the exact position of the fault is detected. At this point the circuit breaker opens in 0,1 second for last time and waits 70 seconds before re-closing. In this period the RGDAT/RGDM, before the fault, sends a message to the control room indicating blocks in opens. Than the operator in the control room opens the closest IMS/DY800 to the fault, closes the IMS in the border secondary substation within 180 seconds and configures the RGDAT/RGDM, downstream to the fault, in the reverse direction.

The FSL (Funzione Selettività Logica) automation is adopted on cable, aerial and mixed networks in any case of connection to earth and any kind of faults. It can be used only in case of RGDM, for its possibility to communicate with the primary station protection system by IEC 61650 protocol.

It allows the detection of the fault branch without re-closing cycle operation in primary station for any kind of faults.

Each RGDM is blocked by the corresponding downstream one. The RGDM, that doesn't receive the blocking signal, opens its DY800.

2 | Test set-up

In order to guarantee a correct operation, all the components introduced before must be calibrated. For this reason Gridspertise, a company of the Enel group which helps the DSO supporting the digitalization of the power grids, recreated the working condition of a secondary voltage substation equipped with RGDM in order to test sensors called smart termination in different conditions.

In this section the test set-up will be explained according to the sources: [3] [5] [6] [7] [8] [9] [10] [11] [14] [15].

2.1 The test bench layout

In this part of the thesis the set-up of the chain will be briefly shown, Figure 2.1, 2,2, in order to give a short idea of what will be deepened in the next sections. The goal of this test bench is to test the smart terminations (DJ5400, GSCC012), to guarantee a correct working condition.

To do that, current and voltage are generated in LV side by the same instrument, CMC 256plus. To respect all the working conditions, the current is increased by an amplifier, CMS 356.

Then both voltage and current signal are increased in MV side by the secondary substation thanks to voltage and current transformers, respectively CTV20 and RTA 36-2.

To verify the correct function of the smart terminations, two couple of sensors (the smart termination under test and the reference smart termination) are connected as in figure 2.3. To acquire and measure the signals smart terminations are equipped with Rogowski coil and voltage dividers.

The last part of the chain is the RGDM, TMPR, which receives and records the output data of smart terminations.

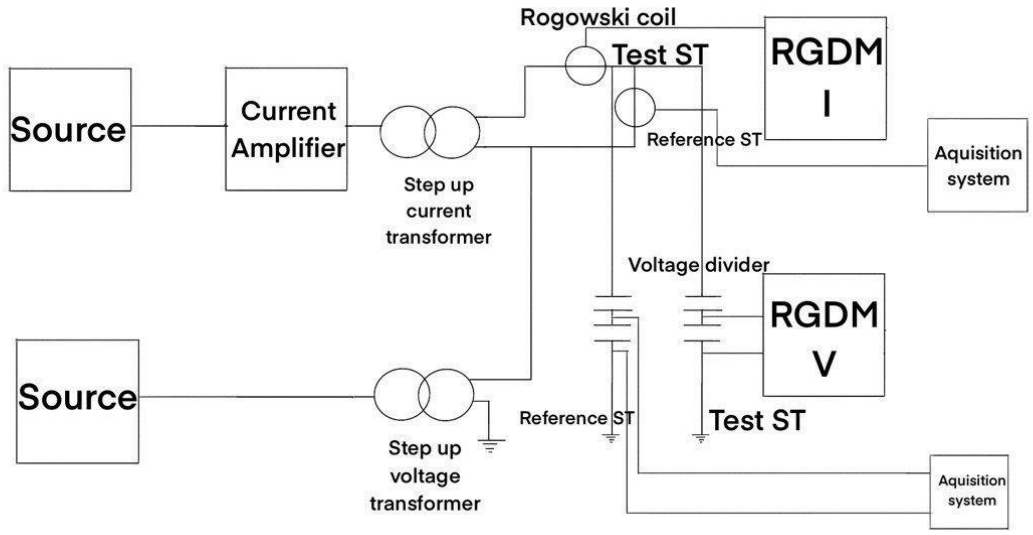

Figure 2. 1: Block diagram of the set-up chain

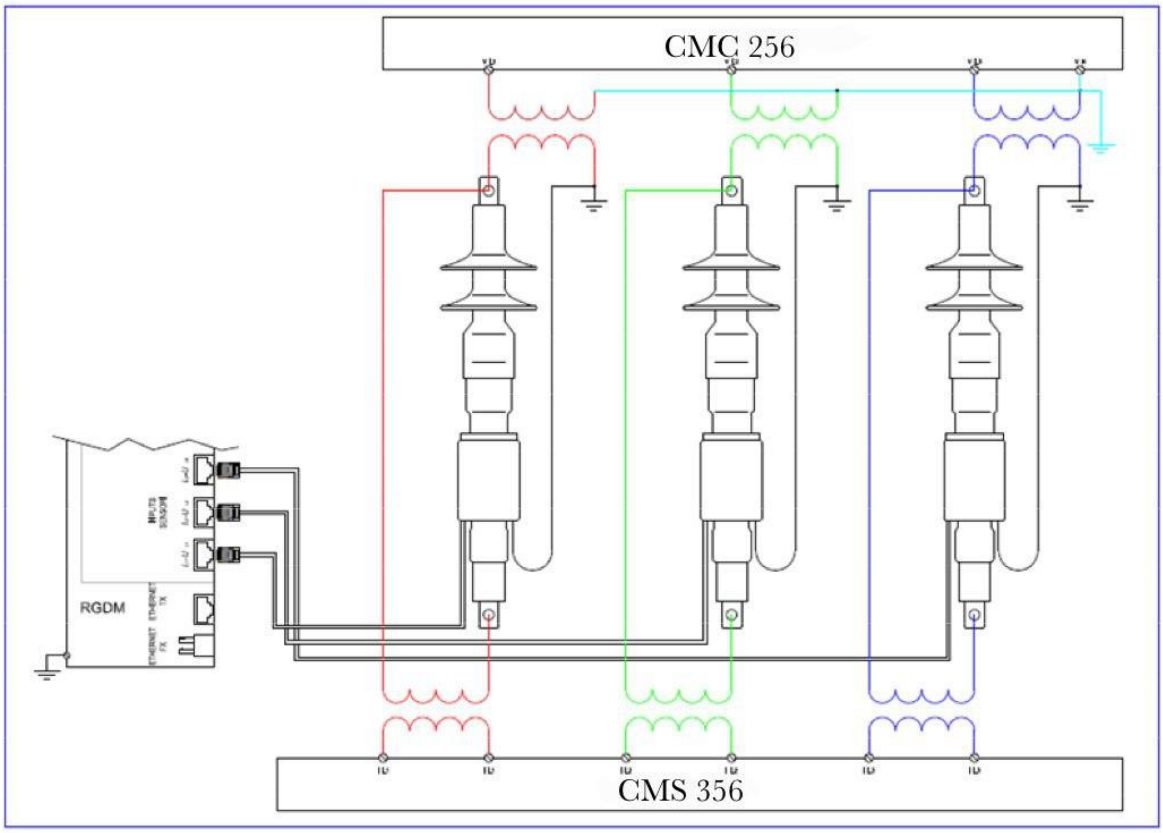

Figure 2. 2: Set-up scheme

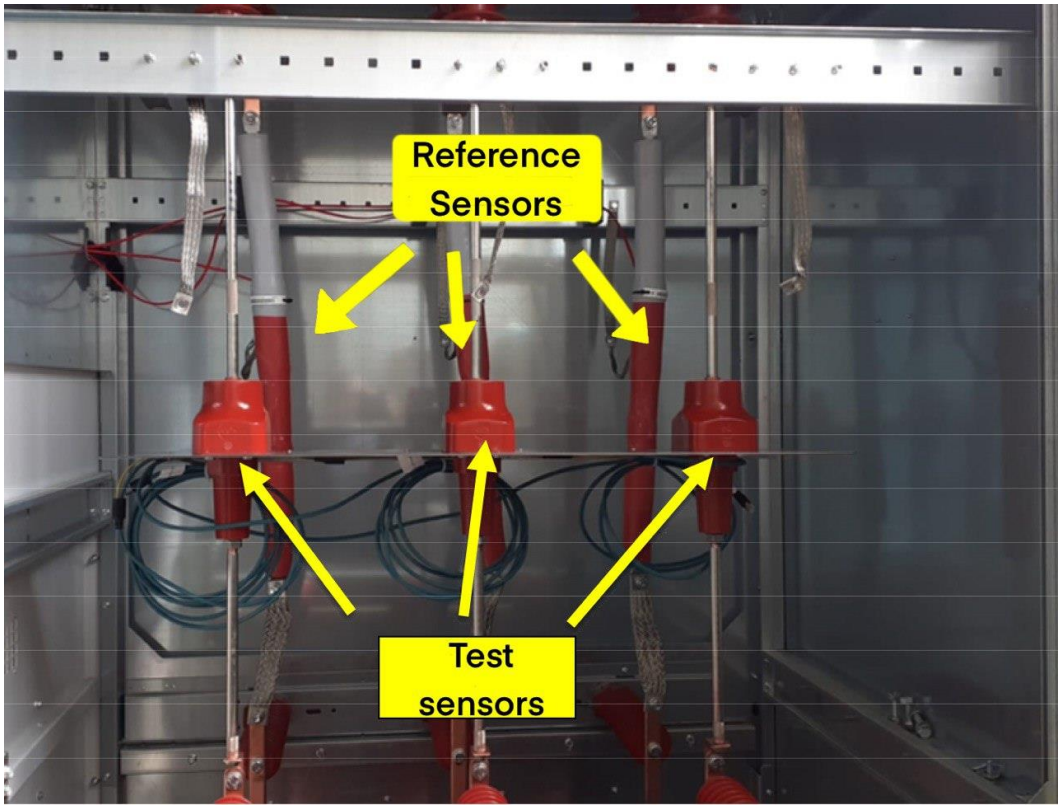

Figure 2.3: Test and reference sensors

2.2 The signal source CMC 256plus

The CMC 256plus is a computer-controlled test set used to generat 4 voltages and two galvanically separated current triples, Figure 2.3, 2.4 .

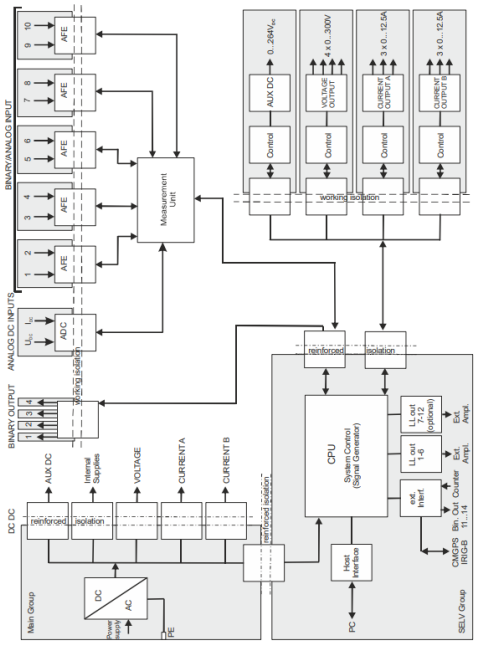

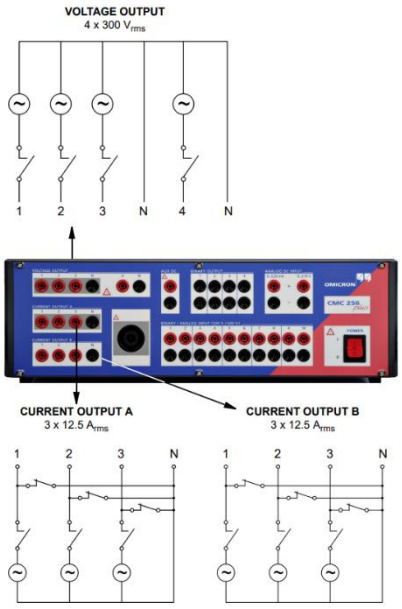

Figure 2. 3: Block diagram CMC 256 plus [8] Figure 2. 4: CMC 256 plus output interface [8]

The four voltage outputs have a common neutral N and are galvanically separated from all other outputs of the CMC 256plus. The two black sockets labeled "N" are galvanically connected with one another, Figure 2.5.

Figure 2. 5: CMC voltage output [8]

Two galvanically separated three-phase current outputs, each with their own neutral (N). Each output is galvanically separated from all other connections of the CMC 256plus.

It operates with a computer equipped with the OMICRON Test Universe software, where the input values are set.

Table 2.1 and 2.2 show the accuracy data of the instrument provider by the manufacturer:

2 x 3 Current Outputs[1] (Groups A and B)		
Output currents 3-phase AC (L-N) 1-phase AC (L-N)[2] DC (L-N)[2] DC (L-N)	3 x 0 ... 12.5 A 1 x 0 ... 37.5 A 1 x 0 ... ±17.5 A 1 x 0 ... ±12.5 A	
Power (range II)	Typical	Guaranteed
3-phase AC (L-N)	3 x 80 VA at 8.5 A	3 x 70 VA at 7.5 A
1-phase AC (L-N)[2]	1 x 240 VA at 25.5 A	1 x 210 VA at 22.5 A
1-phase AC (L-L)[3]	1 x 160 VA at 8.5 A	1 x 140 VA at 7.5 A
DC (L-N)[2]	1 x 240 W at ±17.5 A	1 x 235 W at ±17.5 A
DC (L-N)	1 x 100 W at ±12.5 A	1 x 90 W at ±12.5 A
Power (range I) 3-phase AC (L-N)		3 x 12.5 VA at 1.25 A
Accuracy (range II)	Typical	Guaranteed
$R_{load} \leq 0.5\ \Omega$	Error < 0.015 % rd.[4] + 0.005% of rg.	Error < 0.04 % of rd. + 0.01% of rg.
Accuracy (range I) $R_{load} \leq 1\ \Omega$	Error < 0.015 % of rd. + 0.005 % of rg.	Error < 0.04 % of rd. + 0.01 % of rg.
Harmonic distortion (THD+N)[5]	0.025 %	< 0.07 %
DC offset current range I range II	 < 30 µA < 300 µA	 < 300 µA < 3 mA
Current ranges	Range I: 0 ... 1.25 A Range II: 0 ... 12.5 A	
Resolution	< 50 µA (1.25 A range) < 500 µA (12.5 A range)	
Short-circuit protection	Unlimited to N	
Open-circuit protection	Open outputs (open-circuit) permitted	
Connection	4 mm/0.16 " banana connectors, amplifier connection socket[6] (CURRENT OUTPUT A	
Insulation	Reinforced insulation of power supply and all SELV interfaces	

Table 2. 1: Current output characteristic [8]

4 Voltage Outputs		
Output voltages 4-phase AC (L-N)[1] 1-phase AC (L-L) DC (L-N)	4 x 0 ... 300 V 1 x 0 ... 600 V 4 x 0 ... ± 300 V	
Output power[2]	Typical	Guaranteed
3-phase AC[3] 4-phase AC[4] 1-phase AC (L-N) 1-phase AC (L-L) DC (L-N)	3 x 100 VA at 100 ... 300 V 4 x 75 VA at 100 ... 300 V 1 x 200 VA at 100 ... 300 V 1 x 275 VA at 200 ... 600 V 1 x 420 W at 300 VDC	3 x 85 VA at 85 ... 300 V 4 x 50 VA at 85 ... 300 V 1 x 150 VA at 75 ... 300 V 1 x 250 VA at 200 ... 600 V 1 x 360 W at 300 VDC
Accuracy $R_{load} \geq 250\ \Omega$, U_{L-N} = 0...300V	Error < 0.015 % of rd.[5] + 0.005 % of rg.	Error < 0.04 % of rd. + 0.01 % of rg.
$R_{load} < 250\ \Omega$ $U_{L-N} \geq 30$ V $U_{L-N} < 30$ V	Error < 0.025 % of rd. Error < 10mV	Error < 0.1 % of rd. Error < 30mV
Harmonic distortion (THD+N)[6]	0.015 %	< 0.05 %
DC offset voltage	< 20 mV	< 100 mV
Voltage ranges	Range I: 0 ... 150 V Range II: 0 ... 300 V	
Frequency ranges[7]	sinusoidal signals 10 ... 1000 Hz harmonics/interharm.[8] 10 ... 3000 Hz transient signals DC ... 3.1 kHz	
Resolution	Range I: 5 mV Range II: 10 mV	
Short-circuit protect.	Unlimited for L - N	
Connection	4 mm/0.16 " banana connectors; amplifier connection socket V_{L1}-V_{L3}	
Insulation	Reinforced insulation of power supply and all SELV interfaces	

Table 2. 2: Voltage output characteristic [8]

2.3 The signal amplifier CMS 356

CMS 356, Figure 2.7 and 2.8, is a voltage and current amplifier used as one component in the setup to amplify the current generated by the CMC 256 plus, it receives as input 6 analog low level signals and sand two galvanically separated three-phase current outputs The input signals are filtered, sampled, and used for further digital signal generation for the power amplifiers

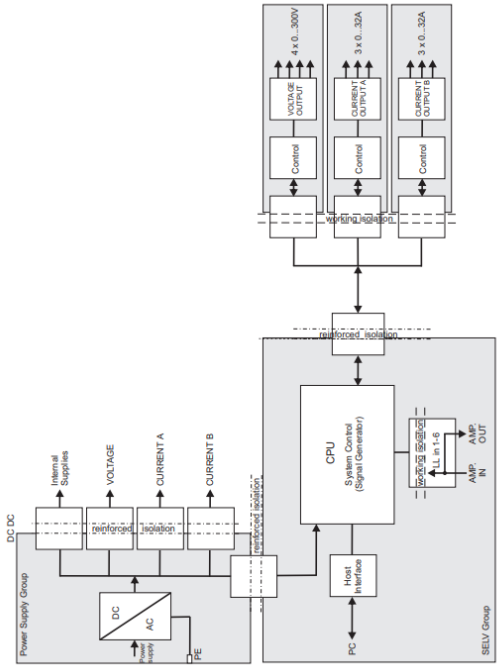

Figure 2. 7: CMS 356 block diagram [9]

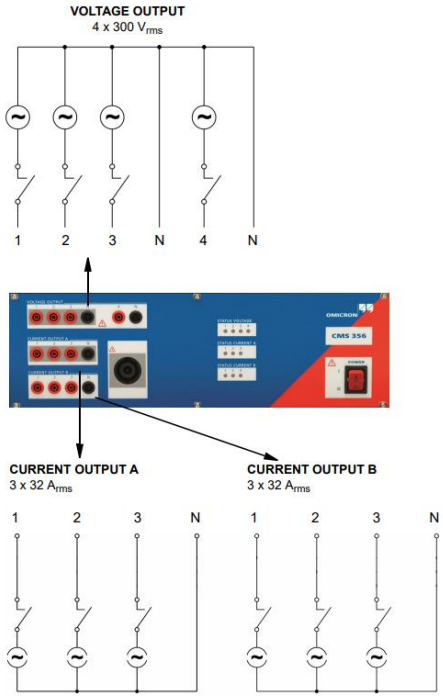

Figure 2. 8: CMS 356 output interface [9]

The table 2.3 shows the accuracy data of the instrument provider by the manufacturer::

Current Outputs[1] (Groups A and B)		
Output currents		
6-phase AC (L-N)	6 x 0 ... 32 A (Group A and B)	
3-phase AC (L-N)	3 x 0 ... 64 A (Group A + B parallel)	
2-phase AC (L-L)[2, 3]	2 x 0 ... 32 A (Group A and B)	
1-phase AC (L-L)[2, 3]	1 x 0 ... 64 A (Group A + B parallel)	
1-phase AC (L-L-L-L)[2, 3]	1 x 0 ... 32 A (Group A + B in series)	
2-phase AC (LL-LN)[2]	2 x 0 ... 64 A (Group A and B)	
1-phase AC (LL-LN)[2]	1 x 0 ... 128 A (Group A + B parallel)	
DC (LL-LN)[2]	1 x 0 ... ±180 A (Group A + B parallel)	
Power[7]	Typical	Guaranteed
6-phase AC (L-N)	6 x 430 VA at 25 A	6 x 250 W at 20 A
3-phase AC (L-N)	3 x 860 VA at 50 A	3 x 500 W at 40 A
2-phase AC (L-L)[2, 3]	2 x 870 VA at 25 A	2 x 550 W at 20 A
1-phase AC (L-L)[2, 3]	1 x 1740 VA at 50 A	1 x 1100 W at 40 A
1-phase AC (L-L-L-L)[2, 3]	1 x 1740 VA at 25 A	1 x 1100 W at 20 A
2-phase AC (LL-LN)[2]	2 x 500 VA at 40 A	2 x 350 W at 40 A
1-phase AC (LL-LN)[2]	1 x 1000 VA at 80 A	1 x 700 W at 80 A
DC (LL-LN)[2]	1 x 1400 W at ±80 A	1 x 1000 W at ±80 A
Accuracy	Typical	Guaranteed
$R_{load} \leq 0.5\ \Omega$	Error < 0.1 % rd.[4] + 0.04% of rg.	Error < 0.3 % of rd. + 0.1% of rg.
Harmonic distortion (THD+N)[5,6]	0.1 %	< 0.3 %
Phase error[5]	0.1 °	< 0.25 °
DC offset current	< 3 mA	< 10 mA
Resolution	1 mA, 2 mA (2 phases in parallel), ...	
Bandwidth (-3 dB)[8]	guaranteed: > 1 kHz typical: > 2.5 kHz[10]	
Propagation delay with input type "analog"	500 us (error < ± 2 us typ., ± 5 us guar.)	
Output delay with input type "Sampled Values"	Configurable, setting range[11]: 1000 – 6000 µs	
Short-circuit protection	Unlimited	

Table 2. 3: CMS 356 current output characteristic [9]

2.4 The step up voltage transformer CTV 20

In order to recreate a MV voltage triad a triad of inductive VTs, CTV 20 Figure 2.9, is used, obtaining a value in a range of 0-11 kV.

It receives from the generation side the voltage triad and send the increased values to the measuring side.

Figure 2. 9: CTV 20 [10]

The CTV 20 is a two pole transformer made according to the standard IEC 61869-1/3. It works with a nominal frequency of 50 Hz, or in case 60 Hz, with a rated voltage factor of 1,2, continuous, and a rated thermal duty of 500 VA.

It covers different classes of accuracy in base on the rated primary voltage, the secondary primary voltage and the number of ratios, single primary ratio, as in this case, or double ratio with switch secondary, Table 2.4 and 2.5.

After the definition of the accuracy class, the limits of the ratio and phase error introduced by the transformer can be obtained from the table 2.6 referred to the standard IEC 61869-3.

Rated primary Voltage (V)	Rated secondary Voltage (V)	Cl. 0,2 (VA)	Cl. 0,5 (VA)	Cl. 1 (VA)	Cl. 3 (VA)
Up to 20000	100 or 110	25	50	100	300

Table 2. 4 Accuracy class for CTV 20 in case of single primary ratio [10].

Rated primary Voltage (V)	Rated secondary Voltage (V)	Cl. 0,2 (VA)	Cl. 0,5 (VA)	Cl. 1 (VA)	Cl. 3 (VA)
Up to 10000/20000	100 or 110	10-20	25-50	50-100	150-300

Table 2. 5 Accuracy class for CTV 20 in case of double ratio with switch secondary [10].

Class	Voltage (ratio) error ε_u ±%	Phase displacement $\Delta\varphi$	
		±Minutes	±Centiradians
0,1	0,1	5	0,15
0,2	0,2	10	0,3
0,5	0,5	20	0,6
1,0	1,0	40	1,2
3,0	3,0	Not specified	Not specified

Table 2. 6 Limits of ratio error and phase error according to the standard IEC 61869-3

2.5 The step up current transformer RTA 36-2

In order to recreate a triad of high value currents a triad of inductive CTs are employed. The CTS installed in the test bench are the CT RTA 36-2 Figure 2.10. it is able to produce current values in the range from 0 A to 600 A.

It receives from the generation side the current triad and send the increased values to the measuring side through to the smart terminations.

Figure 2. 10: RTA 36-2 [11]

The RTA 36-2 is a double or triple core transformer complying with IEC 61869-1/2. It works with a nominal frequency of 50 Hz, or in case 60 Hz, and with normal secondary rated current of 5 A or 1 A.

It covers different classes of accuracy in base on the rated primary current and the number of ratios, single primary ratio, as in this case, double ratio with switch primary or double ratio with switch secondary, Table 2.7, 2.8 and 2.9.

After the definition of the accuracy class, the ratio and phase error introduced by the transformer can be obtained from the table 2.10 referred to the standard IEC 61869-2.

Rated primary current (A)	Cl. 0,2 Burden/ VA	Cl. 0,5 Burden/ VA	Cl. 1 Burden/ VA	Cl. 5P10 Burden/ VA
5-600	15	30	60	20
650-1250	20	50	100	30
1300-3000	20	50	100	30

Table 2. 7 Accuracy class for RTA 36-2 in case of single primary ratio [11]

Rated primary current (A)	Cl. 0,2 (VA)	Cl. 0,5 (VA)	Cl. 1 (VA)	Cl. 5P10 (VA)
Form 5-10 up to 300-600	15	30	60	20

Table 2. 8 Accuracy class for RTA 36-2 in case of double ratio with switch primary [11]

Rated primary current (A)	Cl. 0,2 (VA)	Cl. 0,5 (VA)	Cl. 1 (VA)	Cl. 5P10 (VA)
Form 350-750 up to 625-1250	10-20	20-40	40-80	15-30
Form 625-1250 up to 1500-3000	10-20	20-40	40-80	15-30

Table 2. 9 Accuracy class for RTA 36-2 in case of double ratio with switch secondary [11]

Accuracy class	Ratio error				Phase displacement							
	± %				± Minutes				± Centiradians			
	at current (% of rated)				at current (% of rated)				at current (% of rated)			
	5	20	100	120	5	20	100	120	5	20	100	120
0,1	0,4	0,2	0,1	0,1	15	8	5	5	0,45	0,24	0,15	0,15
0,2	0,75	0,35	0,2	0,2	30	15	10	10	0,9	0,45	0,3	0,3
0,5	1,5	0,75	0,5	0,5	90	45	30	30	2,7	1,35	0,9	0,9
1	3,0	1,5	1,0	1,0	180	90	60	60	5,4	2,7	1,8	1,8

Table 2. 10 Limits of ratio error and phase error according to the standard IEC 61869-2

2.6 Rogowski coil in the reference smart termination

The smart terminations, DJ5400, integrate a Rogowski coil for current measurement which is interfaced with the ENEL RGDM equipment.

It is a current to voltage transducer, it receives the current on MV side as input, that is converted in a voltage signal proportional to the measured current. The voltage signal is acquired and stored in the RGDM apparatus.

$$e(t) = M\frac{d\mathbf{i}}{dt} \tag{2. 1}$$

Where:

- i is the input current

- e is the output voltage

- M is the mutual inductance

For more specific details see [3].

Rogowski coil installed in the smart termination DJ5400 has a rated current transformation ratio, k_{sf} equals to (1000 A)/ (31 mV).

Since at rated frequency f_r it is:

$$|\underline{E}| = \frac{|\underline{I}|}{k_{sf}} \tag{2. 2}$$

According to the formula (2.1) it is:

$$|\underline{E}| = 2\pi f_r |\underline{I}| \tag{2. 4}$$

We derive the relationship between M and k_{sf} is

$$k_{sf} = \frac{1}{2\pi\, f_r\, M} \tag{2. 5}$$

With f_r considered as 50 Hz.

The accuracy class introduced by the Rogowski coil is declared in the document [5] referred to the standard IEC 61869-10, Table 2.11.

Accuracy class

0,5 S / 5P 10000 A. Summarization in following tables:

Accuracy class	Ratio error ε, $\varepsilon_{cor\,I}$ ± % at current					± phase error at primary current shown below: Minutes at current					Centiradians at current				
	$0{,}01\,I_{pr}$	$0{,}05\,I_{pr}$	$0{,}2\,I_{pr}$	I_{pr}	$K_{pcr} \times I_{pr}$	$0{,}01\,I_{pr}$	$0{,}05\,I_{pr}$	$0{,}2\,I_{pr}$	I_{pr}	$K_{pcr} \times I_{pr}$	$0{,}01\,I_{pr}$	$0{,}05\,I_{pr}$	$0{,}2\,I_{pr}$	I_{pr}	$K_{pcr} \times I_{pr}$
0,5 S	1,5	0,75	0,5	0,5	0,5	90	45	30	30	30	2,7	1,35	0,9	0,9	0,9

Accuracy class	± Ratio error at rated primary current ε, $\varepsilon_{cor\,I}$ in %	± Phase error at rated primary current: Minutes	Centiradians	Composite error at rated accuracy limit primary current ε_c, $\varepsilon_{cor\,I}$ in %	Maximum peak instantaneous error at rated primary short circuit current I_{psc} %
5P	1	60	1,8	5	-

Table 2. 11 Limits of ratio error and phase error considering a nominal current of 500 A [5]

2.7 Voltage dividers in the reference smart termination

The smart terminations, DJ5400, integrate voltage divider, Figure 2. 11, to measure voltage which is interfaced with the ENEL RGDM equipment.

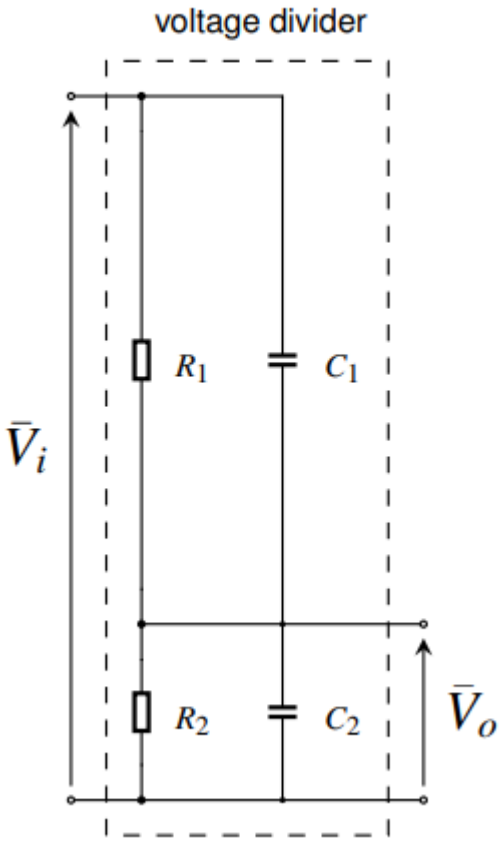

Figure 2. 11: Voltage divider [3]

The formula of the output voltage varies in case of DC, AC and AC with high frequency.

$$\bar{V}_0(\bar{s}) = \frac{R_2}{R_1 + R_2}\bar{V}_i(\bar{s}) \tag{2. 6}$$

$$\overline{V}_0(\bar{s}) = \frac{\frac{R_2}{(1+\bar{s}R_2C_2)}}{\frac{R_1}{(1+\bar{s}R_1C_1)} + \frac{R_2}{(1+\bar{s}R_2C_2)}}\overline{V}_i(\bar{s}) \tag{2. 7}$$

In case of high frequency $\bar{s}R_2C_2 \gg 1$ and $\bar{s}R_1C_1 \gg 1$ for this reason the formula can be rewrite in the following way:

$$\overline{V}_0(\bar{s}) = \frac{\frac{1}{\bar{s}C_2}}{\frac{1}{\bar{s}C_1} + \frac{1}{\bar{s}C_2}}\overline{V}_i(\bar{s}) \tag{2. 8}$$

Its nominal transformation ratio is equal to 10000.

The accuracy class introduced by the voltage instrument is declared in the document [5] referred to the standard IEC 61869-11, Table 2.12.

Accuracy class	Ratio error ε, $\varepsilon_{cor\ U}$ ± %					Phase error φ_e, $\varphi_{cor\ \varphi o}$									
						± minutes					± centiradiants				
	at voltage (% of rated)					at voltage (% of rated)					at voltage (% of rated)				
	2	20	80	100	F_v x100	2	20	80	100	F_v x100	2	20	80	100	F_v x100
1P	4	2	1	1	1	160	80	40	40	40	4,8	2,4	1,2	1,2	1,2

Table 2. 12 Limits of ratio error and phase error considering a nominal voltage between 6/√3 ÷ 34,5/√3 kV [5]

2.8 RGDM

The data acquisition from the reference smart termination is obtained using a specific RGDM unit, TMPR. RGDM acquires data from by Low Power Instrument Transformers (LPIT) that are integrated in reference Smart Termination (DJ5400, GSCC012), Figure 2.12 and 2.13.

The current sensor is completely insulated with respect to any part of the primary circuit.

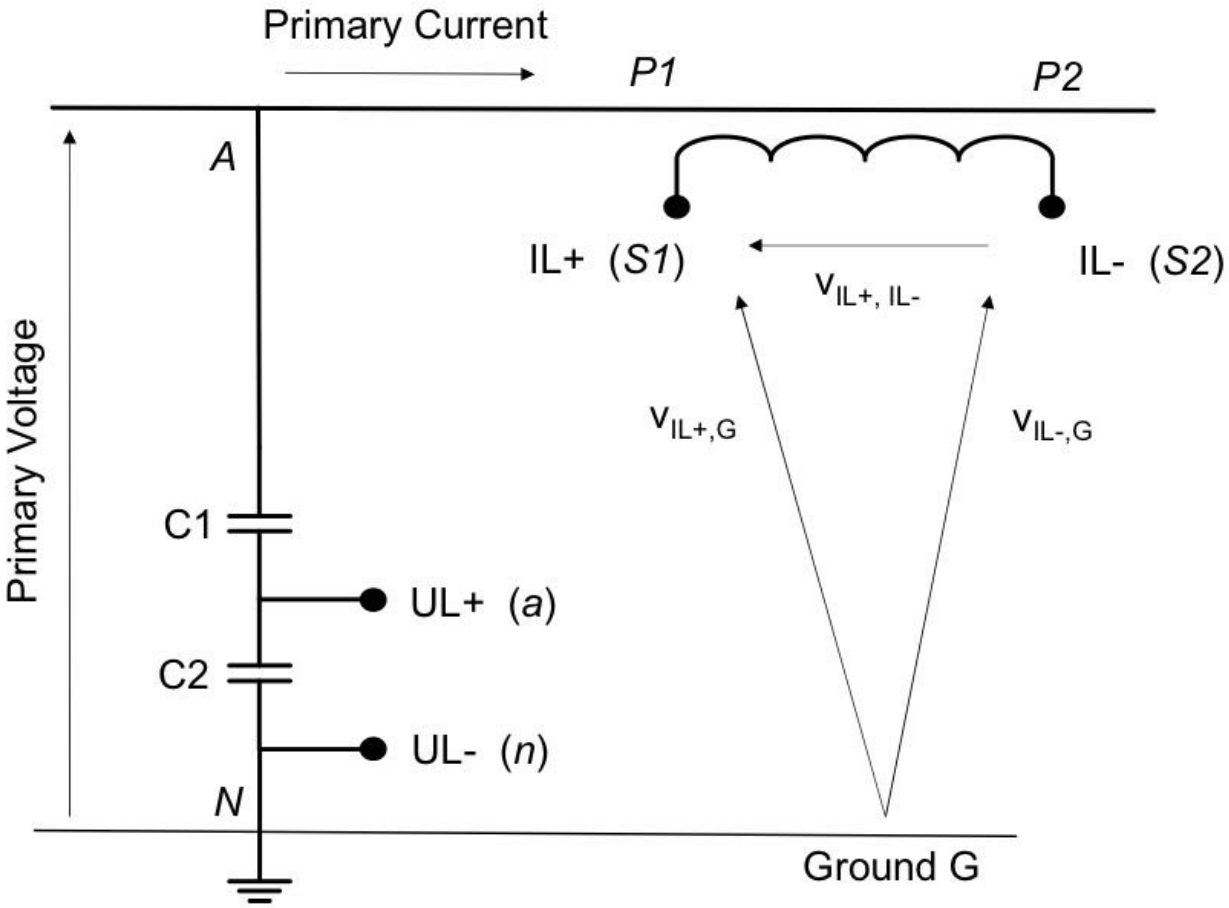

Figure 2. 12: General schema of an integrated low power voltage-current sensor [5]

With reference to Figure 2.12, to respect the correct operation of the protection system both open-circuit voltages $V_{IL+,G}$ and $V_{IL-,G}$ must be less than 10 mV, as Root Mean Square (RMS), in case of maximum voltage of equipment during a no load test, their values must go to zero when a resistive pull-down load is connected at least one wire of the current sensor and the ground. Overall the differential-mode voltage, $V_{IL+,IL-}$, must not be influenced by eventually transient.

Enel tests the LPCT, Figure 2.13, and LPVT, Figure 2.14, according to IEC 61869-10 and IEC 61869-11 standards, including the verification of deviation requirements, and performs also integration test, to guarantee the correct operation of the entire system. It consists on a series of tests like: accuracy level, sensor impedance measurement,

transient response, noise measurement, harmonic response, common-mode voltage and effect on the differential voltage test.

For more specific details see [15].

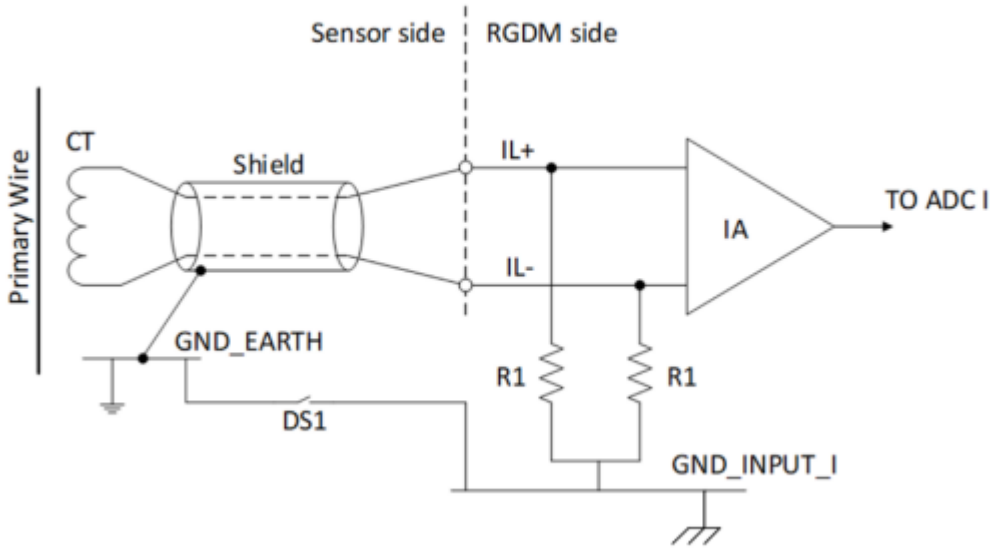

Figure 2. 13: Schematic principle for the current input [15]

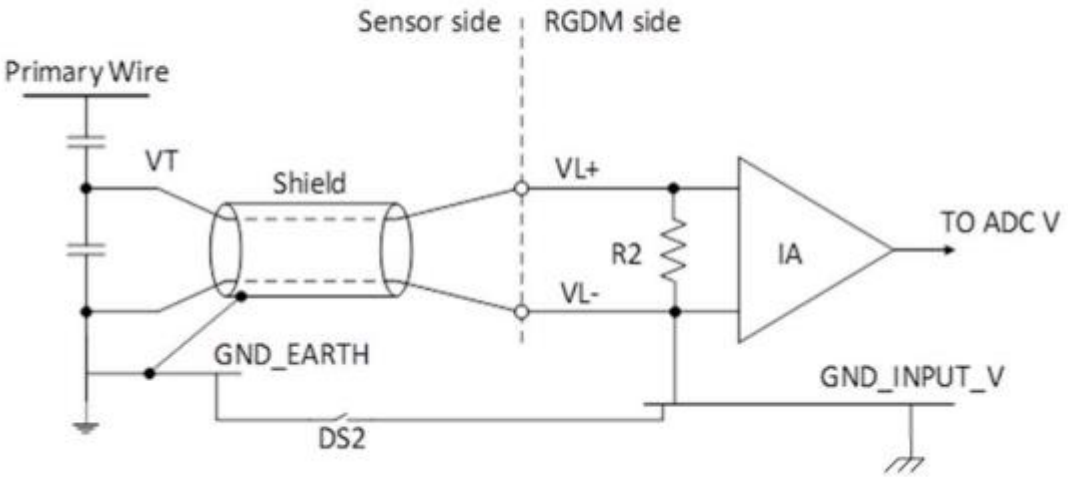

Figure 2. 14: Schematic principle for voltage input [15]

3| Calibration of the chain

After defining the entire chain, calibration is necessary to ensure compliance with all standards and to guarantee proper functioning conditions.

In this section, two different cases will be analysed. The first one is related to an unexpected phase shift between current and voltage signal. The second one is related to the estimation of error introduced by voltage and current transformers, CTV 20 and RTA 36-2.

3.1 First test case

Gridspertise reported a phase shift, around 11°, between the current and voltage signals acquired by the RGDM, Figure 3.1. This first test case investigates the origin of the unexpected phase shift that was compensated it manually.

This phenomenon is still present and constant for any kind of values of current and voltages.

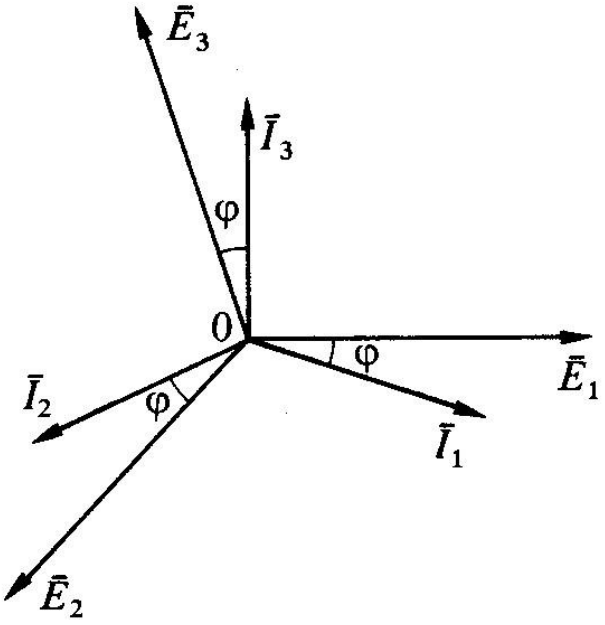

Figure 3. 1: Current and voltage output

In order to study this phenomenon, the measurement chain was split in three different parts to understand their contribution on the phase shift. The three parts are: the generation side, figure 3.2., the loop of the secondary station, figure 3.3. and the RGDM.

The plan to solve this problem involved a step-by-step process, analysing each cause separately. This approach would help determine if any part introduced a phase shift, if there was any correlation between the parts, and if any part could be excluded entirely.

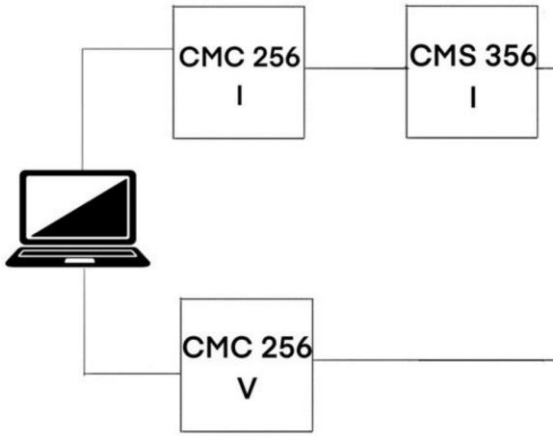

Figure 3. 2: Generation side

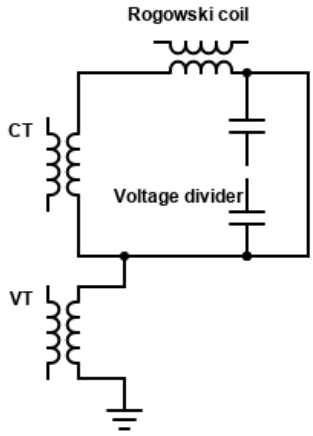

Figure 3. 3: Secondary substation loop

3.1.1 Laboratory test

In this section all the test are reported.

The first test is related to the generation side, Figure 3.2, and two different cases are distinguished. The first one with the MV secondary substation connected to the generator, like in the figure 2.1, and the second one without substation.

The idea is to understand if there is any kind of phase shift since the generation and if it is related or no to the load. For this reason the following set-up is recreated, Figure 3.4

For each case a voltage triad and a current triad are generated sending the input from the software Omicron Universe Test to the generator CMC 256 plus, figure 3.8. The current output goes to the CMS 356 amplifier, Figure 3.9, instead for the voltage the neutral and one single phase are acquired and connected to the junction box, figure 3.6.

The current output of the amplifier is acquired with an AC current clamp "FLUKE i200s", figure 3.7.

To acquire and analyse the wanted signals, a protection device, Figure 3.5, is used with the function of disturbance recorder, which guarantees the possibility to obtain the current and voltage behaviour in a variable time section.

It receives the voltage signals from a junction box and the current signal form AC current clamp, both signals are acquired simultaneously at different frequencies.

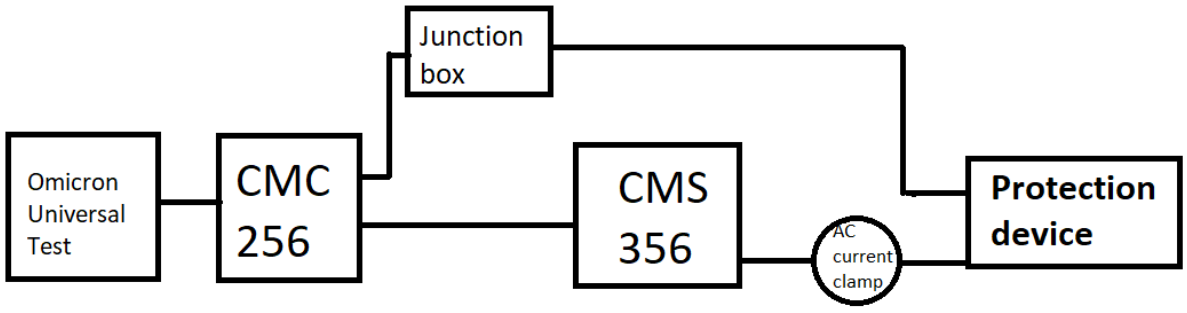

Figure 3. 4: Set-up block diagram

Figure 3. 5: Protection device

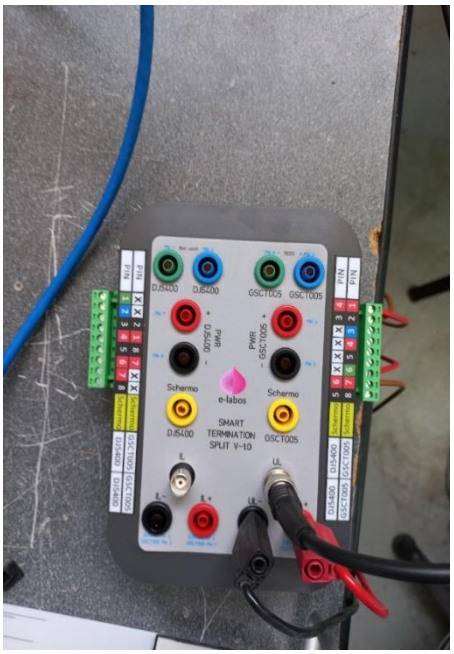

Figure 3. 6: Junction box

20A Range (i200s only)

Measuring range	0.1 to 24A
Maximum current	24A
Crest factor *	< 3
Maximum non-destructive current	200A (Frequency ≤ 1 kHz and crest factor < 3)
Output signal	100 mV/A
Output impedance	≤ 20 Ω @ 1 kHz
Basic accuracy	
48 Hz to 65 Hz	≤ 2% + 0.5A
Additional error:	
40 Hz to 48 Hz and 65 Hz to 1 kHz	+ < 10%
1 kHz to 10 kHz	+ < 15%
Phase shift	Unspecified

200A Range	i200	i200s
Measuring range	0.5 to 240A	0.5 to 240A
Maximum current	240A	240A
Crest factor *	< 3	< 3
Maximum non-destructive current	@ Frequency ≤ 1 kHz and crest factor < 3	
Continuous	200A	
10 min ON /30 min OFF	240A	
Output signal	1 mA/A	10 mV/A
Output impedance	-	≤ 10 Ω @ 1 kHz
Basic accuracy		
48 Hz to 65 Hz		
0.5A to 10A	≤ 3% + 0.5A	≤ 3.5% + 0.5A
10A to 40A	≤ 2.5% + 0.5A	≤ 3% + 0.5A
40A to 100A	≤ 2% + 0.5A	≤ 2.5% + 0.5A
100A to 240A	≤ 1% + 0.5A	≤ 1.5% + 0.5A
Additional error:		
40 Hz to 48 Hz and 65 Hz to 1 kHz	+ < 3%	+ < 3%
1 kHz to 10 kHz	+ < 12%	+ < 12%
Phase shift		
0.5A to 10A	Unspecified	Unspecified
10A to 40A	≤ 5 °	≤ 6 °
40A to 100A	≤ 3 °	≤ 4 °
100A to 240A	≤ 2.5 °	≤ 3 °

Figure 3. 7: AC current clamp and its accuracy range

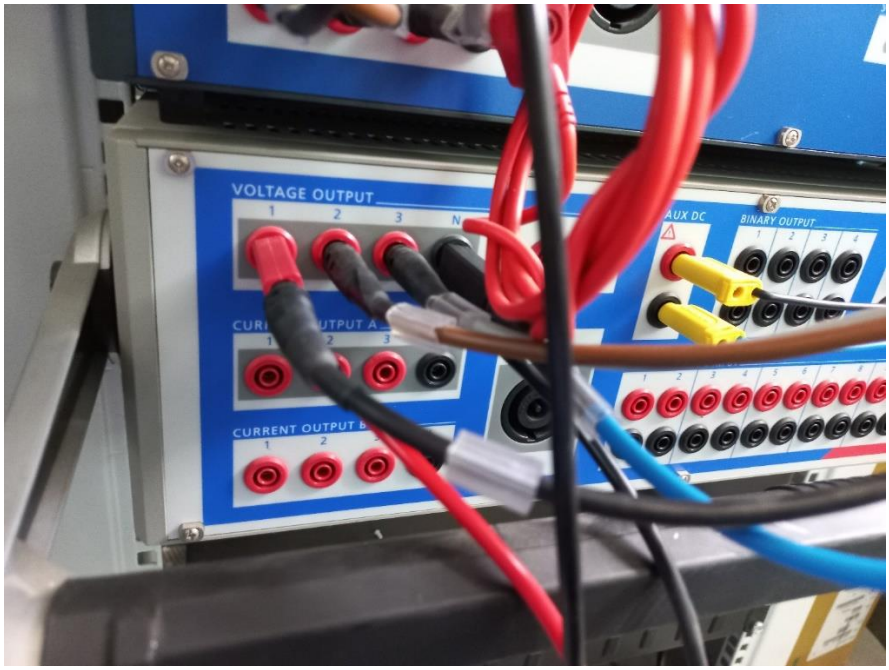

Figure 3. 8: CMC 256 plus voltage output

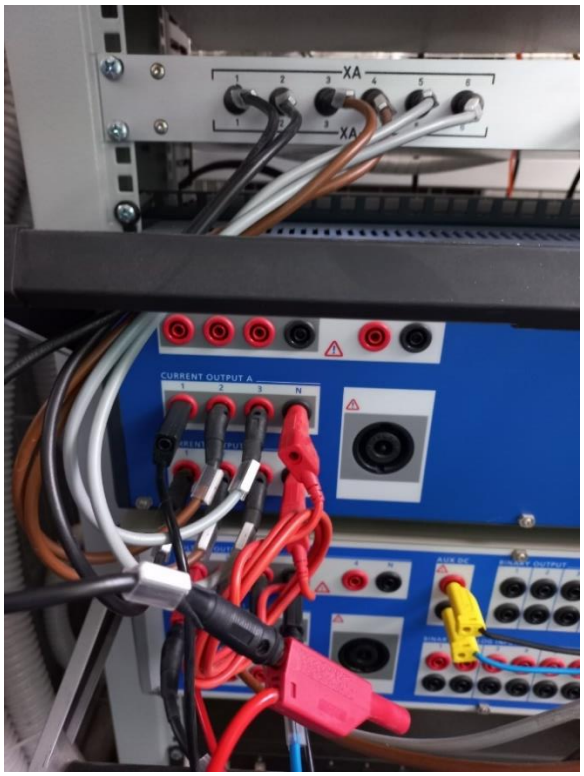

Figure 3. 9: CMS 356 current output

3.1.2 Result

The acquired current signal is recreated with the following formula:

$$i(t_K) = I_q \sin(2\pi f t_k) + I_d \cos(2\pi f t_k) \tag{3. 1}$$

While the voltage:

$$v(t_K) = V_q \sin(2\pi f t_k) + V_d \cos(2\pi f t_k) \tag{3. 2}$$

The x vector of unknown quantities can be expressed in the following way:

$$x = \begin{bmatrix} I_q \\ I_d \\ V_q \\ V_d \\ f \end{bmatrix} \tag{3. 3}$$

Where:

- I_q is the imaginary part of the current
- I_d is the real part of the current
- V_q is the imaginary part of the voltage
- V_d is the real part of the current
- f is the frequency

The data-measurands model vector $h(x)$ is organized in a 2Nx1 vector, with N is the number of samples.

$$h(x) = \begin{bmatrix} I_q \sin(\omega t_1) + I_d \cos(\omega t_1) \\ \vdots \\ I_q \sin(\omega t_N) + I_d \cos(\omega t_N) \\ V_q \sin(\omega t_1) + V_d \cos(\omega t_1) \\ \vdots \\ V_q \sin(\omega t_N) + V_d \cos(\omega t_N) \end{bmatrix} \tag{3. 4}$$

The acquired data are placed in the vector y as shown in the equation below:

$$y = \begin{bmatrix} i(t_1) \\ \vdots \\ i(t_N) \\ v(t_1) \\ \vdots \\ v(t_N) \end{bmatrix} \tag{3. 5}$$

Where:

$$y = h(x) + e_y \tag{3. 6}$$

With e_y, the error between the estimated data and the acquired data.

The Jacobian matrix A of h(x) with respect to x is the following 2Nx5 matrix:

$$A = \frac{dh_k(x)}{dx_i} =$$

$$= \begin{vmatrix} sin(2\pi f t_1) & cos(2\pi f t_1) & 0 & 0 & 2\pi f \cdot \left(I_q cos(2\pi f t_1) - I_d sin(2\pi f t_1)\right) \\ \vdots & \vdots & \vdots & \vdots & \vdots \\ sin(2\pi f t_N) & cos(2\pi f t_N) & 0 & 0 & 2\pi f \cdot \left(I_q cos(2\pi f t_N) - I_d sin(2\pi f t_N)\right) \\ 0 & 0 & sin(2\pi f t_1) & cos(2\pi f t_N) & 2\pi f \cdot \left(V_q cos(2\pi f t_1) - V_d sin(2\pi f t_1)\right) \\ \vdots & \vdots & \vdots & \vdots & \vdots \\ 0 & 0 & sin(2\pi f t_N) & cos(2\pi f t_N) & 2\pi f \cdot \left(V_q cos(2\pi f t_N) - V_d sin(2\pi f t_N)\right) \end{vmatrix} \tag{3. 7}$$

The x vector can be estimated with the non-linear least-square estimation:

$$\tilde{x}_{NLS}^{k+1} = \tilde{x}_{NLS}^{k} + [A(\tilde{x}_{NLS}^{k})^T \cdot R_y^{-1} \cdot A(\tilde{x}_{NLS}^{k})]^{-1} \cdot A(\tilde{x}_{NLS}^{k}) \cdot R_y^{-1} \cdot [y - h(\tilde{x}_{NLS}^{k})] \tag{3. 8}$$

Where $\tilde{x}_{NLS}^{k}$ is the estimate of the recursive number k

For the first iteration the vector x was initialized with f as the rated frequency, I_d and V_d as zero, I_q and V_q as the max value of the signal.

The initialized and estimated values can be observed in the appendix at the table A.1 and A.2.

The measured data error covariance matrix R is assumed as diagonal:

$$R = \begin{bmatrix} \sigma^2 & \cdots & 0 \\ \vdots & \ddots & \vdots \\ 0 & \cdots & \sigma^2 \end{bmatrix} \tag{3. 9}$$

Where σ^2 is the variances of the measured data error e_y

$$\sigma^2 = var\big(y - h(x)\big) \tag{3. 20}$$

Once computed the Non-linear least-square estimates of x, (3.8), the values of the voltage and current phases are derived as:

$$\varphi_v = \arctan\left(\frac{V_q}{V_d}\right) \tag{3. 11}$$

$$\varphi_i = \arctan\left(\frac{I_q}{I_d}\right) \tag{3. 12}$$

The phase shift can be estimated as:

$$\Delta\varphi = \varphi_v - \varphi_i \tag{3. 13}$$

And the time delay:

$$\Delta T = \frac{\Delta\varphi}{f \cdot 2 \cdot \pi} \tag{3. 34}$$

For what concern the variance of the time variation, it can be estimated with the following formula:

$$\sigma^2 = J \cdot P \cdot J'$$

(3. 15)

Where:

- J is the Jacobian of the formula (3.14) respect to the vector (3.5)

$$J = \begin{vmatrix} -\frac{1}{f \cdot 2 \cdot \pi} \cdot \frac{1}{1 + \left(\frac{I_q}{I_d}\right)^2} \cdot \frac{1}{I_d} \\ \frac{1}{f \cdot 2 \cdot \pi} \cdot \frac{1}{1 + \left(\frac{I_q}{I_d}\right)^2} \cdot \frac{I_q}{{I_d}^2} \\ \frac{1}{f \cdot 2 \cdot \pi} \cdot \frac{1}{1 + \left(\frac{V_q}{V_d}\right)^2} \cdot \frac{1}{V_d} \\ -\frac{1}{f \cdot 2 \cdot \pi} \cdot \frac{1}{1 + \left(\frac{V_q}{V_d}\right)^2} \cdot \frac{V_q}{{V_d}^2} \\ -\frac{\arctan\left(\frac{I_q}{I_d}\right) - \arctan\left(\frac{V_q}{V_d}\right)}{f^2 \cdot 2 \cdot \pi} \end{vmatrix}$$

(3. 16)

- P is the matrix of variance and covariance obtained in the following way:

$$P = (A \cdot R^{-1} \cdot A')^{-1}$$

(3. 17)

With A derived with the formula (3.7) and R obtained with the formula (3.9).

Instead, for what concern the variance of the phase shift, it can be estimated with the formula (3.15) where J stands for the Jacobian of the formula (3.13) respect to first four quantities of the vector x (3.3).

For this reason the Jacobian vector J will be:

$$J = \begin{vmatrix} -\cdot\dfrac{1}{1+\left(\dfrac{I_q}{I_d}\right)^2}\cdot\dfrac{1}{I_d} \\ \cdot\dfrac{1}{1+\left(\dfrac{I_q}{I_d}\right)^2}\cdot\dfrac{I_q}{{I_d}^2} \\ \cdot\dfrac{1}{1+\left(\dfrac{V_q}{V_d}\right)^2}\cdot\dfrac{1}{V_d} \\ -\cdot\dfrac{1}{1+\left(\dfrac{V_q}{V_d}\right)^2}\cdot\dfrac{V_q}{{V_d}^2} \end{vmatrix} \tag{3. 18}$$

And the Jacobian matrix A will be:

$$A = \begin{vmatrix} sin(2\pi f t_1) & cos(2\pi f t_1) & 0 & 0 \\ \vdots & \vdots & \vdots & \vdots \\ sin(2\pi f t_N) & cos(2\pi f t_N) & 0 & 0 \\ 0 & 0 & sin(2\pi f t_1) & cos(2\pi f t_N) \\ \vdots & \vdots & \vdots & \vdots \\ 0 & 0 & sin(2\pi f t_N) & cos(2\pi f t_N) \end{vmatrix} \tag{3. 19}$$

In this part of the thesis the result of the first test case will be briefly shown. In the Table 3.1, the phase shift and the time delay are reported for any frequency and for any condition.

Secondary Substation	f	$\varphi_v - \varphi_i$	ΔT
Connected	50 Hz	10,71(2) °	595(1) μs
Connected	60 Hz	11,28(3) °	522(2) μs
Disconnected	50 Hz	8,83(3)°	491(2) μs
Disconnected	60 Hz	9,81(3)°	454(2) μs
Disconnected	100 Hz	14,45(3)°	401(1) μs
Disconnected	200 Hz	27,38(4)°	380,3(5) μs

Table 3. 1 Estimated values of frequency shift and time variation

Looking at Table 3.1, it can be observed that the phenomenon is not a phase shift, as originally thought, but rather a time delay. The delay falls within a range of 500 μs for all cases, but it is not constant. The most probable cause of this delay is a lack of synchronization between the generator and amplifier, which imposes a random delay for each individual case. Therefore, it isn't impossible to derive a mathematical law to predict the delay for any specific case. However, this study has obtained more specific values of the delay, Figure 3.13, which can be used to compensate more accurately.

Another thing to note is that the entire delay is present from the generation stage. Therefore, the loop of the secondary substation and the RGDM can be excluded as causes of this delay.

Contrary to what Gridspertise had initially assumed, the current is not leading respect to the voltage, as shown in Figures 3.10 and 3.11. Instead, it is lagging, as shown in Figures from 3.12.

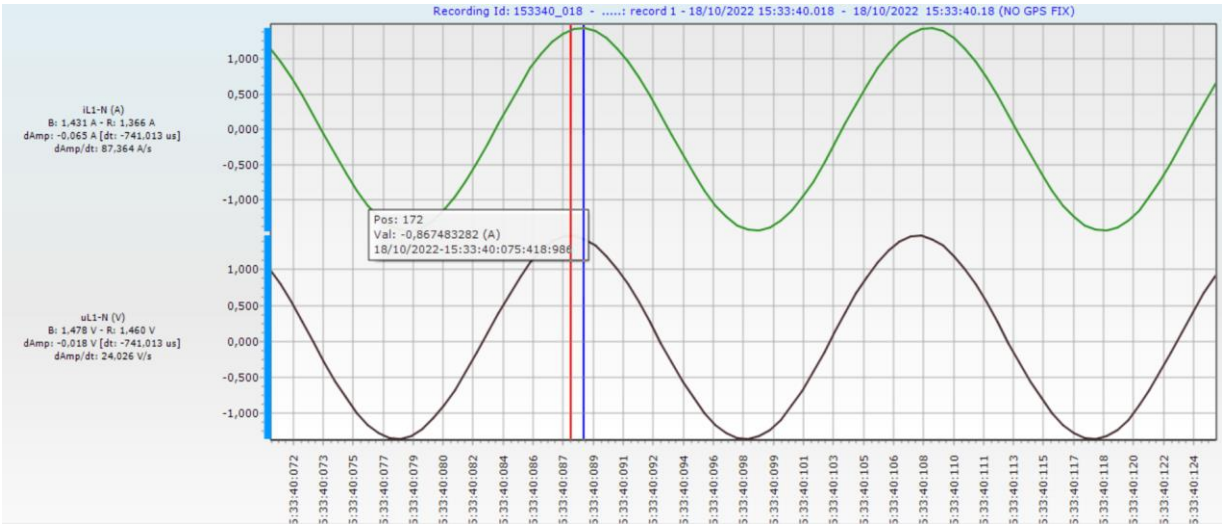

Figure 3. 10: Current and voltage behavior acquired by the disturbance recorder at 50 Hz

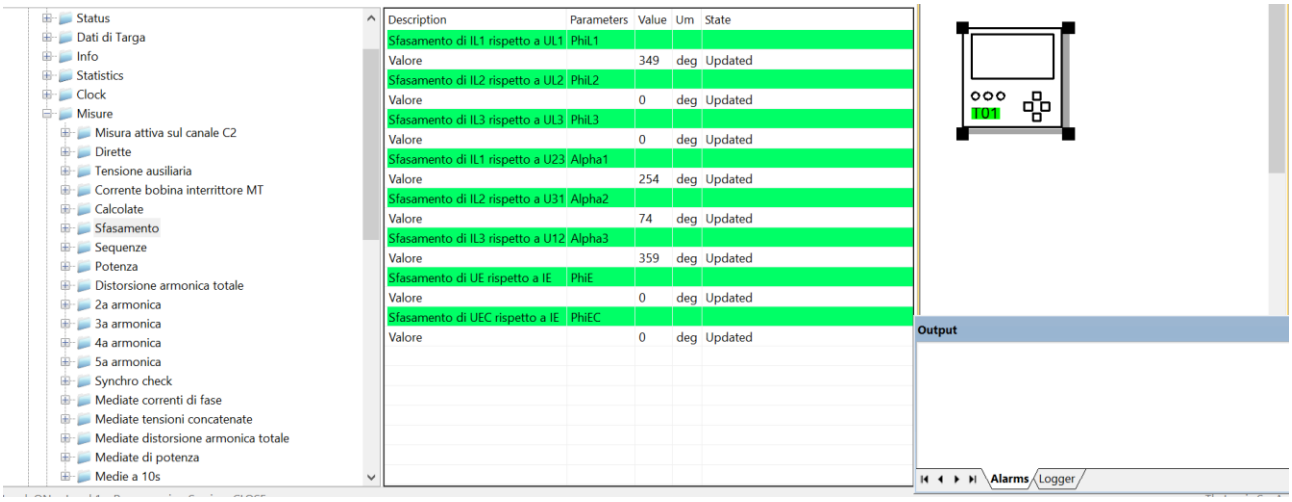

Figure 3. 11: Data acquired by protection panel at 50 Hz

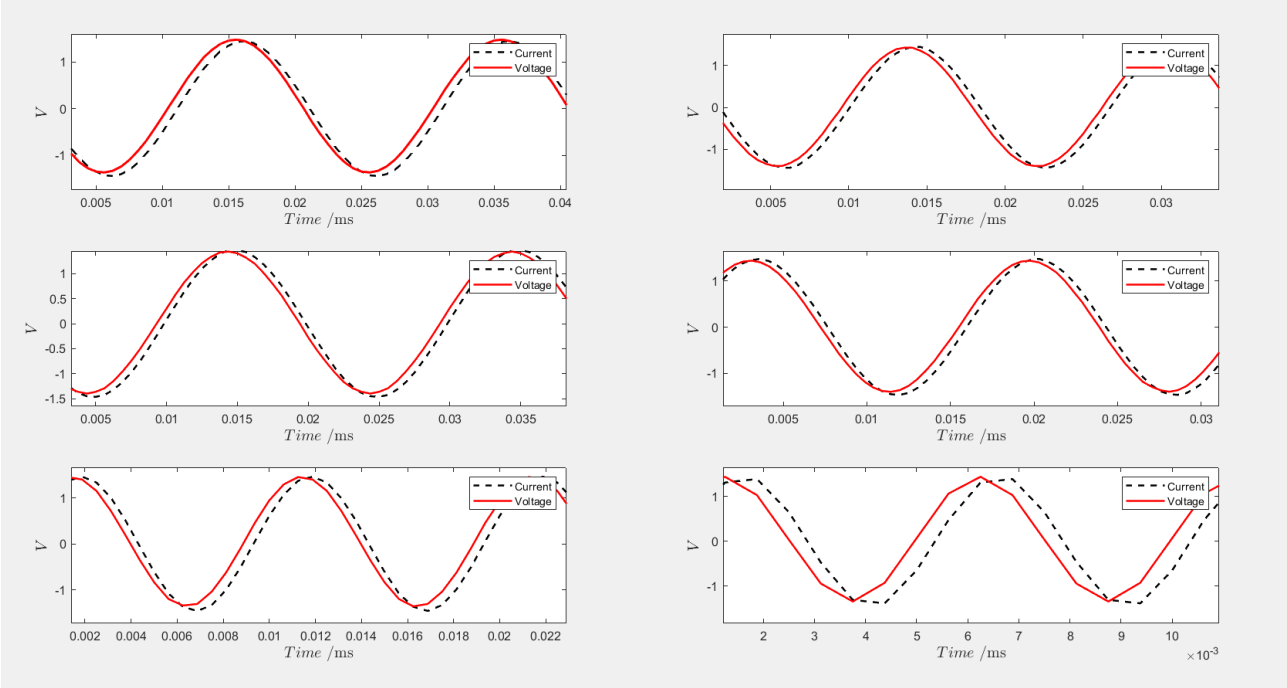

Figure 3. 12: Voltage and current signals for each single case from the first one to the last one clockwise, all the plots can be found in the appendix in the figure from A.1 to A.6.

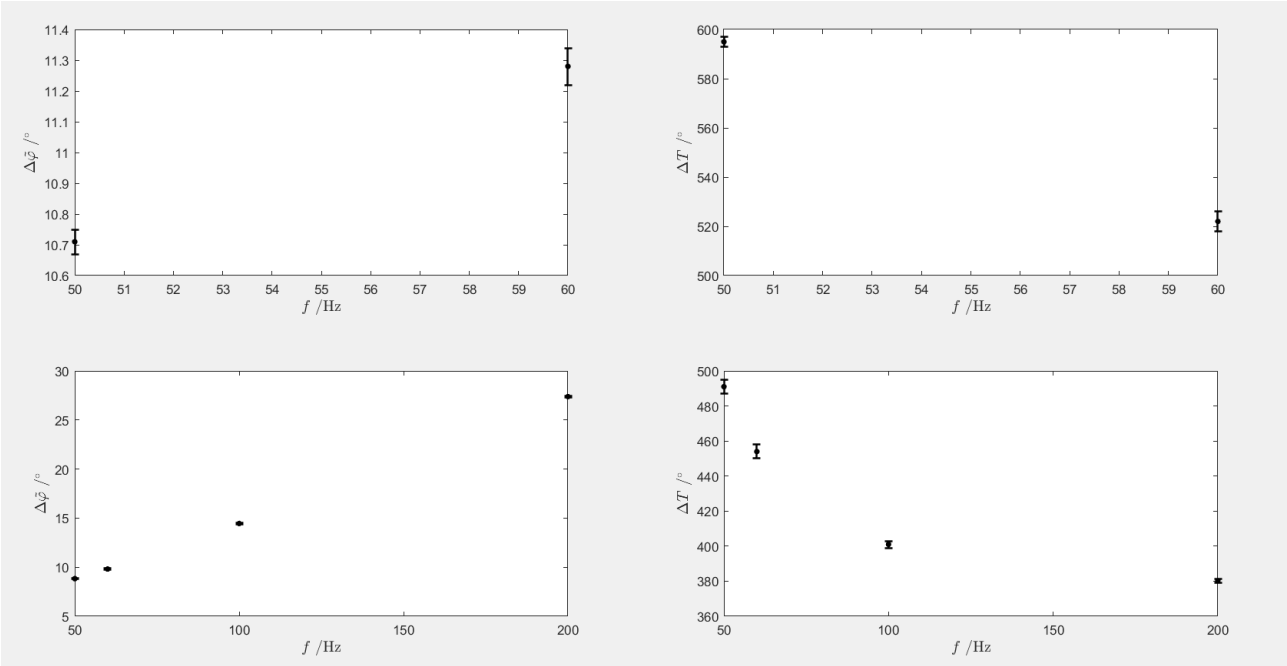

Figure 3. 13: Plots of the results in the Table 3.1, each single plot is present in the appendix, Figure from A.7 to A.10

3.2 Second test case

The second point of this thesis is the estimation of the error introduced by the voltage and current transformers for each possible condition. This is due to the working conditions which don't respect the accuracy range of the transformers reported in the tables (2.4) (2.7).

The procedure to solve this problem is similar to the previous one. First a laboratory test is done in order to collect the wanted data and after that an analysis on Matlab was implemented.

3.2.1 Laboratory test

The idea of this test is to collect the current and voltage signal at the output of the generation side, output of the generator for the voltage and output of the amplifier for the current, and at the input of the RGDM, output of the Rogowski coil for the current and output of the voltage divider for the voltage.

For a practical reason, related to the number of instruments, this work is done for one single phase.

To collect and see the signal a scopemeter, FLUKE 190-204, is used, Figure 3.14 and Table 3.2.

Figure 3. 14: Scopemeter, FLUKE 190-204

Oscilloscope

Isolated Inputs A,B, C and D (Vertical)

Number of Channels
- Fluke 190-xx2 ..... 2 (A, B)
- Fluke 190-xx4 ..... 4 (A,B,C,D)

Bandwidth, DC Coupled
- FLUKE 190-502 ..... 500 MHz (-3 dB)
- FLUKE 190-2xx ..... 200 MHz (-3 dB)
- FLUKE 190-1xx ..... 100 MHz (-3 dB)
- FLUKE 190-062 ..... 60 MHz (-3 dB)

Lower Frequency Limit, AC Coupled
- with 10:1 probe ..... <2 Hz (-3 dB)
- direct (1:1) ..... <5 Hz (-3 dB)

Rise Time
- FLUKE 190-502 ..... 0.7 ns
- FLUKE 190-2xx ..... 1.7 ns
- FLUKE 190-1xx ..... 3.5 ns
- FLUKE 190-062 ..... 5.8 ns

Analog Bandwidth Limiters ..... 20 MHz and 20 kHz

Input Coupling ..... AC, DC

Polarity ..... Normal, Inverted

Sensitivity Ranges
- with 10:1 probe ..... 20 mV to 1000 V/div
- direct (1:1) ..... 2 mV to 100 V/div

Dynamic Range ..... > ±8 div (< 10 MHz)
..... > ±4 div (> 10 MHz)

Trace Positioning Range ..... ±4 divisions

Input Impedance on BNC
- DC Coupled ..... 1 MΩ (±1 %)//14 pF (±2 pF)

⚠ Max. Input Voltage
For detailed specifications, see "Safety" on page 125

Vertical Accuracy ..... ±(2.1 % + 0.04 range/div)
2 mV/div: ..... ±(2.9 % + 0.08 range/div)
For voltage measurements with 10:1 probe, add probe accuracy, see section '10:1 Probe' on page 127

Digitizer Resolution ..... 8 bits, separate digitizer for each input

Horizontal

Minimum Time Base Speed (Scope Record) ..... 2 min/div

Real Time Sampling Rate

FLUKE 190-502
- 2 ns to 4 µs /div (2 channels) ..... up to 2.5 GS/s
- 2 ns to 4 µs /div (1 channel) ..... up to 5 GS/s
- 10 µs to 120 s/div ..... 125 MS/s

FLUKE190-202,-204:
- 2 ns to 4 µs /div (1 or 2 channels) ..... up to 2.5 GS/s
- 2 ns to 4 µs /div (3 or 4 channels) ..... up to 1.25 GS/s
- 10 µs to 120 s/div ..... 125 MS/s

Table 3. 2: Scopemeter FLUKE 190-204 characteristic

It receives the first voltage signal from the generation with a simple cable trough a junction box, Figure 3.6.

Instead the first current signal is acquired thanks to an AC Current Clamp, FLUKE i200s, figure 3.7.

For what concerns the other signals the outputs of the smart terminations are removed from the RGDM and are insert in the junction box in order to use compatible cables for the scopemeter, Figure 3.15.

At this point two kind of test are done, the first one varying the current and keeping the voltage constant and the second one varying the voltage and keeping the current constant.

The values are chosen in accord to the Tables 2.11 and 2.12.

For the test with a variable current the fixed value of voltage is 3464 V and the nominal value of the current is 500 A, both values are referred to the MV side.

For the test with a variable current the fixed value of current is 300 A and the nominal value of the voltage is 11 kV, both values are referred to the MV side.

Figure 3. 15: Junction box which receives the output of the smart termination

3.2.2 Result

The analysis of the data is done considering separately the two cases. The first one is the case with variable voltage and fixed current, the equivalent circuit of the voltage side is represented in the figure 3.16:

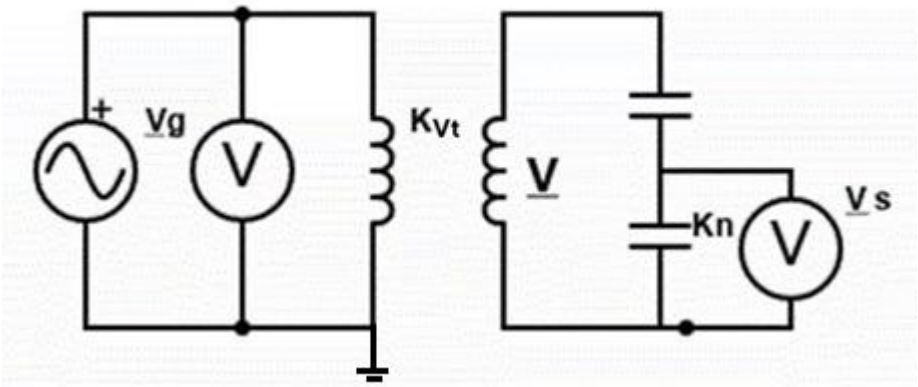

Figure 3. 16: Voltage side equivalent circuit

With:

$$\underline{V} = K_{VT}\underline{V}_g = K_N\underline{V}_s \tag{3. 20}$$

Where:

- $\underline{V}_g$ the voltage acquired from the generator
- $\underline{V}_s$ the voltage acquired by the smart termination
- $\underline{V}$ the voltage at medium voltage side
- K_N is the nominal transformation ratio of the voltage divider
- K_{VT} is the nominal transformation ratio of voltage transformer

In order to estimate the voltage signals, the Non-linear Least-square estimation, (3.8), is adopted.

The voltage acquired from the generator is recreated with the following formula

$$V_{gen}(t_K) = V_{q,gen}\sin(2\pi f t_k) + V_{d,gen}\cos(2\pi f t_k) \tag{3. 21}$$

The x vector of unknown quantities can be expressed in the following way:

$$x_{gen} = \begin{bmatrix} V_{q,gen} \\ V_{d.gen} \\ f \end{bmatrix} \tag{3. 22}$$

Where:

- $V_{q,gen}$ is the imaginary part of the voltage
- $V_{d,gen}$ is the real part of the current
- f is the frequency

The data-measurands model vector $h(x)$ is organized in a Nx1 vector, with N is the number of samples.

$$h_{gen}(x) = \begin{bmatrix} V_{q,gen}\sin(\omega t_1) + V_{d,gen}\cos(\omega t_1) \\ \vdots \\ V_{q,gen}\sin(\omega t_N) + V_{d,gen}\cos(\omega t_N) \end{bmatrix} \tag{3. 23}$$

The acquired data are placed in the vector y as shown in the equation below:

$$y_{gen} = \begin{bmatrix} V_{gen}(t_1) \\ \vdots \\ V_{gen}(t_N) \end{bmatrix} \tag{3. 24).}$$

The Jacobian matrix A of h(x) with respect to x is the following Nx3 matrix:

$$A = \begin{vmatrix} sin(2\pi f t_1) & cos(2\pi f t_1) & 2\pi f \cdot \left(V_{q,gen}cos(2\pi f t_1) - V_{d,gen}sin(2\pi f t_1)\right) \\ \vdots & \vdots & \vdots \\ sin(2\pi f t_N) & cos(2\pi f t_N) & 2\pi f \cdot \left(V_{q,gen}cos(2\pi f t_N) - V_{d,gen}sin(2\pi f t_N)\right) \end{vmatrix} \tag{3. 25}$$

The x vector can be estimated with the Non-linear Least-square estimation, (3.8)

For the first iteration the vector x was initialized with f as the rated frequency, $50\ Hz$, $V_{d,gen}$ as zero and $V_{q,gen}$ as the max value of the signal.

The initialized and estimated values can be observed in the appendix at the table A.3 and A.4.

Once computed the Non-linear least-square estimates of x, the values of the voltage phase and of the voltage module are derived as:

$$\varphi_{v,gen} = \arctan\left(\frac{V_{q,gen}}{V_{d,gen}}\right) \tag{3. 26}$$

$$|\underline{V}_g| = \sqrt{{V_{q,gen}}^2 + {V_{d,gen}}^2} \tag{3. 27}$$

This process can be repeated for the voltage acquired from the sensor, that is recreated with the following formula

$$V_{sen}(t_K) = V_{q,sen}\sin(2\pi f t_k) + V_{d,sen}\cos(2\pi f t_k) \tag{3. 28}$$

The x vector of unknown quantities can be expressed in the following way:

$$x_{sen} = \begin{bmatrix} V_{q,sen} \\ V_{d.sen} \\ f \end{bmatrix} \tag{3. 29}$$

Where:

- $V_{q,gen}$ is the imaginary part of the voltage
- $V_{d,gen}$ is the real part of the current
- f is the frequency

The data-measurands model vector $h(x)$ is organized in a Nx1 vector, with N is the number of samples.

$$h_{sen}(x) = \begin{bmatrix} V_{q,sen}\sin(\omega t_1) + V_{d,sen}\cos(\omega t_1) \\ \vdots \\ V_{q,sen}\sin(\omega t_N) + V_{d,sen}\cos(\omega t_N) \end{bmatrix} \tag{3. 30}$$

The data vector y is:

$$y_{sen} = \begin{bmatrix} v_{sen}(t_1) \\ \vdots \\ v_{sen}(t_N) \end{bmatrix}$$

(3. 31)

The Jacobian matrix A of h(x) with respect to x is the following Nx3 matrix:

$$A = \begin{vmatrix} sin(2\pi f t_1) & cos(2\pi f t_1) & 2\pi f \cdot \left(V_{q,sen} cos(2\pi f t_1) - V_{d,sen} sin(2\pi f t_1)\right) \\ \vdots & \vdots & \vdots \\ sin(2\pi f t_N) & cos(2\pi f t_N) & 2\pi f \cdot \left(V_{q,sen} cos(2\pi f t_N) - V_{d,sen} sin(2\pi f t_N)\right) \end{vmatrix}$$

(3. 32)

For the first iteration the vector x was initialized with f as the rated frequency, $50\ Hz$, $V_{d,sen}$ as zero and $V_{q,sen}$ as the max value of the signal.

The initialized and estimated values can be observed in the appendix at the table A.5 and A.6.

Once computed the Non-linear least-square estimates of x, (3.8), the values of the voltage phase and of the voltage module are derived as:

$$\varphi_{v,sen} = \arctan\left(\frac{V_{q,sen}}{V_{d,sen}}\right)$$

(3. 33)

$$|\underline{V}_s| = \sqrt{{V_{q,sen}}^2 + {V_{d,sen}}^2}$$

(3. 34)

At this point, the real transformation ration of the voltage transformer can be estimated:

$$\widetilde{K}_{VT} = \frac{K_N |\underline{V}_{sen}|}{|\underline{V}_{gen}|}$$

(3. 35)

The phase shift introduced by the voltage transformer is:

$$\Delta\widetilde{\varphi}_{VT} = \varphi_{v,gen} - \varphi_{v,sen} \tag{3. 36}$$

Their variances can be estimated with the following formula:

$$\begin{bmatrix} \sigma^2_{K_{VT}} \\ \sigma^2_{\varphi_{VT}} \end{bmatrix} = J_V \cdot P_V \cdot J_V{}' \tag{3. 37}$$

With:

J_V is the Jacobian of the variances of the formulas, (3. 35) (3. 36), respect to the variable vector x

The variance of the transformation ratio is:

$$\sigma^2_{K_{VT}} = \sigma^2_{K_N}\left(\frac{|\underline{V_s}|}{|\underline{V_g}|}\right)^2 + \sigma^2_{|V_s|}\left(\frac{K_N}{|\underline{V_g}|}\right)^2 + \sigma^2_{|V_g|}\left(\frac{K_N|\underline{V_s}|}{|\underline{V_g}|^2}\right)^2 \tag{3. 38}$$

The variance of the phase shift introduced by the voltage transformer is:

$$\sigma^2_{\varphi_{VT}} = \sigma^2_{\varphi_{vg}} + \sigma^2_{\varphi_{vs}} + \sigma^2_{\varphi_D} \tag{3. 39}$$

The variable vector x is:

$$\mathrm{x} = \begin{bmatrix} \sigma^2_{\varphi_D} \\ \sigma^2_{K_N} \\ \sigma^2_{|\underline{V_g}|} \\ \sigma^2_{\varphi_{vg}} \\ \sigma^2_{|\underline{V_g}|} \\ \sigma^2_{\varphi_{vs}} \end{bmatrix} \tag{3. 40}$$

The Jacobian J_V is:

$$J_V = \begin{bmatrix} 0 & \frac{|\underline{V_s}|}{|\underline{V_g}|} & \frac{K_{Dn}}{|\underline{V_g}|} & 0 & -\frac{K_{Dn}|\underline{V_s}|}{|\underline{V_g}|^2} & 0 \\ 1 & 0 & 0 & 1 & 0 & -1 \end{bmatrix} \tag{3. 41}$$

Where:

- $\sigma^2_{K_{VT}}$is the variance of the transformation ratio of the voltage transformer
- $\sigma^2_{K_N}$ is the variance of the transformation ratio of the voltage divider
- $\sigma^2_{|\underline{V_s}|}$ is the variance of the module of the voltage acquired from the sensor
- $\sigma^2_{|\underline{V_g}|}$ is the variance of the module of the voltage acquired from the generator
- $\sigma^2_{\varphi_{VT}}$is the variance of the phase displacement introduced by the voltage transformer
- $\sigma^2_{\varphi_D}$ is the variance of the phase displacement introduced by the voltage divider
- $\sigma^2_{\varphi_{vg}}$ is the variance of the phase of the voltage acquired from the generator
- $\sigma^2_{\varphi_{vs}}$ is the variance of the phase of the voltage acquired from the sensor

Instead P_V is the matrix of variance and covariance

$$P_V = \begin{bmatrix} \sigma^2_{\varphi_D} & 0 & 0 & 0 \\ 0 & \sigma^2_{K_N} & 0 & 0 \\ 0 & 0 & [P_{Vg}] & 0 \\ 0 & 0 & 0 & [P_{Vs}] \end{bmatrix} \tag{3. 42}$$

Where:

- $\sigma^2_{\varphi_D}$was estimated with the formula

$$\sigma^2_{\varphi_P} = \frac{{\varphi_e}^2}{3} \tag{3. 43}$$

φ_e the phase error related to the voltage divider, its value can be obtained from (Table 2.12) .
An uniform distribution was considered

- $\sigma_{K_N}^2$ was estimated with the formula

$$\sigma_{K_N}^2 = \frac{\varepsilon^2}{3} \tag{3. 44}$$

ε the ratio error related to the voltage divider, its value can be obtained from (Table 2.12) .

An uniform distribution was considered

- $P_{Vg}$is the submatrix 2X2 of variances and covariances related to the voltage acquired from the generator.

$$P_{Vg} = \begin{bmatrix} \sigma_{|\underline{V}_g|}^2 & \sigma_{|\underline{V}_g|,\varphi_{vg}} \\ \sigma_{|\underline{V}_g|,\varphi_{vg}} & \sigma_{\varphi_{vg}}^2 \end{bmatrix} \tag{3. 45}$$

- $\sigma_{|V_g|,\varphi_{vg}}$is the covariance between the module and the phase of the voltage signal acquired from the generator
- $P_{Vs}$is the submatrix 2X2 of variances and covariances related to the voltage acquired from the sensor.

$$P_{Vs} = \begin{bmatrix} \sigma_{|\underline{V}_s|}^2 & \sigma_{|\underline{V}_s|,\varphi_{vs}} \\ \sigma_{|\underline{V}_s|,\varphi_{vs}} & \sigma_{\varphi_{vs}}^2 \end{bmatrix} \tag{3. 46}$$

- $\sigma_{|V_s|,\varphi_{vs}}$is the covariance between the module and the phase of the voltage signal acquired from the sensor

Both submatrix are estimated with the formula (3. 17), where R is the diagonal matrix 2x2 of variances expressed as in the formula (3. 9) and A is the Jacobian of the acquired signal respect to its module and its phase.

Considering the case of voltage acquired from the generator:

$$v_{gen} = |\underline{V}_g|\sin(\omega t + \varphi_{vg}) \tag{3. 47}$$

$$A_{vg} = \begin{bmatrix} \sin(\omega t_1 + \varphi_{vg}) & \left|\underline{V}_g\right|\cos(\omega t_1 + \varphi_{vg}) \\ \vdots & \vdots \\ \sin(\omega t_N + \varphi_{vg}) & \left|\underline{V}_g\right|\cos(\omega t_N + \varphi_{vg}) \end{bmatrix} \tag{3. 48}$$

The variance of the matrix R is related to the accuracy of the scopemeter, Table 3.2.

$$\sigma^2 = \frac{2{,}1\% * reading\ value + 0{,}04 * division}{3} \tag{3. 49}$$

The error of the estimated transformation ratio and its variance are estimated in the following way:

$$\varepsilon = \frac{K_N - \widetilde{K}_{VT}}{\widetilde{K}_{VT}} * 100 \tag{3. 50}$$

$$\sigma_\varepsilon^2 = \sigma_{\widetilde{K}_{VT}}^2 \left(\frac{K_N}{\widetilde{K}_{VT}^{\ 2}} \right)^2 \tag{3. 51}$$

Instead, for what concern the case with variable current and constant voltage, the equivalent circuit of the current side is represented in the figure 3.17:

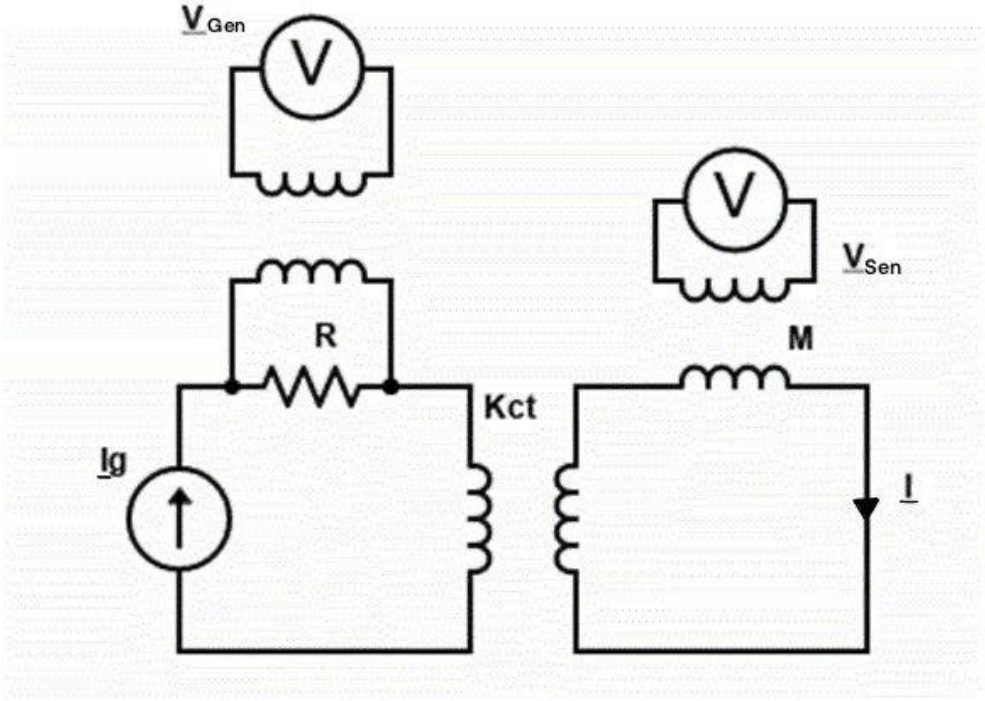

Figure 3. 17: Current side equivalent circuit

With

$$\underline{I} = K_{CT}\frac{\underline{V_g}}{R} = \frac{\underline{V_s}}{\omega M} \tag{3. 52}$$

Where:

- R is the current traductor sensibility
- M is the mutual inductance, its value can be obtained from the formula (2.3)

$$M = \frac{1}{2\pi f \mathrm{k}_{sf}} \tag{3. 53}$$

- $\underline{V_g}$ the voltage acquired by the AC current clamp
- $\underline{V_s}$ the voltage acquired by the smart termination

The procedure will be the same of the previous one, for this reason the formulas from (3. 22) to (3. 33) are applied.

At this point the phase shift can be estimated with the formula (3.35) and the transformation ration with the formula (3. 36):

After the estimation of the unknown quantities with the non-linear least-square, see Tables from A.7 to A.10, the real transformation ration of the current transformer and the phase shift introduced by the transformer can be calculated:

$$\widetilde{K}_{CT} = \frac{|\underline{V}_s|}{|\underline{V}_g|} * \frac{R}{\omega M} \tag{3. 54}$$

$$\Delta\widetilde{\varphi}_{CT} = \angle_1 - \angle_2 + 90° \tag{3. 55}$$

Their variances are obtained with the following formula:

$$\begin{bmatrix} \sigma^2_{K_{CT}} \\ \sigma^2_{\varphi_{CT}} \end{bmatrix} = J_I \cdot P_I \cdot J_I{}' \tag{3. 56}$$

With:

J_I is the Jacobian of the variances of the formulas, (3. 54) (3. 55), respect to the variable vector x

The variance of the transformation ratio:

$$\sigma^2_{K_{CT}} = \sigma^2_M \left(\frac{|\underline{V}_s|}{|\underline{V}_g|}\right)^2 + \sigma^2_{|V_s|} \left(\frac{K_M}{|\underline{V}_g|}\right)^2 + \sigma^2_{|V_g|} \left(\frac{K_M |\underline{V}_s|}{|\underline{V}_g|^2}\right)^2 \tag{3. 57}$$

The variance of the phase shift introduced by the transformer:

$$\sigma^2_{\varphi_{CT}} = \sigma^2_{\varphi_{vg}} + \sigma^2_{\varphi_{vs}} + \sigma^2_{\varphi_R} \tag{3. 58}$$

The variable vector x:

$$x = \begin{bmatrix} \sigma^2_{\varphi_D} \\ \sigma^2_{K_N} \\ \sigma^2_{|\underline{V}_g|} \\ \sigma^2_{\varphi_{vg}} \\ \sigma^2_{|\underline{V}_g|} \\ \sigma^2_{\varphi_{vs}} \end{bmatrix} \tag{3. 59}$$

The Jacobian J_I:

$$J_I = \begin{bmatrix} 0 & \frac{|\underline{V}_s|}{|\underline{V}_g|} & \frac{M}{|\underline{V}_g|} & 0 & -\frac{M|\underline{V}_s|}{|\underline{V}_g|^2} & 0 \\ 1 & 0 & 0 & 1 & 0 & -1 \end{bmatrix} \tag{3. 60}$$

Where:

- $\sigma^2_{K_{CT}}$is the variance of the transformation ratio of the current transformer
- σ^2_M is the variance of the mutual inductance
- $\sigma^2_{|\underline{V}_s|}$ is the variance of the module of the voltage acquired from the sensor
- $\sigma^2_{|\underline{V}_g|}$ is the variance of the module of the voltage acquired from the generator
- $\sigma^2_{\varphi_{CT}}$is the variance of the phase displacement introduced by the current transformer
- $\sigma^2_{\varphi_R}$ is the variance of the phase displacement introduced by the Rogowski coil
- $\sigma^2_{\varphi_{vg}}$ is the variance of the phase of the voltage acquired from the generator
- $\sigma^2_{\varphi_{vs}}$ is the variance of the phase of the voltage acquired from the sensor

Instead P_I is the matrix of variance and covariance

$$P_I = \begin{bmatrix} \sigma_{\varphi_R}^2 & 0 & 0 & 0 \\ 0 & \sigma_M^2 & 0 & 0 \\ 0 & 0 & [P_{Vg}] & 0 \\ 0 & 0 & 0 & [P_{Vs}] \end{bmatrix} \quad (3.\ 61)$$

Where:

- $\sigma_{\varphi_R}^2$ was estimated with the formula

$$\sigma_{\varphi_R}^2 = \frac{{\varphi_e}^2}{3} \quad (3.\ 62)$$

  φ_e the phase error related to the Rogowski, its value can be obtained from (Table 2.11) .
  An uniform distribution was considered
- σ_M^2 was estimated with the formula

$$\sigma_{K_M}^2 = \frac{(\varepsilon M)^2}{3} \quad (3.\ 63)$$

  ε the ratio error related to the Rogowski coil, its value can be obtained from (Table 2.11) .

  An uniform distribution was considered
- P_{Vg} is the submatrix 2X2 of variances and covariances related to the voltage acquired from the generator.

$$P_{Vg} = \begin{bmatrix} \sigma_{|\underline{V_g}|}^2 & \sigma_{|\underline{V_g}|,\varphi_{vg}} \\ \sigma_{|\underline{V_g}|,\varphi_{vg}} & \sigma_{\varphi_{vg}}^2 \end{bmatrix} \quad (3.\ 64)$$

- $\sigma_{|V_g|,\varphi_{vg}}$ is the covariance between the module and the phase of the voltage signal acquired from the generator
- P_{Vs} is the submatrix 2X2 of variances and covariances related to the voltage acquired from the sensor.

$$P_{Vs} = \begin{bmatrix} \sigma^2_{|\underline{V_s}|} & \sigma_{|\underline{V_s}|,\varphi_{vs}} \\ \sigma_{|\underline{V_s}|,\varphi_{vs}} & \sigma^2_{\varphi_{vs}} \end{bmatrix} \tag{3. 65}$$

- $\sigma_{|V_s|,\varphi_{vs}}$is the covariance between the module and the phase of the voltage signal acquired from the sensor

The submatrix, P_{Vs}, can be estimated with the formals from (3. 47) to (3. 49).

The same process can be adopt also for the submatrix P_{Vg}, but in this case the variance of the matrix R is related to the accuracy of the scopemeter and to the accuracy of the AC current clamp, Figure 3.7.

$$\sigma^2 = \frac{(2{,}1\% * reading\ value + 0{,}04 * division)^2 + (2\% * reading\ value + 0{,}5)^2}{3} \tag{3. 66}$$

The error of the estimated transformation ratio and its variance are estimated in the following way:

$$\varepsilon = \frac{K_N - \widetilde{K}_{CT}}{\widetilde{K}_{CT}} * 100 \tag{3. 67}$$

$$\sigma^2_{\varepsilon} = \sigma^2_{\widetilde{K}_{CT}} \left(\frac{M}{\widetilde{K}_{CT}^{\ 2}} \right)^2 \tag{3. 68}$$

In this part of the thesis the results of the first case will be briefly shown.

In the Table 3.3 results of the test at constant voltage and variable current are reported instead in the Table 3.4. the results of the test at constant current and variable voltage are reported. All the result are present in the figure 3.18.

I [A]	$\widetilde{K}_{CT}$	ε	$\Delta\widetilde{\varphi}_{CT}$
5	11(5)*10^2	5(2)*10%	-4 (2)*10^2 °
25	7(2) *10^2	1(2)%	-16(1)°
100	63(4)	5(5)%	-12(1)°
500	62(2)	3(1)%	-8,99(1)°
600	62(1)	2(1)%	-8,84(1)°

Table 3. 3: Results of the test at constant voltage and variable current

V [V]	$\widetilde{K}_{VT}$	ε	$\Delta\widetilde{\varphi}_{VT}$
220	226,0(7)	2,7(2)%	0,56 (4)°
2200	225,87(7)	2,66(2)%	0,46(1)°
8800	226,04(2)	2,75(1)%	0,453(3)°
11000	226,92(1)	3,15(1)%	0,585(3)°

Table 3. 4: Results of the test at constant current and variable voltage

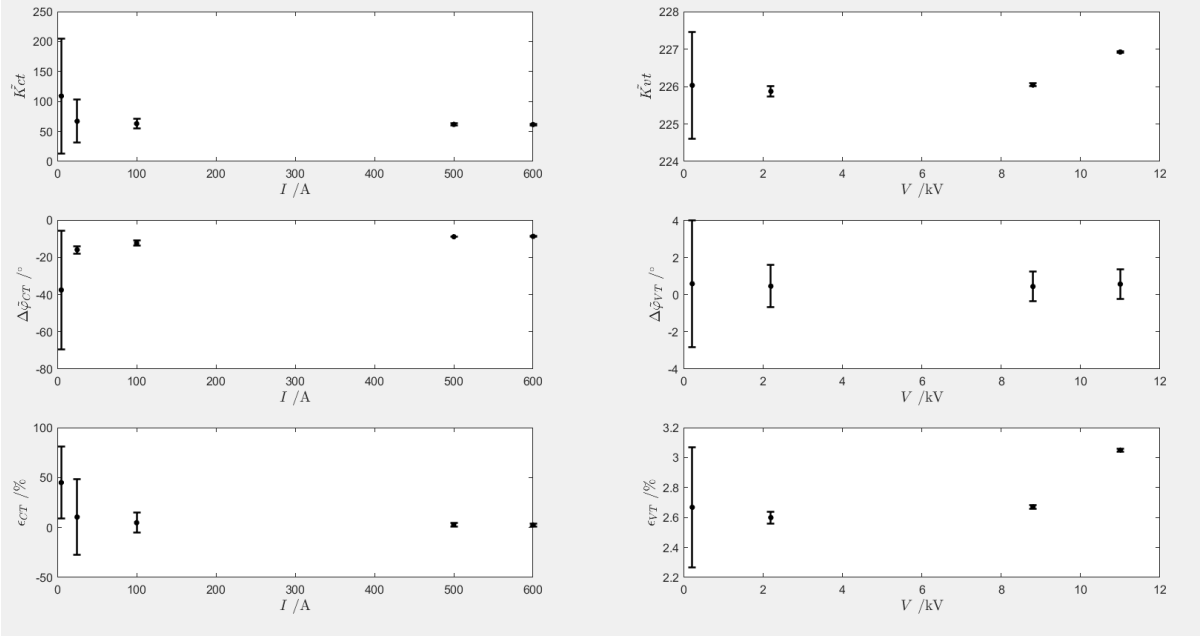

Figure 3. 18: Plots of the results in the Tables 3.3 and 3.4 , each single plot is present in the appendix, Figure from A.11 to A.17

4 | Conclusions

In conclusion, this thesis has presented a new calibration for the test bench of Gridspertise laboratory, which ensures more reliable accuracy for future tests.

The results of the first study have shown that the initial hypotheses regarding the nature of the phase shift and that the current is leading respect to the voltage were incorrect.

In fact it has proved that it is a time delay and that the voltage was leading. The most possible reason to this delay was due to a lack of synchronization between the generator and amplifier. The delay remains in a range of 500 μs but it isn't constant, it would be possible in case of random synchronization.

Additionally, the errors introduced by the voltage and current transformers were estimated, with the current transformer showing lower accuracy for secondary currents of 5 A and 25 A. It could be related to the fact that they are to low respect to the nominal value, 300 A.

Instead, for the results related to the voltage transformer have an high accuracy with values similar to the nominal ones.

Future tests on this transformer could be helpful in determining the cause of the displacement introduced by the current transformer. New test related to the other phases, that weren't done for a question of time, can give a more accurate idea.

Overall, this study provides important insights for improving the accuracy of testing equipment in the field of electrical engineering.

Bibliography

[1] Ettore De Berardinis and Roberto Faranda. “Network Automation and Protection Systems” course slide, 2022.
[2] Marco Merlo. “Planning & Operation of Distribution Grids with a high penetration of Res” course slide, 2021.
[3] Gabriele D’Antona. “Sensor, Measurement and Smart Metering” course slide, 2021.
[4] Gianluca Sapienza. “Voltage Control in Smart Grids part 2”, from “Smart Grid: Components, Functionalities and Benefits” course slides, 2022.
[5] F. Mauri, P. Paulon and G. Sapienza, TECHNICAL CHARACTERISTICS OF LPITs FOR RGDM/RGDAT, 2019.
[6] M. Bettinelli, P. Paulon and G. Sapienza, Risultati prove sensori 3M a specifica GSTC05 con RGDM, 2021.
[7] M. Bettinelli, P. Paulon and G. Sapienza, Risultati prove sensori BONOMI a specifica GSTC05 con RGDM, 2022.
[8] CMC 256 plus Manual, 2017.
[9] CMC 356 Manual, 2020.
[10] Q_CTV 20 Manual.
[11] RTA 36-2 Manual.
[12] Fluke 109-104 Manual.
[13] Fluke i200s Manual.
[14] DJ5400 (Smart termination) Manual, 2013.
[15] Gianluca Sapienza, GETP011, 2022.

1 A | Appendix

A.1 First test plots

In this section the Matlab script for the first case is reported. Adopting the formula from (3.1) to (3.19)

```
y = [I;V];

x = [1.4 0 1.4 0 50]'; %[Iq Id Vq Vd f]
A = zeros(2*N,5);
for k = 1:10
   A(1:N,:) = [sin(2*pi*x(5)*t) cos(2*pi*x(5)*t) zeros(N,2)
2*pi*t.*(x(1)*cos(2*pi*x(5)*t)-x(2)*sin(2*pi*x(5)*t))];
    A(N+1:2*N,:) = [zeros(N,2) sin(2*pi*x(5)*t) cos(2*pi*x(5)*t)
2*pi*t.*(x(3)*cos(2*pi*x(5)*t)-x(4)*sin(2*pi*x(5)*t))];
    h = [x(1)*sin(2*pi*x(5)*t)+x(2)*cos(2*pi*x(5)*t);
x(3)*sin(2*pi*x(5)*t)+x(4)*cos(2*pi*x(5)*t)];
    x = x+(A'*A)\A'*(y-h); %R is negligible in case of diagonal matrix
end
f1=atan2(x(1),x(2))*180/pi;
f2=atan2(x(3),x(4))*180/pi;
df=f1-f2;
dt=df/(50*360);
```

In the Tables below, A.1 and A.2 , there are the initial values of the unknown quantities (3.3) and the values estimated with the non-linear least-square estimation (3.8).

I_q	1,4	1,4	1,4	1,4	1,4	1,4
I_d	0	0	0	0	0	0
V_q	1,4	1,4	1,4	1,4	1,4	1,4
V_d	0	0	0	0	0	0
f	50	60	50	60	100	200

Table A. 1 initial values of the unknown quantities vector x, (3.3)

I_q	0,78	-1,35	-1,47	1,43	1,34	1,31
I_d	1,21	-0,49	-0,07	0,36	0,61	-0,65
V_q	0,53	-1,2	-1,38	1,3	1,1	1,4
V_d	1,31	-0,73	-0,28	0,58	0,89	0,02
F	50	60	50	60	100	200

Table A. 2 estimated values of the unknown quantities vector x

```
Iest = x(1)*sin(2*pi*x(5)*t)+x(2)*cos(2*pi*x(5)*t);

Vest = x(3)*sin(2*pi*x(5)*t)+x(4)*cos(2*pi*x(5)*t);

Ierr=I-Iest; %current error

Verr=V-Vest; %voltage error

S2I=var(Ierr); %variance of the current

S2V=var(Verr); %variance of the voltage

R=[S2I*eye(N) zeros(N,N);zeros(N,N) S2V*eye(N)];

P=inv(A'/R*A);

J= zeros (1,5);

J(1)= -1/(2*pi*x(5)*(1+(x(1)/x(2))^2)*x(2));

J(2)= x(1)/(2*pi*x(5)*(1+(x(1)/x(2))^2)*x(2)^2);

J(3)= 1/(2*pi*x(5)*(1+(x(3)/x(4))^2)*x(4));

J(4)= -x(3)/(2*pi*x(5)*(1+(x(3)/x(4))^2)*x(4)^2);

J(5)= (atan(x(1)/x(2))-atan(x(3)/x(4)))/(2*pi*x(5)^2);

sDT=sqrt(J*P*J'); %standard deviation of the time variation
```

This code is referred to the case at 50 Hz but it can be applied for all the cases changing the frequency.

```
Ji=zeros(1,4);

ji(1)=-1/((1+(x(1)/x(2))^2)*x(2));

Ji(2)= x(1)/((1+(x(1)/x(2))^2)*x(2)^2);

Ji(3)= 1/((1+(x(3)/x(4))^2)*x(4));

Ji(4)= -x(3)/((1+(x(3)/x(4))^2)*x(4)^2);

PP=P(1:4,1:4);

sDF=sqrt(Ji*PP*Ji'); %standard deviation of the phase variation
```

The plots in the figure from A.1 to A.6 are refered to the figure 3.12.

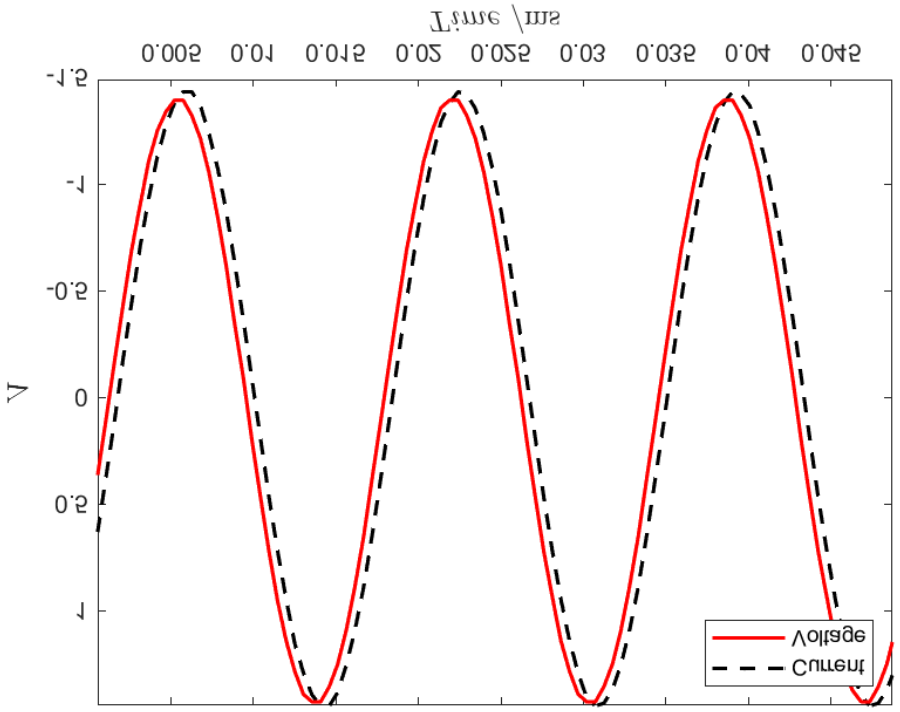

Figure A. 1: Voltage and current signals at 50 Hz with the secondary substation connected

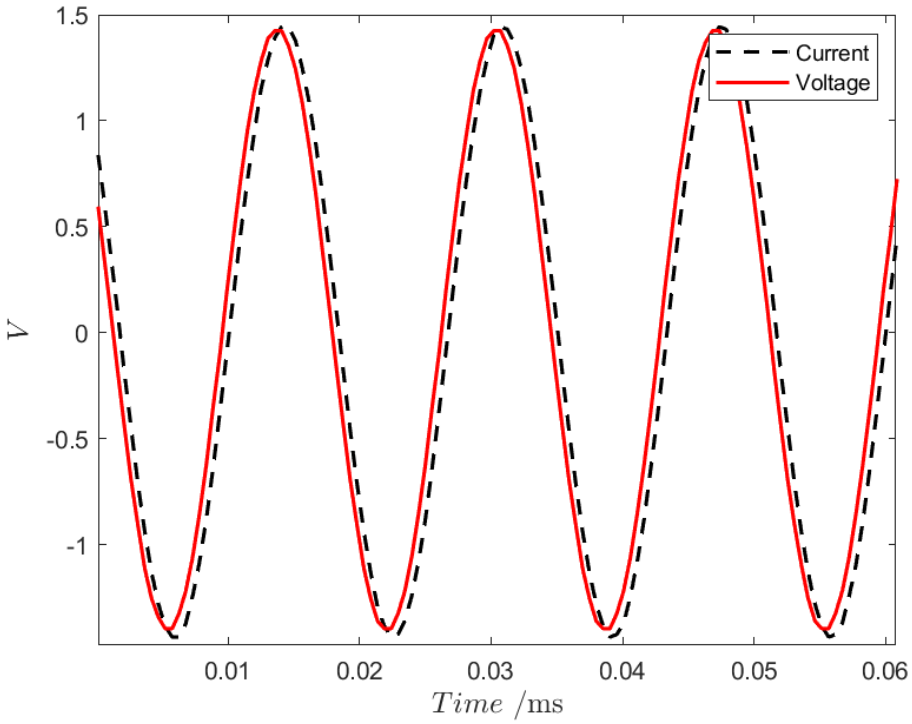

Figure A. 2: Voltage and current signals at 60 Hz with the secondary substation connected

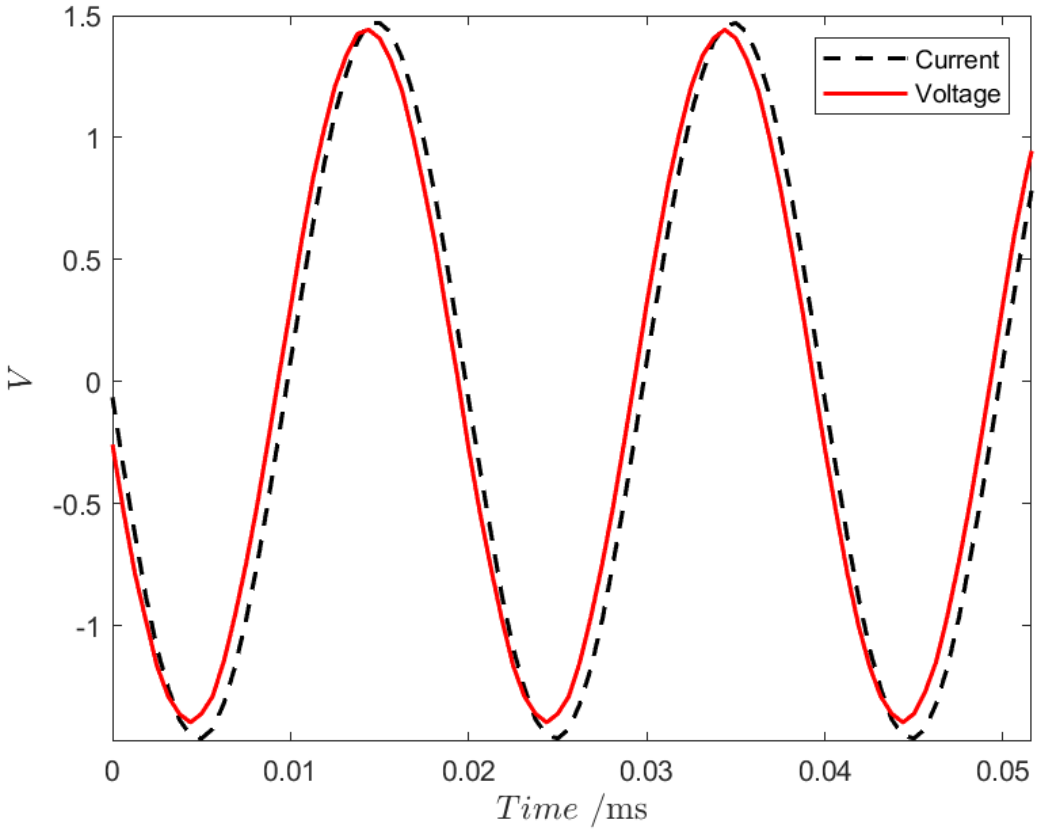

Figure A. 3: Voltage and current signals at 50 Hz with the secondary substation disconnected

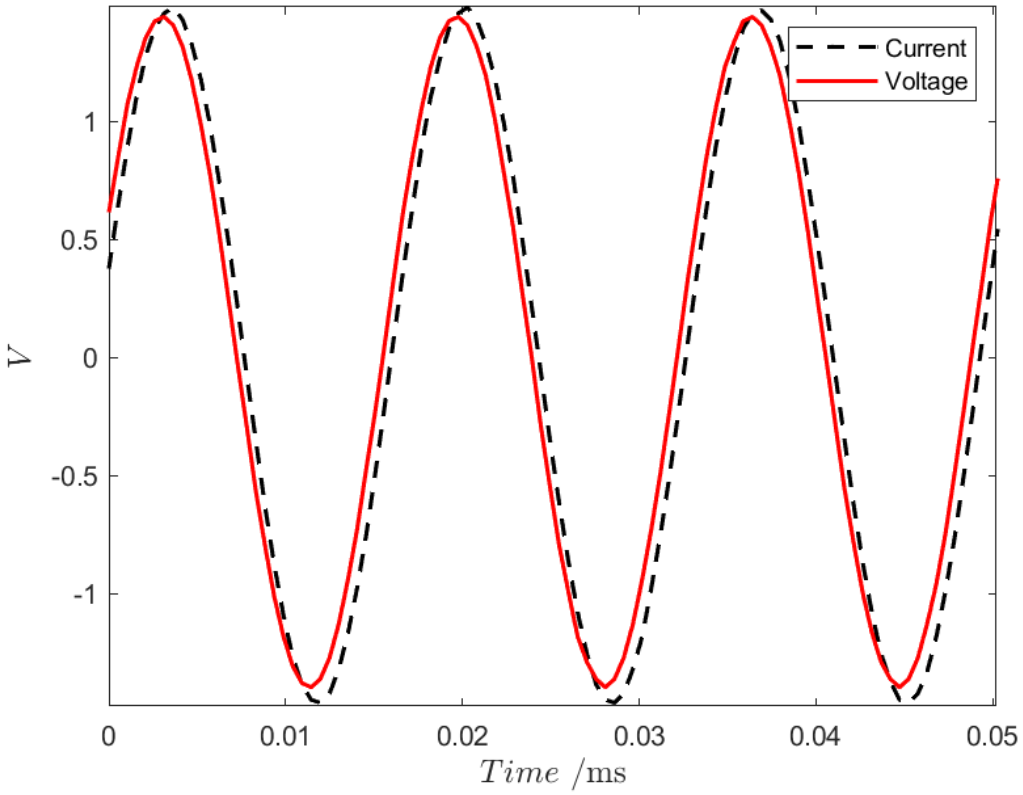

Figure A. 4: Voltage and current signals at 60 Hz with the secondary substation disconnected

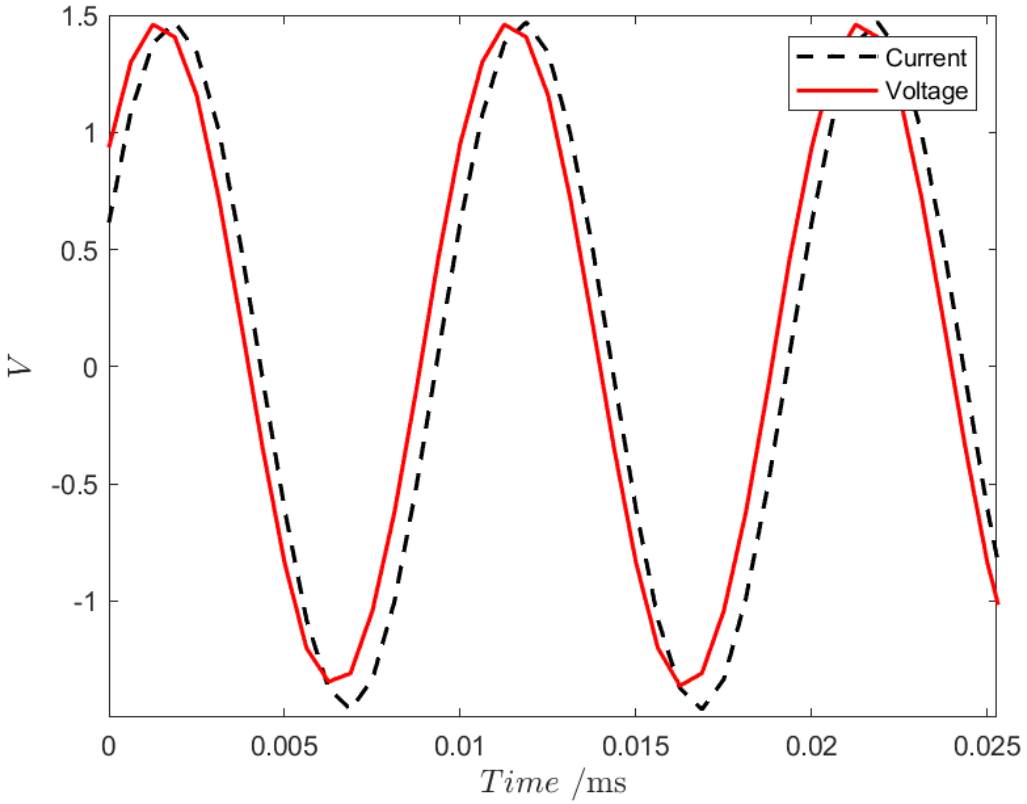

Figure A. 5: Voltage and current signals at 100 Hz with the secondary substation disconnected

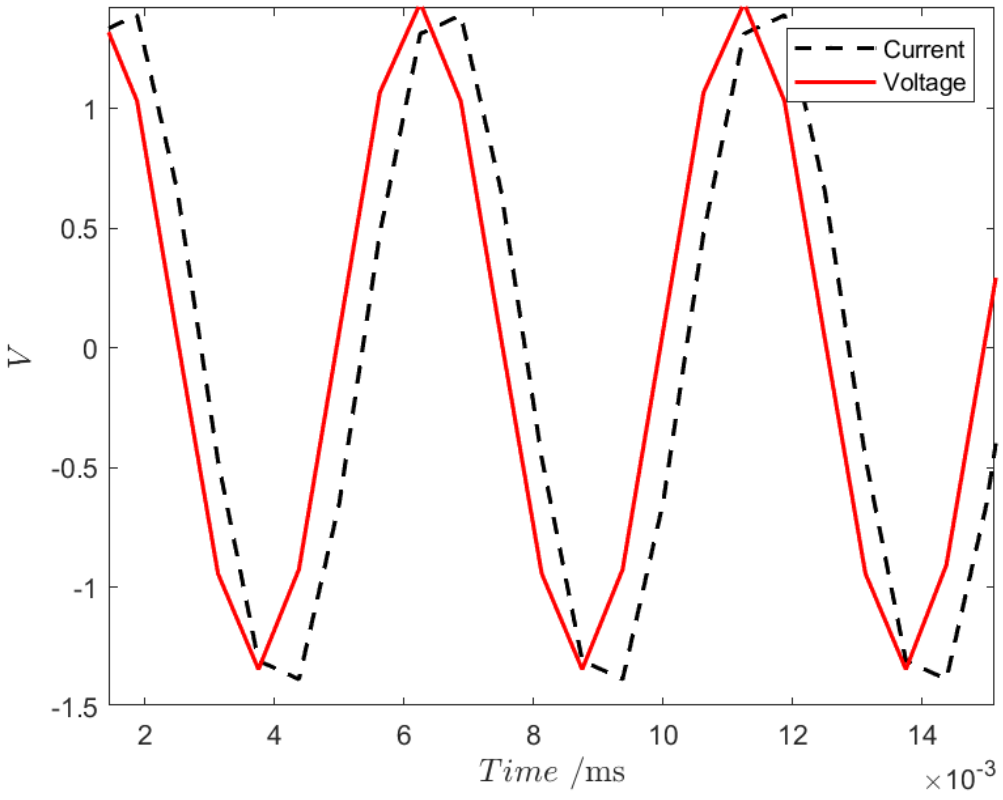

Figure A. 6: Voltage and current signals at 200 Hz with the secondary substation disconnected

The plots in the figure from A.7 to A.10 are refered to the figure 3.13.

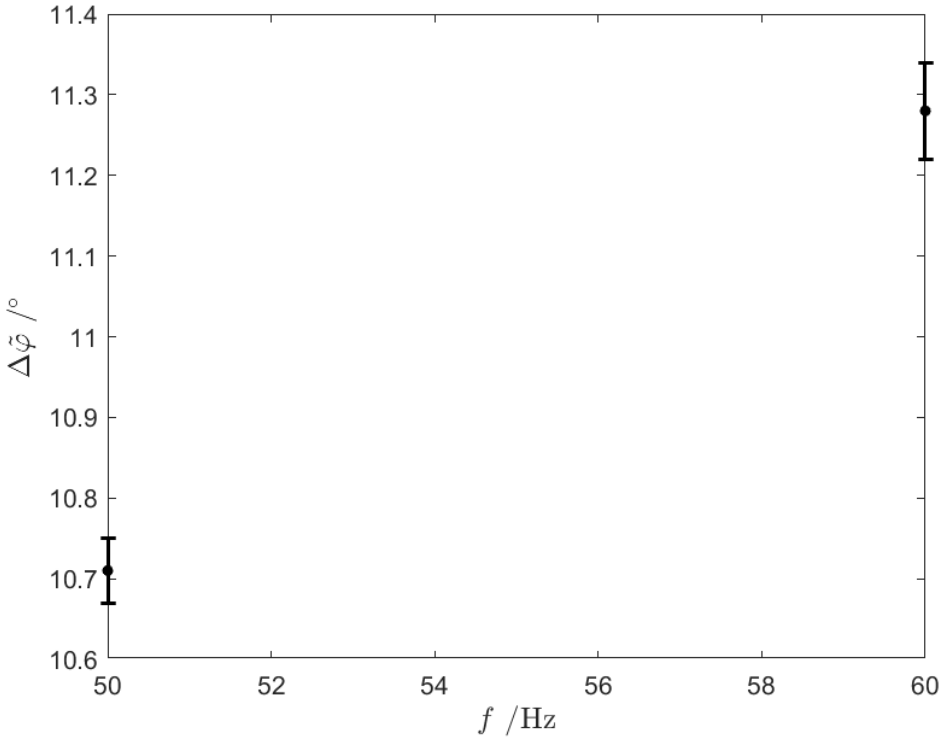

Figure A. 7: phase displacement with the secondary substation connected

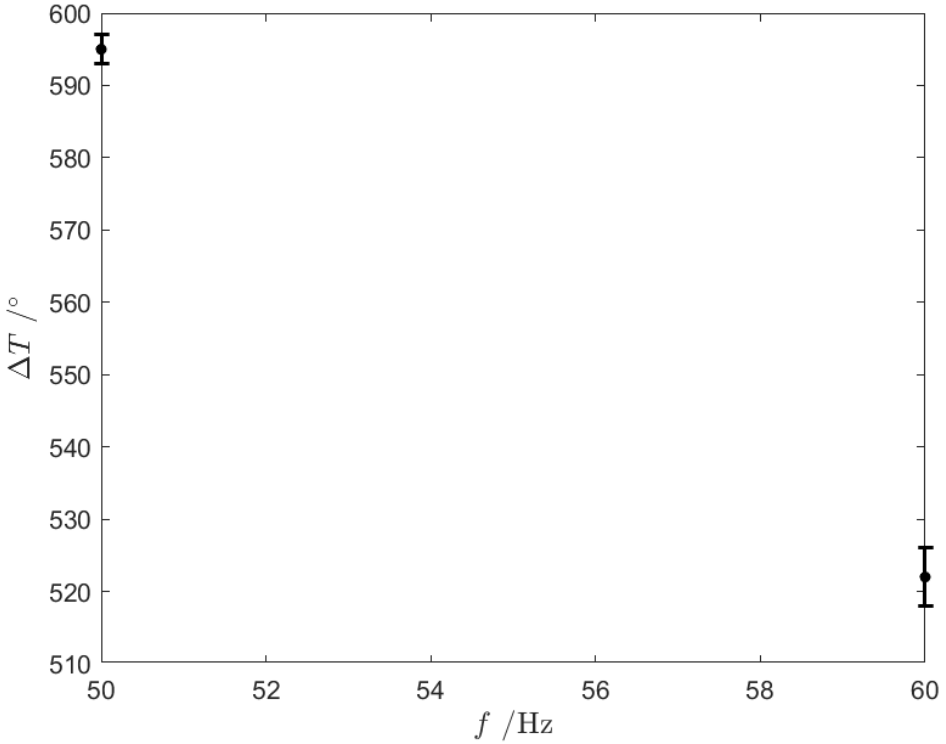

Figure A. 8: Time delay with the secondary substation connected

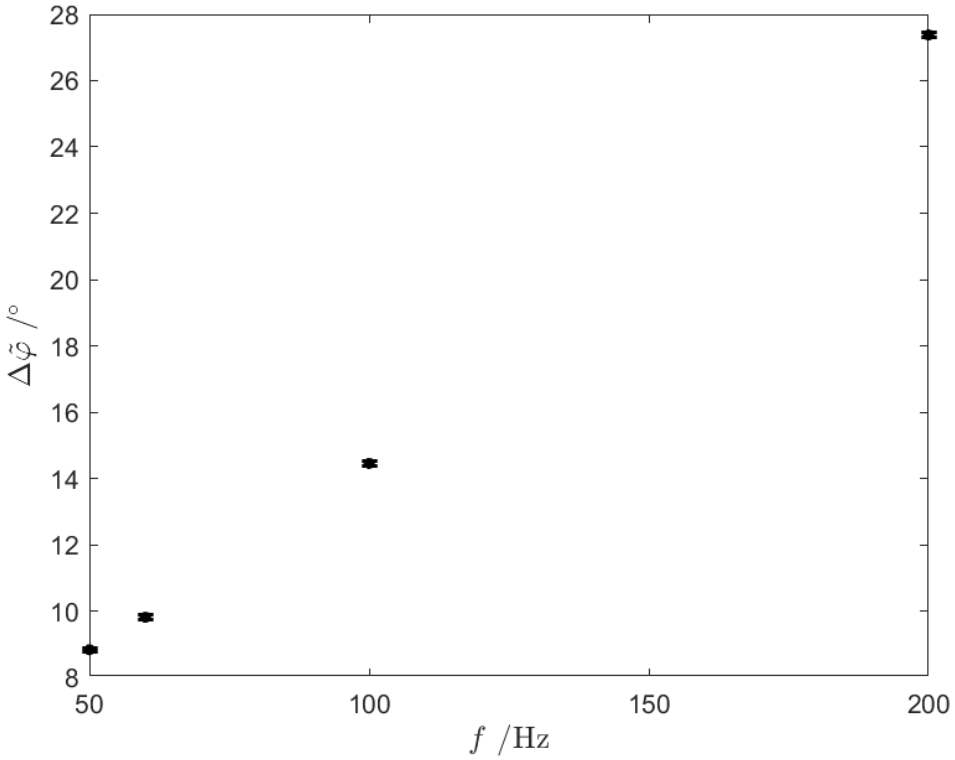

Figure A. 9: phase displacement with the secondary substation disconnected

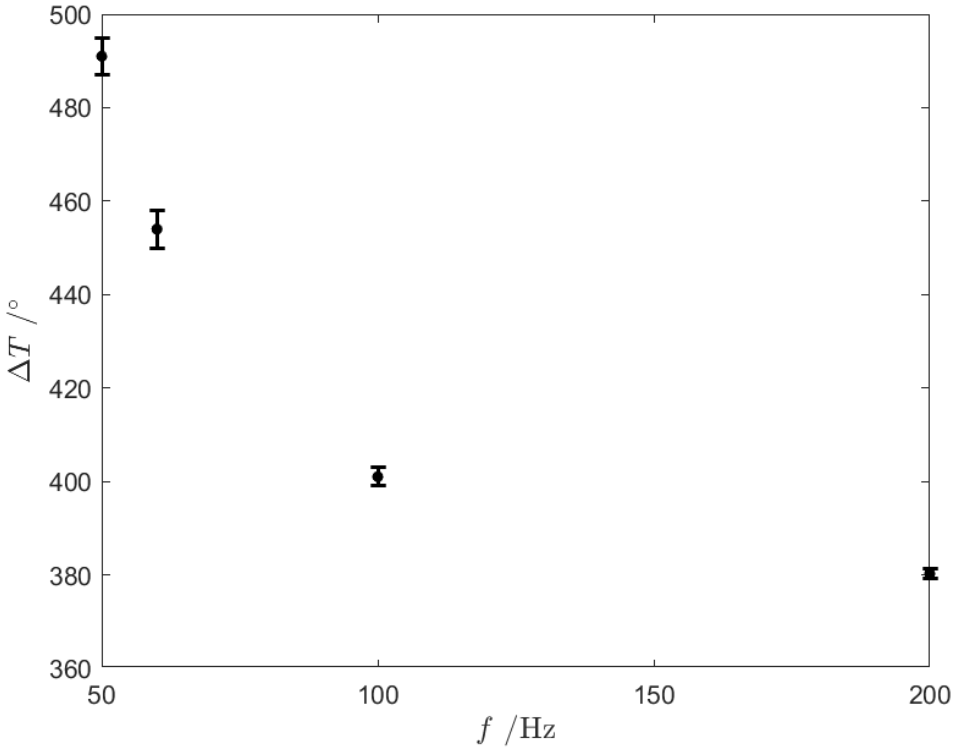

Figure A. 10: Time delay with the secondary substation connected

A.2 Second test plots

In this section the Matlab script for the second case is reported. Adopting the formula from (3.20) to (3.67)

```
xgen=[1.37 0 50]'; %vq,gen vd,gen f

A3 = zeros(length(t),3);

for k = 1:10
   A3(1:length(t),:) = [sin(2*pi* xgen(3)*t) cos(2*pi*xgen(3)*t)
2*pi*t.*(xgen(1)*cos(2*pi* xgen(3)*t)-x3(2)*sin(2*pi*xgen(3)*t))];
    h3 = xgen(1)*sin(2*pi*xgen(3)*t)+xgen(2)*cos(2*pi*xgen(3)*t);
    x3 = xgen+(A3'*A3)\A3'*(Vgen-h3);
end
Vgen_est = xgen(1)*sin(2*pi*xgen(3)*(t))+xgen(2)*cos(2*pi*xgen(3)*t);
f3=atan2(xgen(1),xgen(2))*180/pi;
Veff_gen=sqrt(xgen(1)^2+xgen(2)^2)/sqrt(2);
```

This script is referred to the case with a voltage of 220 V, the 2% of the nominal one, but it is analogue for all the cases.

```
xsen=[0.03 0 50]';

Asen = zeros(length(t),3);

for k = 1:10
   Asen(1:length(t),:) = [sin(2*pi*xsen(3)*t) cos(2*pi*xsen(3)*t)
2*pi*t.*(xsen(1)*cos(2*pi*xsen(3)*t)-xsen(2)*sin(2*pi*xsen(3)*t))];
    hsen = xsen(1)*sin(2*pi*xsen(3)*t)+xsen(2)*cos(2*pi*xsen(3)*t);
    xsen = xsen+(Asen'*Asen)\Asen'*(Vsen-hsen);
end
Vsen_est = xsen(1)*sin(2*pi*xsen(3)*(t))+xsen(2)*cos(2*pi*xsen(3)*t);
fsen=atan2(xsen(1),xsen(2))*180/pi;
Veff_sen=sqrt(xsen(1)^2+xsen(2)^2)/sqrt(2);
```

```
Kvt=Veff_sen/Veff_gen*10000;

df=fgen-fsen;
```

In the Tables below, from A.3 to A.6 , there are the initial values of the unknown quantities and the values estimated (3.22) and (3.29) with the non-linear least-square estimation(3.8)

	220 V	2200 V	8800 V	11000 V
$V_{q,gen}$	1,37	14	56	70
$V_{d,gen}$	0	0	0	0
f	50	50	50	50

Table A. 3 initial values of the unknown quantities vector x, (3.22), for the case with variable voltage and fixed current.

	220 V	2200 V	8800 V	11000 V
$V_{q,gen}$	1,21	10	38	68
$V_{d,gen}$	0,71	10	41	18
f	50	50	50	50

Table A. 4 estimated values of the unknown quantities vector x, for the case with variable voltage and fixed current.

	220 V	2200 V	8800 V	11000 V
$V_{q,sen}$	0,03	0,3	1,3	1,5
$V_{d,sen}$	0	0	0	0
f	50	50	50	50

Table A. 5 initial values of the unknown quantities vector x, (3.29), for the case with variable voltage and fixed current.

	220 V	2200 V	8800 V	11000 V
$V_{q,sen}$	0,03	0,22	0,85	1,5
$V_{d,sen}$	0,02	0,22	0,94	0,43
f	50	50	50	50

Table A. 6 estimated values of the unknown quantities vector x, for the case with variable voltage and fixed current.

```
xgen=[0.06 0 50]'; %vq,gen vd,gen f

Agen = zeros(length(t),3);

for k = 1:10
   Agen(1:length(t),:) = [sin(2*pi*xgen(3)*t) cos(2*pi*xgen(3)*t)
2*pi*t.*(xgen(1)*cos(2*pi*xgen(3)*t)-xgen(2)*sin(2*pi*xgen(3)*t))];
    hgen = xgen(1)*sin(2*pi*xgen(3)*t)+xgen(2)*cos(2*pi*xgen(3)*t);
    xgen = xgen+(Agen'*Agen)\Agen'*(Igen-hgen);
end
Vgen_est = xgen(1)*sin(2*pi*xgen(3)*(t))+xgen(2)*cos(2*pi*xgen(3)*t);
f1=atan2(xgen(1),xgen(2))*180/pi;
Veff_gen=sqrt(xgen(1)^2+xgen(2)^2)/sqrt(2);
```

```
xsen=[0.0003 0 50]';

Asen = zeros(length(t),3);

for k = 1:10
   Asen(1:length(t),:) = [sin(2*pi*xsen(3)*t) cos(2*pi*xsen(3)*t)
2*pi*t.*(xsen(1)*cos(2*pi*xsen(3)*t)-xsen(2)*sin(2*pi*xsen(3)*t))];
    hsen = xsen(1)*sin(2*pi*xsen(3)*t)+xsen(2)*cos(2*pi*xsen(3)*t);
    xsen = xsen+(Asen'*Asen)\Asen'*(Isen-hsen);
end
Vsen_est = xsen(1)*sin(2*pi*xsen(3)*(t))+xsen(2)*cos(2*pi*xsen(3)*t);
fsen=atan2(xsen(1),xsen(2))*180/pi;
Veff_sen=sqrt(xsen(1)^2+xsen(2)^2)/sqrt(2);
```

In the Tables below, from A. 7 to A.10, there are the initial values of the unknown quantities and the values estimated with the non-linear least-square estimation

	5 A	25 A	100 A	500 A	600 A
$V_{q,gen}$	0,06	0,53	2,2	12	13
$V_{d,gen}$	0	0	0	0	0
f	50	50	50	50	50

Table A. 7 initial values of the unknown quantities vector x, for the case with variable current and fixed voltage.

	5 A	25 A	100 A	500 A	600 A
$V_{q,gen}$	0,48	0,34	1,58	8,9	10,3
$V_{d,gen}$	0,44	0,42	1,67	7,9	8,6
f	50	50	50	50	50

Table A. 8 estimated values of the unknown quantities vector x, for the case with variable current and fixed voltage.

	5 A	25 A	100 A	500 A	600 A
$V_{q,sen}$	0,0003	0,001	0,0045	0,02	0,03
$V_{d,sen}$	0	0	0	0	0
f	50	50	50	50	50

Table A. 9 initial values of the unknown quantities vector x, for the case with variable current and fixed voltage.

	5 A	25 A	100 A	500 A	600 A
$V_{q,sen}$	0,48	0,34	1,58	8,9	10,3
$V_{d,sen}$	0,44	0,42	1,67	7,9	8,6
f	50	50	50	50	50

Table A. 10 estimated values of the unknown quantities vector x, for the case with variable current and fixed voltage.

```
Kct=(Veff_sen/Veff_gen)/(2*pi*50*1000000/31);

df=f1-f2+90;
```

```
Agen=[sin(2*pi*50*t+fgen) Veff_gen*(sqrt(2))*(cos(2*pi*50*t+fgen))];

Rgen=diag(((0.021*Vgen_est+0.04*10)/3).^-1);

Pgen=inv(Agen'/Rgen*Agen);

Asen=[sin(2*pi*50*t+f4) Veff4*(sqrt(2))*(cos(2*pi*50*t+f4))];

Rsen=diag(((0.021*Vsen_est+0.04*0.2)/3).^-1);

Psen=inv(Asen'/Rsen*Asen);

P_V=[(0.048/sqrt(3))^2 0 0 0 0 0; 0 (0.04/sqrt(3))^2 0 0 0 0; 0 0 Pgen(1,1)
Pgen(1,2) 0 0; 0 0 Pgen(2,1) Pgen(2,2) 0 0; 0 0 0 0 Psen(1,1) Psen(1,2); 0 0 0 0
Psen(2,1) Psen(2,2)];

JV(1:6,1)=[0 Veff_sen/(Veff_gen) -(sqrt(2)*Veff_sen)/(Veff_gen)^2 0
sqrt(2)/(Veff_gen) 0];

JV(1:6,2)=[1 0 0 1 0 -1];

var_V=JV'*P_V*JV; %[σ²_KVT  σ_KVT,φVT,  σ_KVT,φVT σ²_φVT]
```

This script is referred to the case with a voltage of 220 V, the 2% of the nominal one, but it is analogue for all the cases.

```
Agen=[sin(2*pi*50*t+fgen) Veff_gen*(sqrt(2))*(cos(2*pi*50*t+fgen))];

Rgen=diag(((((0.021*Igen_est+0.04*0.05).^2)+((0.02*Igen_est+0.5).^2))/3).^-1);

Pgen=inv(Agen'/Rgen*Agen);

Asen=[sin(2*pi*50*t+fsen) Veff_sen*(sqrt(2))*(cos(2*pi*50*t+fsen))];

Rsen=diag(((0.021*Isen_est+0.04*0.002)/3).^-1);

Psen=inv(Asen'/Rsen*Asen);

P_I=[(0.027/sqrt(3))^2 0 0 0 0 0; 0 (0.015*M/sqrt(3))^2 0 0 0 0; 0 0 Pgen(1,1)
Pgen(1,2) 0 0; 0 0 Pgen(2,1) Pgen(2,2) 0 0; 0 0 0 0 Psen(1,1) Psen(1,2); 0 0 0 0
Psen(2,1) Psen(2,2)];

JI(1:6,1)=[0 Veff2/Veff1 -(sqrt(2)*Veff2/(Veff1)^2 0 sqrt(2)/(Veff1) 0];

J5(1:6,2)=[1 0 0 1 0 -1];

var_I=JI'*P_I*JI; %[σ²_KCT  σ_KCT,φCT,  σ_KCT,φCT  σ²_φCT]
```

This script is related to the case of current equals to 5 A, 1% of the nominal one, but it is analogue to the other cases.

The plots in the figure from A.11 to A.16 are refered to the figure 3.15.

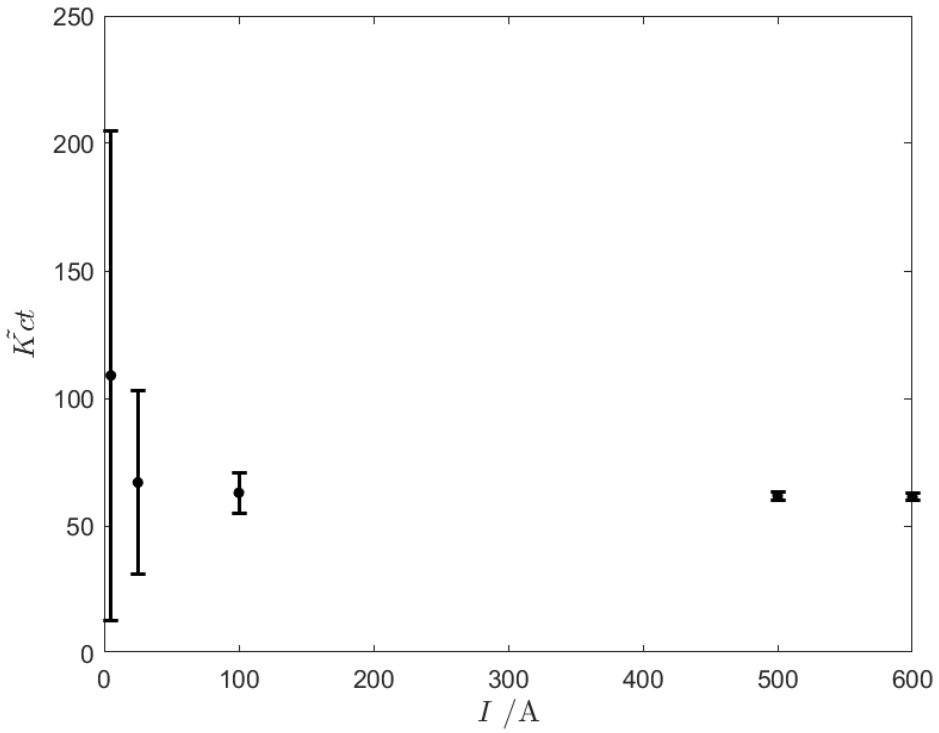

Figure A. 11: Estimated transformation ratio of current transformer

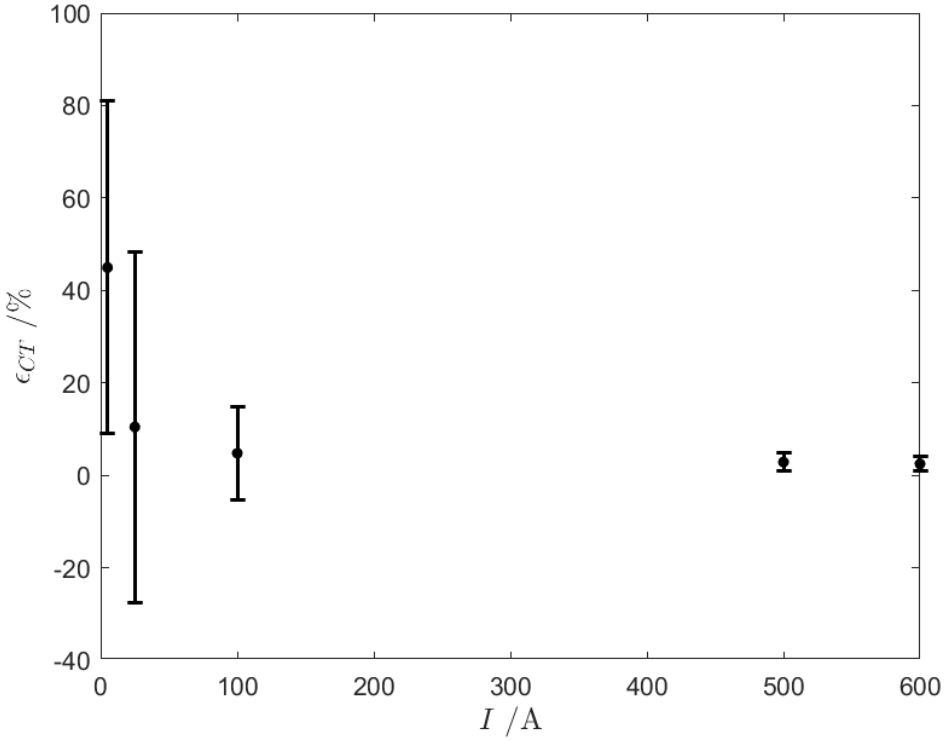

Figure A. 12: Error of the estimated transformation ratio of current transformer

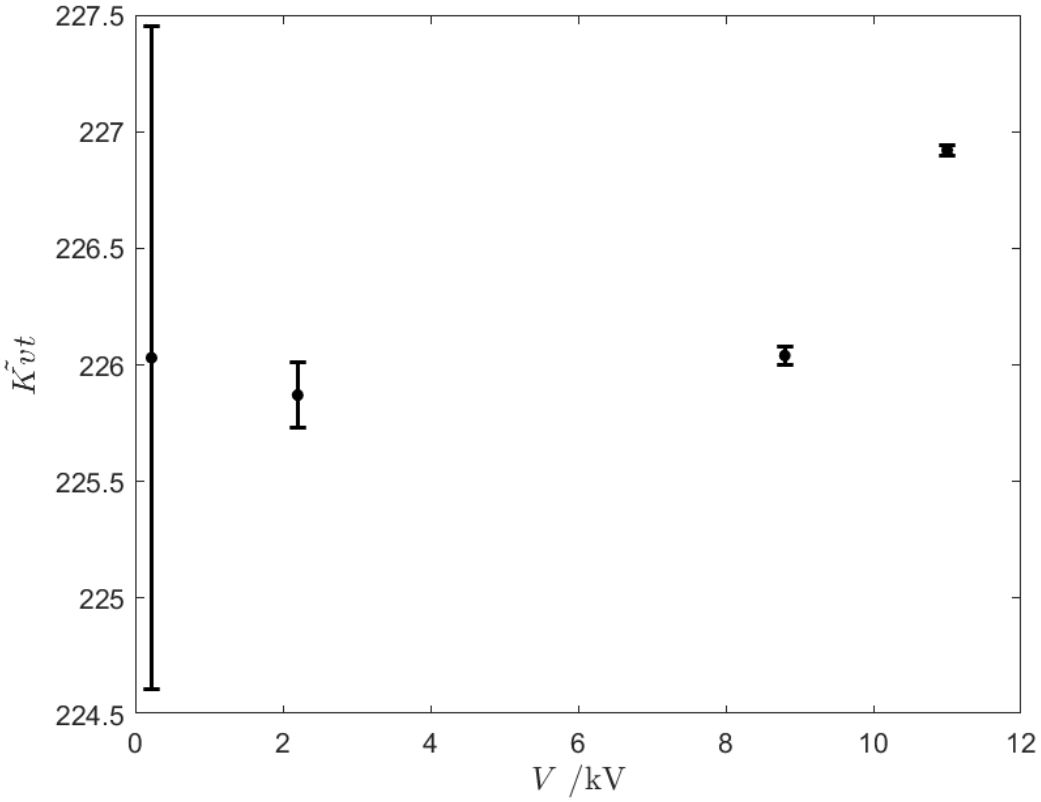

Figure A. 13: Estimated transformation ratio of voltage transformer

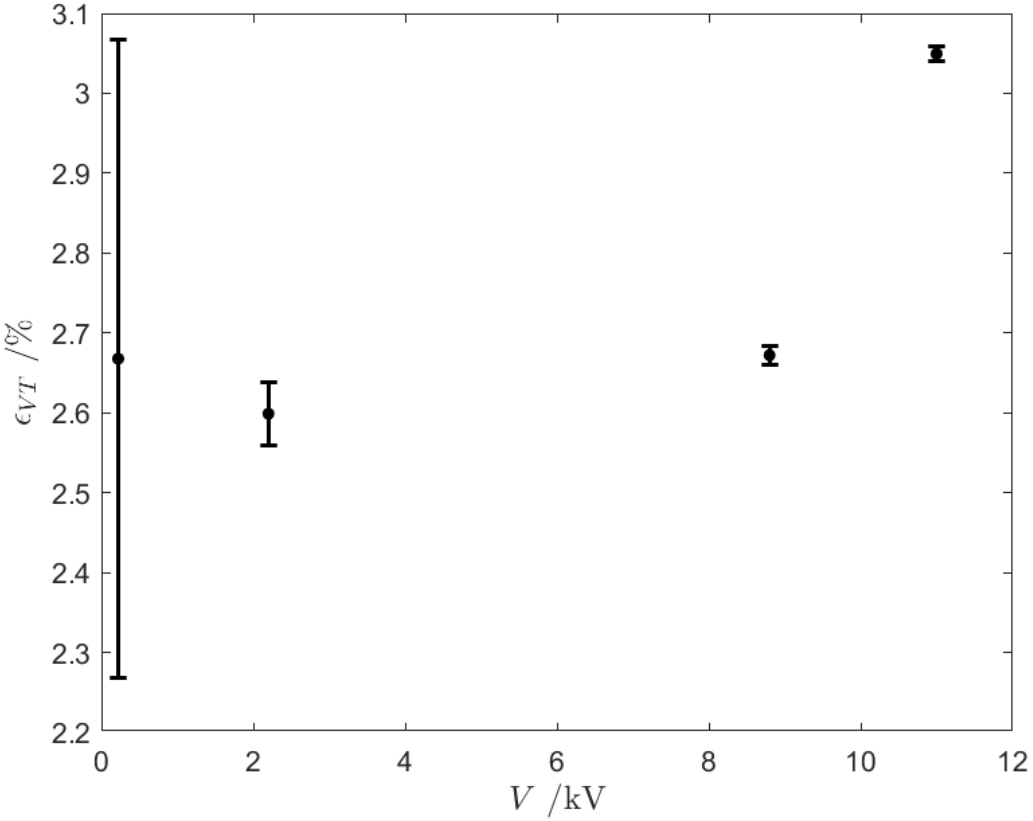

Figure A. 14: Error of the estimated transformation ratio of voltage transformer

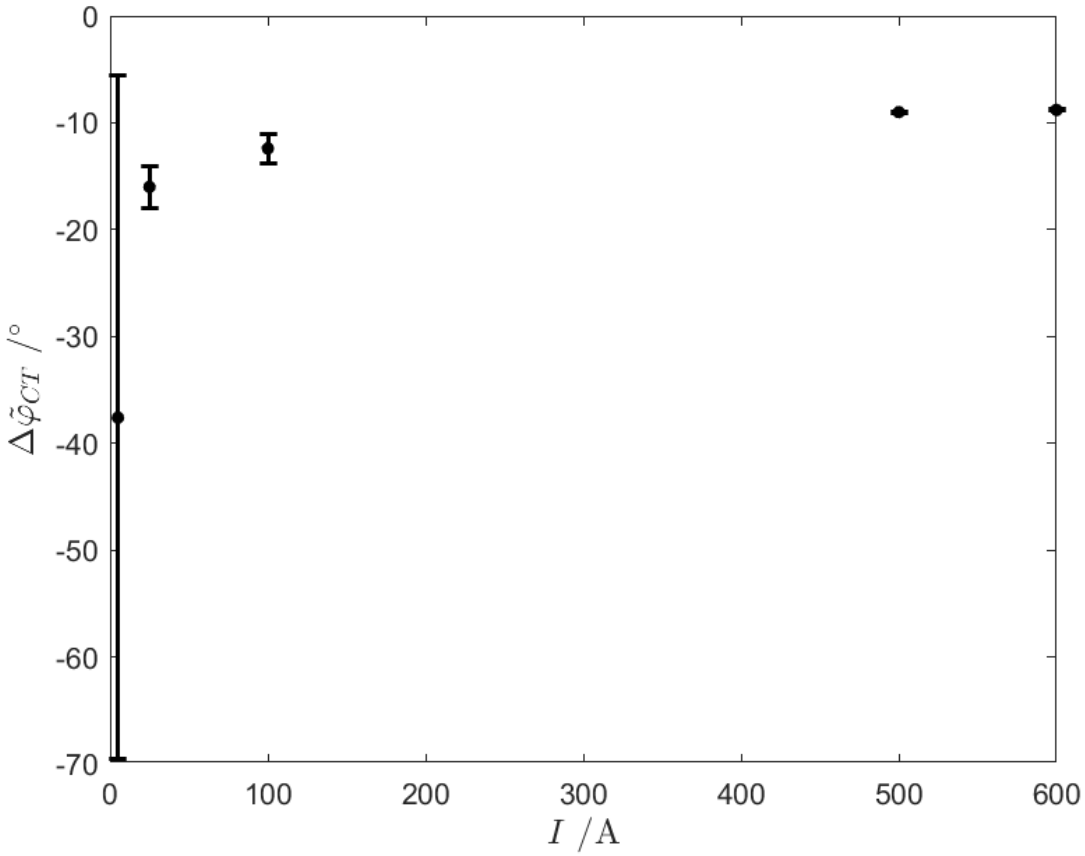

Figure A. 15: Estimated displacement introduced by the current transformer

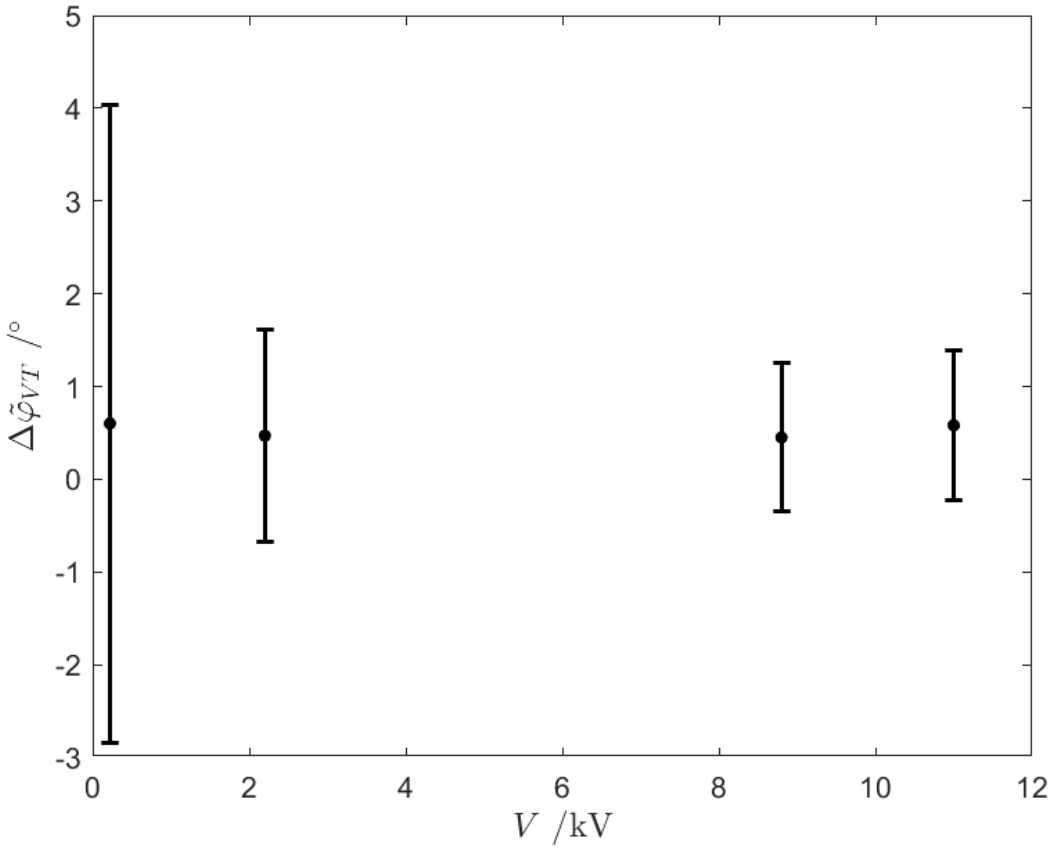

Figure A. 16: Estimated displacement introduced by the voltage transformer

List of Figures

List if Tables